Aus dem
Max-Planck Institut für Hirnforschung
in Frankfurt am Main

Alpha and Gamma-Band Oscillations in MEG-Data: Networks, Function and Development.

Dissertation
zur Erlangung des Doktorgrades
der Naturwissenschaften

vorgelegt am Fachbereich Psychologie und
Sportwissenschaften der Johann Wolfgang Goethe -Universität
in Frankfurt am Main

von Frédéric Roux
aus Friedrichshafen

Frankfurt am Main (2013)
D (30)

vom Fachbereich Psychologie
der Johann Wolfgang Goethe -Universität als Dissertation
angenommen

Dekan: Prof. Dr. Rolf van Dick

1. Gutachter: Prof. Dr. Wolf Singer
2. Gutachter: Prof. Dr. Christian Fiebach

Datum der Disputation: 04.07.2013

Contents

List of Figures

List of Tables

Für Herbert Wegner

1

General Introduction

1.1 Integration through Synchronization

One of the central questions in current cognitive neuroscience is how the highly distributed neuronal activity is coordinated to lead to coherently organized and context-sensitive perception and higher cognitive functions (Singer, 1999; Treisman, 1999). This binding problem arises from the highly segregated functional architecture of the brain where different processing streams operate in parallel (Treisman, 1999). The binding problem was first discussed in relationship to early perceptual processes. Neurophysiological studies had indicated that information regarding the color and shape of individual objects is processed by neurons in the visual cortex (Livingstone and Hubel, 1984; Hubel and Livingstone, 1987), which are differentially tuned to the respective stimulus qualities. Later work indicated that the binding problem generalized also to sensory-motor modalities as well as to higher associative areas (Uhlhaas et al., 2009a). Different mechanisms have been proposed to address this issue.

The first hypothesis is integration through convergence (Barlow, 1972, 1985) where "cardinal cells" at higher levels of the prcessing hierarchy integrate the information processed by cells at lower levels. Through combining different cardinal cells, information converges until the identification of a specific object is achieved. One obstacle for the cardinal cell hypothesis is the combinatorial explosion that occurs if all discriminable objects must have unique cells that code for a particular object. Although the existence of cells with response properties similar to cardinal cells has been documented (Quiroga et al., 2005), it becomes clear that the restricted number of cardinal cells cannot account solely for the perception of all the objects that we perceive (Ghose and Maunsell, 1999). In addition, feature integration based on cardinal cells can only work for familiar pre-stored conjunctions, and it remains unclear how new and unlearned conjunctions would be bound and perceived (Treisman, 1999).

The second hypothesis states that synchrony provides a means to bind cognitive contexts and to disambiguate distributed responses in neuronal networks (Singer, 1999). The central tenant of this hypothesis is that the timing of neuronal activity could act as a mechanism to signal the relatedness of features, such as the different features of an object. A gross simplification of this principle entails that for a blue Warhol portrait of Marylin Monroe, one neuron would be required to signal the color blue, whereas another one would signal the actress's face. The binding of color and shape would be achieved through the synchronous co-activation of both neurons in time. Similarly, for a green portrait, the brain would only require one additional neuron instead of two, in order to represent the change in color, as the same neuron that codes for the form of the face would be kept in the assembly. In a different context, all these neurons could be recombined to bind the features of other colored objects, such as a green triangle and a blue square for example, thereby forming dynamically configured cell assemblies (Singer, 1999). Furthermore, the coding space for neuronal computations is significantly enhanced through the possibility of using different oscillation frequencies. Thus, complementary information is represented on different temporal scales, providing a versatile mechanism that maximizes neural economy and discriminability in neuronal communication (Singer, 1999).

A related perspective is the Communication-through-Coherence (CTC) hypothesis (Fries, 2005). According to this view, activated neuronal groups oscillate and thereby undergo rhythmic excitability fluctuations which establish temporal windows for communication between distributed neuronal ensembles. CTC-has received support from findings which show that CTC can account for the modulation of high-frequency oscillations during attention (Bosman et al., 2012) as well for the relationship between phase relations of high-frequency oscillations and mechanistic interactions of neuronal groups (Womelsdorf et al., 2007), suggesting that the synchrony of neural oscillations can establish flexible communication in cortical networks.

Temporal oscillatory patterning of neuronal responses may not only be relevant for cognitive processes, but could also play an important role in the development of neuronal circuits (Uhlhaas et al., 2010). For example, the timing with which the activity of a pre-synaptic neuron reaches the synapse of a post-synaptic neuron critically determine whether the post-synaptic membrane potential will be potentiated or depressed (Markram et al., 1997). More precisely, if the activity of the pre-synaptic neuron reaches the post-synaptic neuron before it has fired, the membrane potential will be depressed. In turn, if the pre-synaptic spike arrives at the synaptic junction after the post-synaptic neuron has fired, the

membrane potential of the post-synaptic neuron will be potentiated. Both of these processes are referred to as spike timing dependent plasticity (STDP) (Dan and Poo, 2004; Mu and Poo, 2006). Long-term potentiation (LTP) or long-term depression (LTD) critically depends on the relative timing difference between pre- and post-synaptic neurons, and will occur if the pairing is repeated sufficiently often (Markram et al., 1997). While LTP will enhance the likelihood of successive co-activation between the two neurons, LTD will reduce the probability that both cells fire together. Thus, the timing of neural activity will trigger either a reinforcement or weakening of the connection between neurons (Luo and Vallano, 1995; Korte et al., 1998), thereby providing a timing based mechanism that could account for the development of functional circuits. Critically, oscillatory activity at low and higher frequencies has been implicated in the strengthening and weakening of synapses through STDP (Huerta and Lisman, 1996; Wespatat et al., 2004), suggesting that the timing of single spikes relative to the phase of oscillatory activity will determine if a synapse undergoes LTP or LTD.

1.2 Windows of Neuronal Excitability

Edgar Adrian, one of the pioneers of modern electro-physiology, explained the synchronization of neurons in the following way: "[...] synchronous activity can only occur in a group of neurons when the conditions of excitation are uniform throughout the group. When this obtains the neurones will all discharge at the same frequency and they may come to work in phase with one another as a result of their interconnection. " (Adrian and Matthews, 1934). In this quote Sir Adrian refers to the physiological origin of the large amplitude alpha oscillations at 10 Hz, which can be observed in the electro-encephalogram (EEG) of humans during eyes closed rest (Berger, 1929). He also highlights the importance of two general factors which will critically contribute to the emergence of rhythmic fluctuations of activity in the central nervous system: uniform excitation and connectivity.

Subsequent studies revealed that the cortex is capable of producing synchronous activity not only during eyes closed rest but also in response to sensory input and at frequencies $>$ 10 Hz (Adrian, 1950; Bressler and Freeman, 1980; Gray and Singer, 1989). Seminal work by Singer and colleagues showed that visual stimulation induces the synchronization of local neuronal populations at frequencies in the gamma (30-100Hz) range (Gray et al., 1989; Engel et al., 1990). These discoveries lead to the hypothesis that neuronal networks exploit rhythmic activity to process distributed inputs and transmit sensory information with high temporal precision (Singer, 1999). A large body of evidence has confirmed oscillatory activity in the gamma-band during different cognitive tasks,

suggesting a functional relationship between gamma-band activity and cognition (for a review see, Tallon-Baudry and Bertrand, 1999; Varela et al., 2001; Herrmann et al., 2004; Jensen et al., 2007; Fries, 2009; Uhlhaas et al., 2011).

In addition to oscillation at alpha and gamma-band frequencies, the spectrum of EEG activity displays frequencies between 0.1 and 600 Hz (Buzsáki and Draguhn, 2004; Buzsáki, 2011; Uhlhaas et al., 2011). During sleep for example, slow wave activity at delta frequencies (0.5-2Hz) can be prominently observed during sleep stages 3 and 4, whereas faster oscillations in the beta (15-20 Hz) and gamma (30-100 Hz) frequency ranges occur predominantly during alert states, active cognitive processing and paradoxical sleep (Steriade, 2000). Thus, the frequency of oscillatory activity depends on the behavioral state and reflects inhibition based fluctuations in the excitability of neuronal networks, thereby providing temporal windows of reduced and enhanced neuronal excitability (for a review see, Haider and McCormick, 2009; Buzsáki and Watson, 2012).

While slower oscillations provide a temporally broader framing of spiking activity, fast oscillations determine the probability of spiking in the millisecond range (Mainen and Sejnowski, 1995; Cardin et al., 2009). In addition, slower oscillations have been reported to synchronize activity over longer distances, whereas fast oscillations tend to occur at more local scales (Kopell et al., 2000; von Stein and Sarnthein, 2000). In many experiments slower brain rhythms are observed to occur simultaneously with faster oscillations and different forms of cross-frequency coupling (CFC) may exist between these rhythms (for a review see, Jensen and Colgin, 2007; Buzsáki and Wang, 2012). On form of CFC is phase amplitude coupling (PAC), where the amplitude of a high frequency oscillations is modulated by the phase of a slower rhythm. Other forms include amplitude to amplitude coupling as well as n:m phase locking, and refer to power and phase co-fluctuations between different frequencies (Jensen and Colgin, 2007). Importantly, the modulation of local high frequency activity through the phase of a slower rhythm has been proposed as a putative mechanism to synchronize fast oscillations across distant sites (Buzsáki and Wang, 2012).

In agreement with this hypothesis, slower rhythms have been proposed to provide the background activity necessary to keep cortical networks near spiking threshold over longer time scales, thereby allowing the network to rapidly react to fast changing fluctuations in local population dynamics (Haider and McCormick, 2009). Such a dynamical regime has been proposed to enhance the network's sensitivity towards synchronous inputs (Salinas and Sejnowski, 2001),

which play an important role in neuronal communication and functional connectivity (Schoffelen et al., 2005; Womelsdorf et al., 2007). Hence, these data suggest that the co-occurrence of multiple rhythms provides several advantages as it may a) balance excitation and inhibition in recurrent networks, b) maximize the sensitivity of neurons towards correlated inputs and c) promote the routing of information between networks (Mainen and Sejnowski, 1995; Salinas and Sejnowski, 2001; Sejnowski and Paulsen, 2006; Haider and McCormick, 2009).

Together these data suggest that the intrinsic dynamics of large-scale networks contribute to the emergence of both slow and fast rhythmic activity and that coherence among sub threshold membrane potential fluctuations could be exploited to express selective functional relationships (Fries, 2005), thereby allowing the coupling of different frequencies which may facilitate the grouping of distributed neuronal responses for further processing (Buzsáki and Wang, 2012).

1.3 Mapping Cerebral Large-Scale Dynamics

In humans, the measurement of rhythmic fluctuations of activity and the localization of underlying sources requires techniques that can track the spatio-temporal dynamics of cerebral activity with high precision in space and time. Electro-encephalography (EEG) and magneto-encephalography (MEG) are techniques that measure fluctuations of electromagnetic activity outside of the brain and offer high temporal (ms) and spatial resolution (mm^3). Both techniques are thus ideally suited to investigate the oscillatory dynamics of large-scale neuronal networks in the human brain (Hari and Salmelin, 1997; Salmelin and Baillet, 2009; Liu et al., 2010).

Biophysically, the emergence of measurable electro-magnetic fields has been related to the synchronous activity of hundreds of thousands of neurons (10^5) which can be modeled by the activity of current dipoles (Salmelin and Hämäläinen, 1995). Depending on the orientation of the dendrites, a current dipole will therefore have either a radial (perpendicular) or a tangential (parallel) orientation towards the scalp surface. Therefore, neurons organized in vertical macro-columns will tend to produce dipoles that have a radial orientation, whereas dipoles generated by neurons organized in horizontal macro-columns will be tangentially oriented (Ilmoniemi, 1993; Ahlfors et al., 2010). Radial and tangential dipoles each have their own spatial signature, and both techniques will pick up dipoles with mixed orientations (Renault and Garnero, 2004). However, while EEG is equally sensitive towards radial and tangential electric fields, MEG

is most sensitive to the activity generated by tangential sources (Renault and Garnero, 2004; Ahlfors et al., 2010).

One important advantage of MEG in comparison to EEG, however, is that the magnetic field will not be distorted by the conductive properties of the tissue surrounding the brain (skull & skin). Thus, MEG has a greater sensitivity towards higher frequencies and also higher spatial resolution, making it an optimal tool to examine rhythmic fluctuations of activity at source level during different behavioral states and cognitive processes (Hari and Salmelin, 1997; Salmelin and Baillet, 2009; Liu et al., 2010).

1.4 Temporally Structured Selection and Maintenance of Information

Recent theoretical work has proposed that the coupling between alpha and gamma oscillations may serve as a physiological gating mechanism, in which bursts of high-frequency activity occur preferentially during the phase of the alpha rhythm at which the network is in its most excitable state (Jensen and Mazaheri, 2010; Jensen et al., 2012). This hypothesis is based on observations which suggest that alpha oscillations lead to the phasic modulation of neural activity (Klimesch et al., 2007; Busch et al., 2009; Lorincz et al., 2009; Dugué et al., 2011; Haegens et al., 2011; Scheeringa et al., 2011; Vijayan and Kopell, 2012) and the phasic modulation of gamma-band oscillations (Chorlian et al., 2006; Osipova et al., 2008; Saalmann and Kastner, 2009; Foster and Parvizi, 2012; Spaak et al., 2012; Yanagisawa et al., 2012). According to this hypothesis, the amplitude modulation (AM) of gamma-band activity through the phase of the alpha oscillation may provide a mechanism that allows for the selective read out of relevant information (Jensen et al., 2012) (Fig. 2.1).

A similar mechanism involving theta (5-7 Hz) oscillations has been proposed to account for the maintenance of sequential information in working memory. According to this theoretical model, gamma oscillations are coupled to the phase of the theta rhythm, and this coupling is thought to provide a phase code for the serial order of memorized items (Lisman and Idiart, 1995). The hippocampus has been proposed to be involved in the formation of sequential memories and has been shown to be a key pacemaker of theta activity (Scoville and Milner, 2000; Kesner et al., 2002; Colgin and Moser, 2009), suggesting that theta-gamma coupling may be a specific mechanism for sequential information processing in

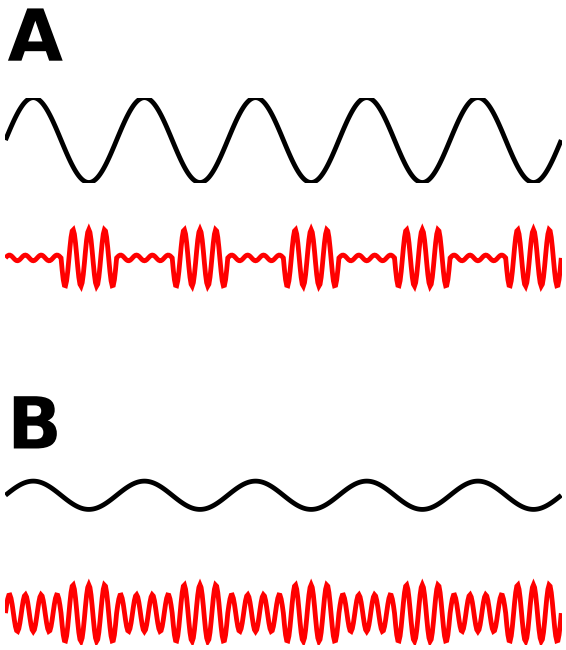

Figure 1.1: **Amplitude modulation of gamma-band activity through the phase of alpha oscillations.(A)**, The presence of strong rhythmic alpha activity will break the duty cycle of gamma oscillations into bouts of activity because only gamma oscillations which occur near the peak of excitability will be amplified. As a consequence, the amplitude of gamma-band activity will be strongly modulated by the phase of the alpha rhythm, producing a phase code for the gating of information. **(B)**, By contrast, weak alpha activity produces a continuous gamma signal, as the gamma cycle remains uninterrupted. Figure adapted from Jensen & Bonnefond (2012).

the hippocampus (Sirota et al., 2008; Colgin et al., 2009; Tort et al., 2009; Axmacher et al., 2010).

Accordingly, shifts in gamma phase-amplitude coupling from theta to alpha may reflect the recruitment of different functional networks (Voytek et al., 2010). So far, however, only few studies have attempted to examine the sources involved into the genesis of alpha-gamma coupling (Saalmann et al., 2012). The thalamus has been implicated in the gating of sensory information and the generation of alpha oscillations (Da Silva et al., 1973; Shuliak and Trush, 1983; Hughes and Crunelli, 2005; Lorincz et al., 2008, 2009; Saalmann and Kastner, 2009; Wang et al., 2010; Purushothaman et al., 2012; Vijayan and Kopell, 2012), suggesting that thalamo-cortical networks may utilize alpha-gamma coupling as a mechanism to selectively gate relevant or inhibit irrelevant information (Saalmann et al., 2012). However, direct evidence for such a relationship is so far lacking.

From a psychological perspective, the ability to gate relevant information and to inhibit distractors is strongly related with an individual's ability to remember information over a short period of time (Dempster, 1992). This ability is referred to as working memory (WM) (Baddeley and Hitch, 1974; Baddeley, 2003). WM-capacity has been estimated at 4-9 items (Miller, 1956; Cowan, 2001) which has been related to the ability to suppress irrelevant items (Vogel et al., 2005).

The available evidence suggests that oscillatory activity at alpha and gamma frequencies may provide the temporal structure to gate and maintain relevant information (Jensen et al., 2012), but the brain regions involved as well as the functional role of each frequency remain unclear.

Moreover, resistance to interference is a major factor in the development of cognitive abilities (Dempster, 1992; Harnishfeger and Bjorklund, 1994; Brainerd, 1995; Harnishfeger, 1995) and maturational changes in synchronous rhythmic activity at alpha and gamma frequencies have been related to the development of cognitive functions (Uhlhaas et al., 2009b; Werkle-Bergner et al., 2012). Thus, an important question is whether developmental changes in alpha and gamma band activity also account for age-related changes in distractor-inhibition and WM-capacity.

The present thesis addresses these questions in four chapters:

1. Neural Synchrony and the Development of Cortical Networks. Chapter three discusses the theoretical implications of late physiological and anatomical changes for the development of oscillatory activity. Specifically, this chapter highlights the importance of late developmental periods such as adolescence for the maturation of large-scale functional networks. Adolescence is accompanied by profound physiological and psychological changes, suggesting that the brain may undergo a structural and functional reorganization during this period of time. This hypothesis is supported by a growing body of evidence showing late structural and functional changes in cerebral networks which are correlated with the development of cognitive capacities. In addition, developmental changes in myelination and neurotransmission may greatly impact the precise timing of neuronal activity, suggesting that late developmental changes in oscillatory activity may provide important insights into the mechanisms underlying the development of functional networks associated with higher cognitive functions.

2. Gamma-band Activity in Prefrontal Cortex Codes for the Number of Relevant Items Maintained in Working Memory. Chapter four of this thesis presents the results of experiment one, which was designed to assess the frequency bands and functional networks which contribute to the selection and maintenance of relevant information. To address this question, MEG activity was recorded while healthy adult participants performed a delayed response task in which the amount of task-relevant and irrelevant information was manipulated.

The main outcome of this research showed enhanced alpha and gamma oscillations during the delay period. Importantly, alpha oscillations during the delay phase showed a similar modulation in the presence of task-relevant and irrelevant items, whereas gamma band oscillations were specifically modulated by the amount of behaviorally relevant information maintained in WM, suggesting a differential contribution of alpha and gamma oscillations towards the processing of relevant and irrelevant information during WM.

4. The Phase of Thalamic Alpha Activity Differentially Entrains Cortical Gamma-Band Activity: Evidence from Resting State MEG Recordings. Chapter five contains the results from experiment two, which examined the modulation of cortical gamma band oscillations by the phase of spontaneous alpha oscillations in different brain regions. Strong coupling was found between cortical alpha oscillations and cortical gamma-band activity in the occipital cortex. Because recent evidence suggests that the thalamus may coordinate cortical gamma-band activity through alpha synchronization (Saalmann et al., 2012), we performed a seed based analysis which revealed that cortical gamma-band activity was strongly modulated by the phase of thalamic alpha oscillations. This effect was found in parietal regions belonging to the default mode network and connected with higher order nuclei of the thalamus, supporting the hypothesis that alpha-gamma coupling may provide a mechanism to selectively gate cortical gamma-band oscillations.

5. Age Related Changes of MEG Alpha and Gamma-Band Activity Reflect the Late Maturation of Distractor-Inhibition during Working Memory Maintenance. Finally, in chapter six, late developmental changes in alpha and gamma band activity were investigated during WM and distractor-inhibition. The findings from experiment one and from experiment two both highlight the importance of alpha and gamma oscillations in large-scale functional networks for the selection and maintenance of relevant information. To investigate developmental changes of activity in both frequency bands in relationship to age related differences in behavioral performance, MEG activity was recored in a sample of participants aged between 12 and 24 years while they performed a similar version of the WM task employed in experiment one. The findings of this research show that young adolescents have a reduced WM capacity as compared to adult participants. This reduction in WM capacity in young adolescents was also associated with markedly decreased behavioral performances in the presence of distractors and with developmental changes in alpha and gamma band activity. Importantly, developmental changes in rhythmic activity at alpha and gamma frequencies were found only in the distractor

condition, further highlighting the importance of alpha and gamma oscillations during distractor inhibition and the selection of relevant information. The results from experiment three confirm the results from experiment one by showing that alpha and gamma oscillations differentially contribute to the maintenance of information in WM and provide important evidence for a functional relationship between the development of WM capacity, distractor-inhibition and rhythmic activity in the alpha and gamma frequency bands.

1.5 References

Adrian E (1950) The electrical activity of the mammalian olfactory bulb. Electroencephalogr Clin Neurophysiol 2:377–388.

Adrian E, Matthews B (1934) The Berger rhythm: Potential changes from the occipital lobe in man. Brain 57:356–385.

Ahlfors SP, Han J, Belliveau JW, Hämäläinen MS (2010) Sensitivity of MEG and EEG to source orientation. Brain Topogr 23:227–232.

Axmacher N, Henseler MM, Jensen O, Weinreich I, Elger CE, Fell J (2010) Cross-frequency coupling supports multi-item working memory in the human hippocampus. Proc Natl Acad Sci USA 107:3228–3233.

Baddeley A (2003) Working memory: looking back and looking forward. Nat Rev Neurosci 4:829–839.

Baddeley A, Hitch G (1974) Working memory. In: The psychology of learning and motivation (Bower G, ed), pp 47–89. New York: Academic Press.

Barlow HB (1972) Single units and sensation: a neuron doctrine for perceptual psychology? Perception 1:371–394.

Barlow HB (1985) The twelfth Bartlett memorial lecture: the role of single neurons in the psychology of perception. Q J Exp Psychol A 37:121–145.

Berger H (1929) Über das Elektroenkephalogramm des Menschen. Archiv für Psychiatrie und Nervenkrankheiten 87:527:570.

Bosman CA, Schoffelen J-M, Brunet N, Oostenveld R, Bastos AM, Womelsdorf T, Rubehn B, Stieglitz T, De Weerd P, Fries P (2012) Attentional stimulus selection through selective synchronization between monkey visual areas. Neuron 75:875–888.

Brainerd CJ (1995) 4 - Interference processes in memory development: The case of cognitive triage. In: Interference and Inhibition in Cognition (Frank N. Dempster and Charles J. Brainerd, eds), pp 105–139. San Diego: Academic Press.

Bressler SL, Freeman WJ (1980) Frequency analysis of olfactory system EEG in cat, rabbit, and rat. Electroencephalogr Clin Neurophysiol 50:19–24.

Busch NA, Dubois J, VanRullen R (2009) The phase of ongoing EEG oscillations predicts visual perception. J Neurosci 29:7869–7876.

Buzsáki G (2011) Rhythms of the Brain. Oxford University Press.

Buzsáki G, Draguhn A (2004) Neuronal oscillations in cortical networks. Science 304:1926–1929.

Buzsáki G, Wang X-J (2012) Mechanisms of gamma oscillations. Annu Rev Neurosci 35:203–225.

Buzsáki G, Watson BO (2012) Brain rhythms and neural syntax: implications for efficient coding of cognitive content and neuropsychiatric disease. Dialogues Clin Neurosci 14:345–367.

Cardin JA, Carlén M, Meletis K, Knoblich U, Zhang F, Deisseroth K, Tsai L-H, Moore CI (2009) Driving fast-spiking cells induces gamma rhythm and controls sensory responses. Nature 459:663–667.

Chorlian DB, Porjesz B, Begleiter H (2006) Amplitude modulation of gamma band oscillations at alpha frequency produced by photic driving. Int J Psychophysiol 61:262–278.

Colgin LL, Denninger T, Fyhn M, Hafting T, Bonnevie T, Jensen O, Moser M-B, Moser EI (2009) Frequency of gamma oscillations routes flow of information in the hippocampus. Nature 462:353–357.

Colgin LL, Moser EI (2009) Hippocampal theta rhythms follow the beat of their own drum. Nat Neurosci 12:1483–1484.

Cowan N (2001) The magical number 4 in short-term memory: a reconsideration of mental storage capacity. Behav Brain Sci 24:87–114; discussion 114–185.

Dan Y, Poo M-M (2004) Spike timing-dependent plasticity of neural circuits. Neuron 44:23–30.

Da Silva FH, Van Lierop TH, Schrijer CF, Van Leeuwen WS (1973) Organization of thalamic and cortical alpha rhythms: spectra and coherences. Electroencephalogr Clin Neurophysiol 35:627–639.

Dempster FN (1992) The rise and fall of the inhibitory mechanism: Toward a unified theory of cognitive development and aging. Developmental Review 12:45–75.

Dugué L, Marque P, VanRullen R (2011) The phase of ongoing oscillations mediates the causal relation between brain excitation and visual perception. J Neurosci 31:11889–11893.
Engel AK, König P, Gray CM, Singer W (1990) Stimulus-Dependent Neuronal Oscillations in Cat Visual Cortex: Inter-Columnar Interaction as Determined by Cross-Correlation Analysis. Eur J Neurosci 2:588–606.
Foster BL, Parvizi J (2012) Resting oscillations and cross-frequency coupling in the human posteromedial cortex. Neuroimage 60:384–391.
Fries P (2005) A mechanism for cognitive dynamics: neuronal communication through neuronal coherence. Trends Cogn Sci (Regul Ed) 9:474–480.
Fries P (2009) Neuronal gamma-band synchronization as a fundamental process in cortical computation. Annu Rev Neurosci 32:209–224.
Ghose GM, Maunsell J (1999) Specialized representations in visual cortex: a role for binding? Neuron 24:79–85, 111–125.
Gray CM, König P, Engel AK, Singer W (1989) Oscillatory responses in cat visual cortex exhibit inter-columnar synchronization which reflects global stimulus properties. Nature 338:334–337.
Gray CM, Singer W (1989) Stimulus-specific neuronal oscillations in orientation columns of cat visual cortex. Proc Natl Acad Sci USA 86:1698–1702.
Haegens S, Nácher V, Luna R, Romo R, Jensen O (2011) α-Oscillations in the monkey sensorimotor network influence discrimination performance by rhythmical inhibition of neuronal spiking. Proc Natl Acad Sci USA 108:19377–19382.
Haider B, McCormick DA (2009) Rapid Neocortical Dynamics: Cellular and Network Mechanisms. Neuron 62:171–189.
Hari R, Salmelin R (1997) Human cortical oscillations: a neuromagnetic view through the skull. Trends Neurosci 20:44–49.
Harnishfeger KK (1995) 6 - The development of cognitive inhibition: Theories, definitions, and research evidence. In: Interference and Inhibition in Cognition (Frank N. Dempster and Charles J. Brainerd, eds), pp 175–204. San Diego: Academic Press.
Harnishfeger KK, Bjorklund D (1994) A developmental perspective on individual differences in inhibition. Learning and Individual Differnces 6:331–355.
Herrmann CS, Munk MHJ, Engel AK (2004) Cognitive functions of gamma-band activity: memory match and utilization. Trends Cogn Sci (Regul Ed) 8:347–355.
Hubel DH, Livingstone MS (1987) Segregation of form, color, and stereopsis in primate area 18. J Neurosci 7:3378–3415.
Huerta PT, Lisman JE (1996) Low-frequency stimulation at the troughs of theta-oscillation induces long-term depression of previously potentiated CA1 synapses. J Neurophysiol 75:877–884.
Hughes SW, Crunelli V (2005) Thalamic mechanisms of EEG alpha rhythms and their pathological implications. Neuroscientist 11:357–372.
Ilmoniemi RJ (1993) Models of source currents in the brain. Brain Topogr 5:331–336.
Jensen O, Bonnefond M, VanRullen R (2012) An oscillatory mechanism for prioritizing salient unattended stimuli. Trends Cogn Sci (Regul Ed) 16:200–206.
Jensen O, Colgin LL (2007) Cross-frequency coupling between neuronal oscillations. Trends Cogn Sci (Regul Ed) 11:267–269.
Jensen O, Kaiser J, Lachaux J-P (2007) Human gamma-frequency oscillations associated with attention and memory. Trends Neurosci 30:317–324.
Jensen O, Mazaheri A (2010) Shaping functional architecture by oscillatory alpha activity: gating by inhibition. Front Hum Neurosci 4:186.
Kesner RP, Gilbert PE, Barua LA (2002) The role of the hippocampus in memory for the temporal order of a sequence of odors. Behav Neurosci 116:286–290.
Klimesch W, Sauseng P, Hanslmayr S (2007) EEG alpha oscillations: the inhibition-timing hypothesis. Brain Res Rev 53:63–88.
Kopell N, Ermentrout GB, Whittington MA, Traub RD (2000) Gamma rhythms and beta rhythms have different synchronization properties. Proc Natl Acad Sci USA 97:1867–1872.
Korte M, Kang H, Bonhoeffer T, Schuman E (1998) A role for BDNF in the late-phase of hippocampal long-term potentiation. Neuropharmacology 37:553–559.
Lisman JE, Idiart MA (1995) Storage of 7 +/- 2 short-term memories in oscillatory subcycles. Science 267:1512–1515.
Liu H, Tanaka N, Stufflebeam S, Ahlfors S, Hämäläinen M (2010) Functional Mapping with Simultaneous MEG and EEG. J Vis Exp.
Livingstone MS, Hubel DH (1984) Anatomy and physiology of a color system in the primate visual cortex. J Neurosci 4:309–356.
Lorincz ML, Crunelli V, Hughes SW (2008) Cellular dynamics of cholinergically induced alpha (8-13 Hz) rhythms in sensory thalamic nuclei in vitro. J Neurosci 28:660–671.
Lorincz ML, Kékesi KA, Juhász G, Crunelli V, Hughes SW (2009) Temporal framing of thalamic

relay-mode firing by phasic inhibition during the alpha rhythm. Neuron 63:683–696.
Luo Y, Vallano ML (1995) Arachidonic acid, but not sodium nitroprusside, stimulates presynaptic protein kinase C and phosphorylation of GAP-43 in rat hippocampal slices and synaptosomes. J Neurochem 64:1808–1818.
Mainen ZF, Sejnowski TJ (1995) Reliability of spike timing in neocortical neurons. Science 268:1503–1506.
Markram H, Lübke J, Frotscher M, Sakmann B (1997) Regulation of synaptic efficacy by coincidence of postsynaptic APs and EPSPs. Science 275:213–215.
Miller GA (1956) The magical number seven plus or minus two: some limits on our capacity for processing information. Psychol Rev 63:81–97.
Mu Y, Poo M-M (2006) Spike timing-dependent LTP/LTD mediates visual experience-dependent plasticity in a developing retinotectal system. Neuron 50:115–125.
Osipova D, Hermes D, Jensen O (2008) Gamma power is phase-locked to posterior alpha activity. PLoS ONE 3:e3990.
Purushothaman G, Marion R, Li K, Casagrande VA (2012) Gating and control of primary visual cortex by pulvinar. Nat Neurosci 15:905–912.
Quiroga RQ, Reddy L, Kreiman G, Koch C, Fried I (2005) Invariant visual representation by single neurons in the human brain. Nature 435:1102–1107.
Renault B, Garnero L (2004) L'imagerie fonctionenelle EEG-MEG: principes et applications. In: Imagerie cérébrale fonctionelle électrique et mangétique (Renault B, ed), pp 17–32. Paris: Lavoisier.
Saalmann YB, Kastner S (2009) Gain control in the visual thalamus during perception and cognition. Curr Opin Neurobiol 19:408–414.
Saalmann YB, Pinsk MA, Wang L, Li X, Kastner S (2012) The pulvinar regulates information transmission between cortical areas based on attention demands. Science 337:753–756.
Salinas E, Sejnowski TJ (2001) Correlated neuronal activity and the flow of neural information. Nat Rev Neurosci 2:539–550.
Salmelin R, Baillet S (2009) Electromagnetic brain imaging. Hum Brain Mapp 30:1753–1757.
Salmelin RH, Hämäläinen MS (1995) Dipole modelling of MEG rhythms in time and frequency domains. Brain Topogr 7:251–257.
Scheeringa R, Mazaheri A, Bojak I, Norris DG, Kleinschmidt A (2011) Modulation of visually evoked cortical FMRI responses by phase of ongoing occipital alpha oscillations. J Neurosci 31:3813–3820.
Schoffelen J-M, Oostenveld R, Fries P (2005) Neuronal Coherence as a Mechanism of Effective Corticospinal Interaction. Science 308:111–113.
Scoville WB, Milner B (2000) Loss of recent memory after bilateral hippocampal lesions. 1957. J Neuropsychiatry Clin Neurosci 12:103–113.
Sejnowski TJ, Paulsen O (2006) Network oscillations: emerging computational principles. J Neurosci 26:1673–1676.
Shuliak BA, Trush VD (1983) [Possible mechanism of the thalamic pacemaker of alpha-rhythm and fusiform activity]. Biofizika 28:686–692.
Singer W (1999) Neuronal synchrony: a versatile code for the definition of relations? Neuron 24:49–65, 111–125.
Sirota A, Montgomery S, Fujisawa S, Isomura Y, Zugaro M, Buzsáki G (2008) Entrainment of neocortical neurons and gamma oscillations by the hippocampal theta rhythm. Neuron 60:683–697.
Spaak E, Bonnefond M, Maier A, Leopold D., Jensen O (2012) Layer-specific entrainment of gamma-band neural activity by the alpha rhythm in monkey visual cortex. Current Biology.
Steriade M (2000) Corticothalamic resonance, states of vigilance and mentation. Neuroscience 101:243–276.
Tallon-Baudry, Bertrand (1999) Oscillatory gamma activity in humans and its role in object representation. Trends Cogn Sci (Regul Ed) 3:151–162.
Tort ABL, Komorowski RW, Manns JR, Kopell NJ, Eichenbaum H (2009) Theta-gamma coupling increases during the learning of item-context associations. Proc Natl Acad Sci USA 106:20942–20947.
Treisman A (1999) Solutions to the binding problem: progress through controversy and convergence. Neuron 24:105–110, 111–125.
Uhlhaas PJ, Pipa G, Lima B, Melloni L, Neuenschwander S, Nikolić D, Singer W (2009a) Neural synchrony in cortical networks: history, concept and current status. Front Integr Neurosci 3:17.
Uhlhaas PJ, Pipa G, Neuenschwander S, Wibral M, Singer W (2011) A new look at gamma? High-(>60 Hz) γ-band activity in cortical networks: function, mechanisms and impairment. Prog Biophys Mol Biol 105:14–28.
Uhlhaas PJ, Roux F, Rodriguez E, Rotarska-Jagiela A, Singer W (2010) Neural synchrony and the development of cortical networks. Trends in Cognitive Sciences 14:72–80.
Uhlhaas PJ, Roux F, Singer W, Haenschel C, Sireteanu R, Rodriguez E (2009b) The development of neural synchrony reflects late maturation and restructuring of functional networks in humans. Proc Natl Acad Sci U S A 106:9866–9871.
Varela F, Lachaux JP, Rodriguez E, Martinerie J (2001) The brainweb: phase synchronization and

large-scale integration. Nat Rev Neurosci 2:229–239.
Vijayan S, Kopell NJ (2012) Thalamic model of awake alpha oscillations and implications for stimulus processing. Proc Natl Acad Sci USA 109:18553–18558.
Vogel EK, McCollough AW, Machizawa MG (2005) Neural measures reveal individual differences in controlling access to working memory. Nature 438:500–503.
Von Stein A, Sarnthein J (2000) Different frequencies for different scales of cortical integration: from local gamma to long range alpha/theta synchronization. Int J Psychophysiol 38:301–313.
Voytek B, Canolty RT, Shestyuk A, Crone NE, Parvizi J, Knight RT (2010) Shifts in gamma phase-amplitude coupling frequency from theta to alpha over posterior cortex during visual tasks. Front Hum Neurosci 4:191.
Wang Q, Webber RM, Stanley GB (2010) Thalamic synchrony and the adaptive gating of information flow to cortex. Nat Neurosci 13:1534–1541.
Werkle-Bergner M, Freunberger R, Sander MC, Lindenberger U, Klimesch W (2012) Inter-individual performance differences in younger and older adults differentially relate to amplitude modulations and phase stability of oscillations controlling working memory contents. Neuroimage 60:71–82.
Wespatat V, Tennigkeit F, Singer W (2004) Phase sensitivity of synaptic modifications in oscillating cells of rat visual cortex. J Neurosci 24:9067–9075.
Womelsdorf T, Schoffelen J-M, Oostenveld R, Singer W, Desimone R, Engel AK, Fries P (2007) Modulation of neuronal interactions through neuronal synchronization. Science 316:1609–1612.
Yanagisawa T, Yamashita O, Hirata M, Kishima H, Saitoh Y, Goto T, Yoshimine T, Kamitani Y (2012) Regulation of motor representation by phase-amplitude coupling in the sensorimotor cortex. J Neurosci 32:15467–15475.

2

Neural Synchrony and the Development of Cortical Networks

As published in: Peter J. Uhlhaas, Frederic Roux, Eugenio Rodriguez, Anna Rotarska-Jagiela and Wolf Singer (2009): Neural Synchrony and the Development of Cortical Networks. Trends in Cognitive Sciences, 14 (2): 72-80.

2.1 Abstract

Recent data indicate that the synchronisation of oscil- latory activity is relevant for the development of cortical circuits as demonstrated by the involvement of neural synchrony in synaptic plasticity and changes in the frequency and synchronisation of neural oscillations during development. Analyses of resting-state and task-related neural synchrony indicate that gamma- oscillations emerge during early childhood and precise temporal coordination through neural synchrony con- tinues to mature until early adulthood. The late matu- ration of neural synchrony is compatible with changes in the myelination of cortico-cortical connections and with late development of GABAergic neurotransmission. These findings highlight the role of neural synchrony for normal brain development as well as its potential importance for understanding neurodevelopmental disorders, such as autism spectrum disorders (ASDs) and schizophrenia.

2.2 Function and mechanisms of neural synchrony in cortical networks

Synchronised neural oscillations in the low (delta, theta and alpha) and high (beta and gamma) frequency are a fundamental mechanism for enabling coordinated activity in the normally functioning brain (Box 1) [1,2]. A large body of evidence from invasive electrophysiology in non-human primates and electro- and magnetoencephalographic (EEG/MEG) recordings (see Glossary) in humans that have tested the amplitude and synchrony of neural oscillations have demonstrated close relations between synchronous oscillatory activity and a variety of cognitive and percep- tual functions (Box 1). Although the relationship between neural synchrony and cognitive and perceptual processes has received widespread attention, a less explored aspect is the possible role of neural synchrony in the development of cortical networks. Oscillations and the generation of synchronised neuronal activity play a crucial role in the activity-dependent self-organisation of developing networks [3–6] (Figure 3.1).

The development and maturation of cortical networks critically depends on neuronal activity, whereby synchronised oscillations play an important role in the stabilization and pruning of connections [4]. For example, in spike-timing dependent plasticity, pre- and postsynaptic spiking within a critical window of tens of milliseconds has profound functional implications [7]. Stimulation at the depolarizing peak of the theta cycle in the hippocampus favours long-term potentiation (LTP), whereas stimulation in the trough causes depotentiation (LTD) [8]. The same relationship holds for oscillations in the beta- and gamma-frequency range [9], indicating that oscillations provide a temporal structure that allows for precise alignment of the amplitude and temporal relations of presynaptic and postsynaptic activation that determine whether a strengthening or weakening of synaptic contacts occurs. Accordingly, the extensive modifications of synaptic con- nections during the development of cortical networks are critically dependent upon precise timing of neural activity.

Synchronisation of oscillatory activity is furthermore an important index of the maturity and efficiency of cortical networks. Neural oscillations are an energy efficient mech- anism for the coordination of distributed neural activity [1] that are functionally related to anatomical and physiologi- cal parameters that undergo significant changes during development. Thus, synchronisation of oscillatory activity in the beta- and gamma-frequency range is dependent upon cortico-cortical connections that reciprocally link cells situated in the same

Figure 1.

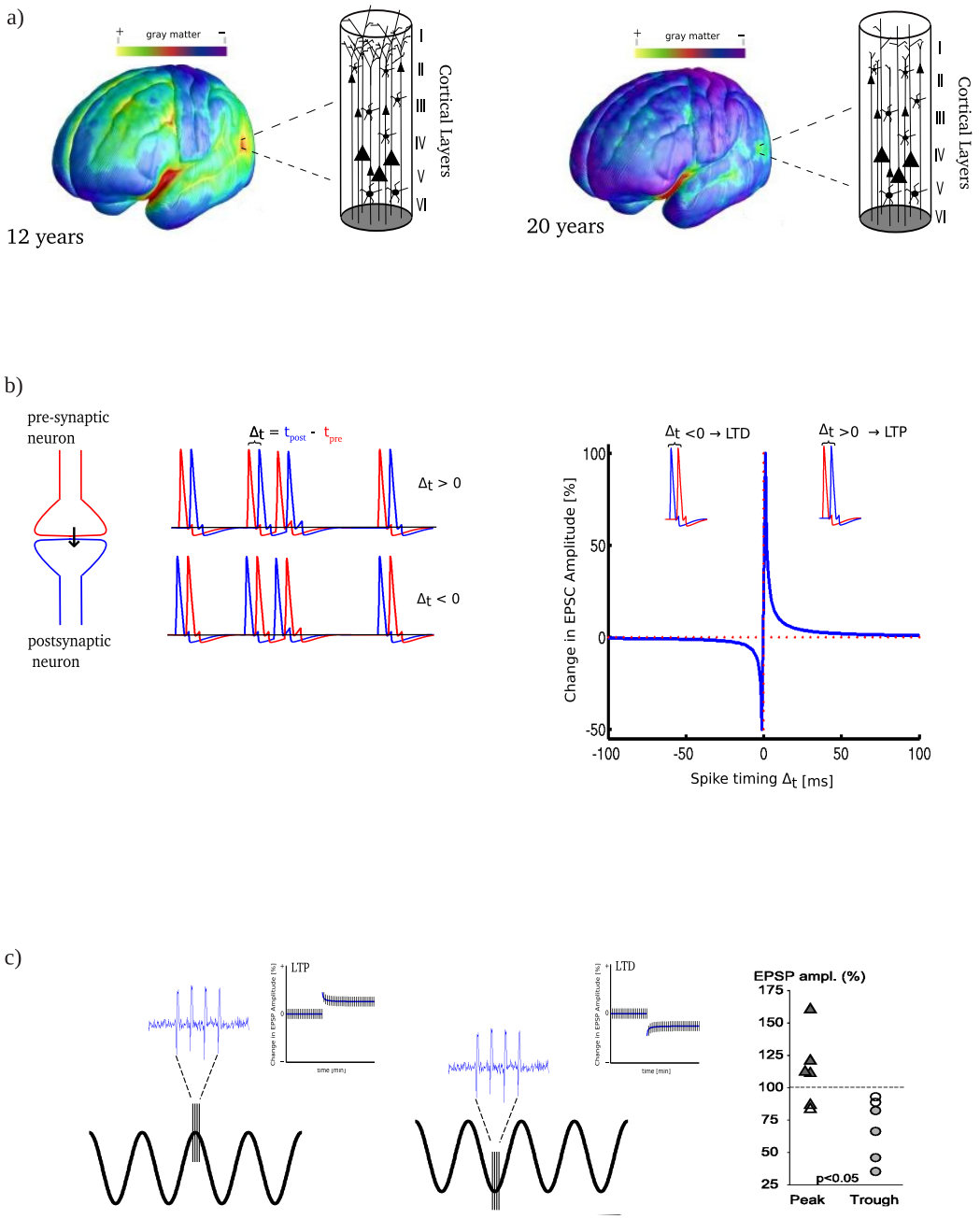

Figure 2.1: **Synchrony, Oscillations and Network Development. (a)** Development of cortical networks. Left panel: Cortical surface representation of grey matter (left) at age 12 (n = 13) and at age 20 (n = 13) (right panel) (adapted from [66]). The colour scale indicates variations in cortical volume and highlight the reduction of grey matter during the adolescent period. A schematic display of a cortical column shows a relative abundance of dendritic arborizations from pyramidal cells in the adolescent brain (left) compared to the adult cortex (right). This pruning process could underlie the observed reductions of grey matter in MR-studies. **(b)** Spike timing dependent plasticity. Left panel: The difference (Dt) at which a pre- (red) and postsynaptic (blue) spike occur is a measure of the temporal order between these spikes. This difference is positive whenever a presynaptic spike precedes a postsynaptic spike. Right panel: Effects of spike timing on synaptic plasticity. If the presynaptic neuron fires prior to the postsynaptic neuron (Dt $>$ 0), the EPSP of the postsynaptic cell is potentiated (long-term potentiation, LTP). However, if the postsynaptic cell fires first (Dt $<$ 0), this effect is reversed and the EPSP of the postsynaptic cell undergoes depression (long-term depression, LTD) (modified and adapted from [67]). **(c)** hase-sensitivity of synaptic modifications. Left panel: Simulated local field potential (LFP)-oscillations (black line) and a burst of high-frequency stimulation (blue line) occurring at the peak of oscillatory cycle. This results in a potentiation of the synaptic potential (LTP) as indicated by the increase in the membrane potential. Middle panel: Stimulation at the through of the oscillation cycle results in a depression of the synaptic membrane potential (LTD). Right panel: Experimental evidence for the phase-sensitivity of synaptic modifications during sustained high-frequency oscillations (40 Hz) in rats. EPSP amplitudes of pyramidal cells in visual cortex are shown during extracellular stimulation. A strong increase in the amplitude of the EPSP is observed when stimulation at the oscillation peak occurs, whereas stimulation at the though decreases the EPSP amplitude (adapted from [9]).

cortical area, across different areas or even across the two hemispheres [10,11]. Furthermore, GABAergic interneurons play a pivotal role in establishing neural synchrony in local circuits as indicated by research that shows that a single GABAergic neuron might be sufficient to synchronise the firing of a large population of pyramidal neurons [12] and the duration of the inhibi- tory postsynpatic potential (IPSP) can determine the domi- nant frequency of oscillations within a network [13]. In addition to chemical synaptic transmission, direct electro- tonic coupling through gap-junctions between inhibitory neurons also contributes to the temporal patterning of population activity and, in particular, to the precise syn- chronisation of oscillatory activity [14,15]. Gap-junctions are functionally important during early brain development [16]. Postnatally, changes in both GABAergic neurotransmission [17,18] and the myelination of long axonal tracts [19,20] occur. Thus, changes can be expected in the frequency and amplitude of oscillation as well as in the precision with which rhythmic activity can be synchronised over longer distances at different developmental stages.

In the following review, we will provide evidence for this hypothesis by summarising the literature on resting state activity as well as during cognitive tasks that indicate important changes in parameters of neural synchrony during childhood and adolescence. Although high-fre- quency activity emerges during early development, cortical networks fully sustain precise synchrony only during the transition from adolescence to adulthood, which is compa- tible with concurrent changes in anatomy and physiology.

2.3 Resting-state oscillations: development of frequency, amplitude and synchronisation

Changes in the frequency spectrum during development were first described by Berger and subsequent studies have confirmed pronounced changes in the amplitude and distribution of oscillations in different frequency bands [for a review see 21]. In adults, resting-state activity is characterised by prominent alpha-oscillations over occipi- tal electrodes whereas low (delta, theta) and high (beta, gamma) frequencies are attenuated. During childhood and adolescence, however, there is a reduction in the amplitude of oscillations over a wide frequency range that is parti- cularly pronounced for delta and theta activity [22] (Figure 3.2a). These development changes occur more rapidly in posterior than in frontal regions [21] and follow a linear trajectory until age 30 [22]. When the relative magnitude is taken into account, oscillations in the alpha- and beta-range increase whereas activity in lower fre- quency decreases with age.

Changes in resting-state activity during adolescence can also be observed during sleep. Campbell and Feinberg [23] analysed delta and theta activity during non-rapid eye movement sleep (non-REM) in a sample of 9- and 12-year-old cohort twice yearly over a 5-year period and observed profound changes in slow frequency oscillations. The power of delta oscillations did not change between 9 and 11 years but then showed a reduction by over 60 per cent until 16.5 years. Similar results were obtained for oscillations in the theta band. According to the authors, the decrease in the power of slow-frequency oscillations reflect synaptic pruning and are independent of pubertal stages.

In contrast to the reduction of slow-wave activity, resting-state gamma band oscillations increase during development. They can be detected around 16 months and continue to increase in amplitude until age 5 [24]. Correlation between the amplitude over frontal electrodes and development of language and cognitive skills indicate a functional role of early gamma band activity in the maturation of cognitive functions [25].

Changes in the amplitude of oscillations are accom- panied by developmental trends in the synchrony of oscil- lations. Thatcher et al. [26] tested the hypothesis that white matter maturation involves the differential devel- opment of short- and long-range fibre connections and is reflected in changes in the coherence of beta-oscillations. EEG coherence between 2 months and 16 years of age was characterised by an increase in coherence at shorter dis- tances ($<$ 6 cm) whereas long-range coherence ($>$ 24 cm) did not vary with age. Pronounced increases in long-range coherence in the alpha band were reported by Srinivasan et al. [27]. The authors tested EEG-coherence in 20 children (6–11 years) and 23 adults (18–23 years). Reduced power over anterior electrodes in children was accompanied by reduced coherence between anterior and posterior electro- des. These findings indicate that in addition to an increase in fast rhythmic activity, the maturation of oscillations during childhood and adolescence is accompanied by an increase in precision with which oscillations are synchronised indicat- ing a continued maturation in the spatial and functional organisation of cortical networks.

2.4 Maturation of Steady-State Responses

Steady-state responses (SSR) represent a basic neural response to a temporally modulated stimulus to which it is synchronised in frequency and phase. Thus, steady-state paradigms are ideally suited to probe the ability of neuronal

networks to generate and maintain oscillatory activity in different frequency bands. Previous research had shown that the power of the auditory SSR (ASSR) is largest in the 40 Hz range [28], indicating a natural reson- ance frequency of cortical networks. Developmental studies have so far focused on the ASSR. Rojas et al. [29] examined the 40 Hz ASSR in MEG data in 69 participants in the age range from 5 to 52 years. Regression analyses showed a significant effect for age indicating that the amplitude of the 40 Hz ASSR between 200 and 500 ms increased significantly during develop- ment. Specifically, a marked increase in 40 Hz power was observed during childhood and adolescence and seemed to reach a plateau during early adulthood. The protracted maturation of the ASSR was confirmed in a recent study by Poulsen et al. [30] (Figure 3.2b).
Sixty- five participants aged 10 were tested with EEG in a longitudinal study that involved a follow up after 18 months. Comparison with an adult group revealed a marked reduction of the 40 Hz ASSR in children relative to adult participants. In addition, to an overall reduction of the amplitude of the ASSR, adults were also characterised by a reduced variability and higher peak frequencies than children. Similar differences were also found between 10 and 11.5-year-old children. Analyses of developmental changes of the source waveforms indicated that adults had significantly higher source power in the left temporal cortex whereas no difference was found for activity in the right temporal source nor in the brainstem.

2.5 Development of task-related oscillations during motor, cognitive and perceptual processes

Csibra et al. [31] measured gamma band responses in EEG data in 6- and 8-months-old infants during the perception of Kanisza squares that require the binding of contour elements into a coherent object representation. Based on prior behavioural studies that showed that infants up to 6 months of age are unable to perceive Kanisza figures, the authors hypothesised that perceptual binding in 8-month- old infants is related to the emergence of gamma band oscillations. This was supported by an induced oscillatory response between 240 and 320 ms over frontal electrodes that was not present in the younger group, indicating that the emergence of gamma band oscillations during infancy is correlated with the maturation of perceptual functions.

Further studies have demonstrated continued matu- ration of neural synchrony during visual processing until adulthood. Werkle-Bergner et al. [32] tested the amplitude and phase-stability of evoked gamma band oscillations during the

Figure 2.

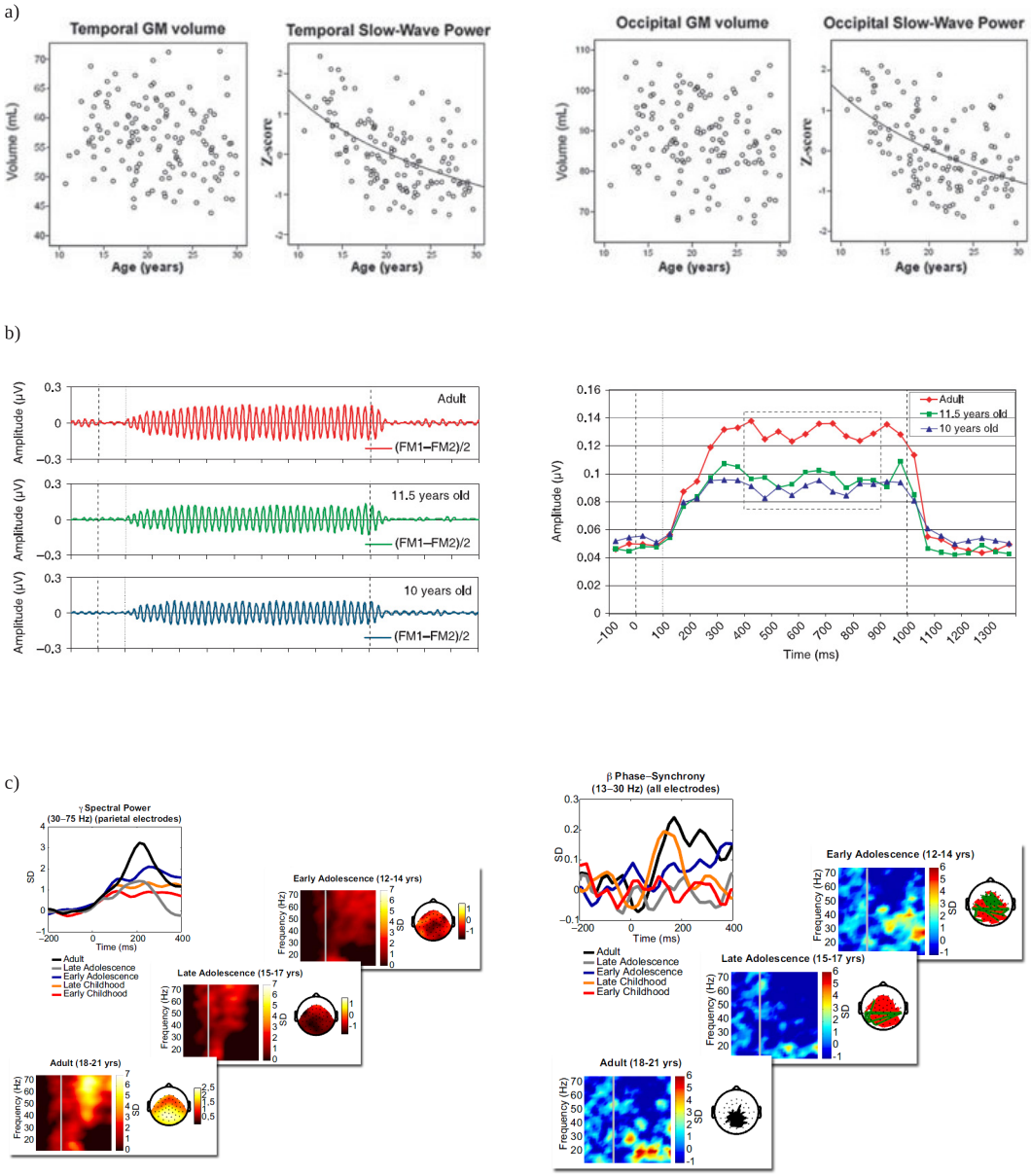

Figure 2.2: **Maturation of Neural Synchrony During the Development of Cortical Networks. (a)** Development of resting state activity in the 0.5–7.5 Hz frequency range in a sample of children, adolescent and adult participants (n = 130) (10–30 years) over temporal and occipital electrodes. The amplitude of delta and theta oscillations decreases over the course of adolescence and early adulthood and is accompanied by reductions in grey matter volume. **(b)** Late maturation of auditory steady state responses. Left panel: Average-referenced, grand-average 40-Hz auditory steady state response (ASSR) at electrode Cz, 30–50-Hz band-pass filtered, for adults (red), children at 10 years of age (blue) and 11.5 years of age (green). Dashed lines indicate time of stimulus onset and offset; dotted lines indicate onset of frequency modulation. Right panel: Root mean square amplitude of ASSRs in 50-ms bins. Data from individual subjects within the time window indicated by the boxed area were subjected to subsequent statistical analyses. Independent-sample t-tests revealed that the amplitude of the 40-Hz ASSR was significantly larger in adults than the children at both 10 and 11.5 years of age (adapted from [30]). **(c)** Development of task-related neural synchrony. Left panel: Comparison of spectral power of oscillations in the 30–75 Hz range across all electrodes between 100 and 300 ms during the presentation of Mooney faces at different ages and time-frequency maps (x-axis: time; y-axis: normalised spectral power in standard deviations (SD)) for early adolescent, late adolescent and adult participants. The data show that gamma oscillations increase significantly during the transition from adolescence to adulthood. Right panel: Comparison of phase-synchrony in the 13–30 Hz frequency range for all electrode pairs between 100–300 ms at different ages (top left panel) and phase synchrony charts of oscillations in the beta and gamma band averaged across all electrodes (x-axis: time; y-axis: normalised phase-synchrony in standard deviations (SD)) for early adolescent, late adolescent and adult participants (adapted from [33]).

perception of squares and circles in children (10–12 years), young adults (20–26 years) and older adults (70–76 years). Evoked oscillations in children were significantly reduced between 30 and 148 Hz over occipital elec- trodes relative to adults. In addition, gamma band activity in children was not modulated by the size of the stimulus as in adult and older participants. Participants in the 70–76 years age range, although displaying a similar degree of phase-locking, were characterised by reduced amplitudes of gamma band oscillations relative to younger adults during the perception of large stimuli.

The development of induced oscillations and their syn- chronisation was examined by Uhlhaas et al. [33] in a study that investigated children's, adolescent participants' and young adults' perception of Mooney faces (Figure 3.2c). In adult participants, perceptual organisation of upright Mooney faces was associated with prominent gamma band oscillations over parietal electrodes as well as long-range synchronisation in the theta and beta band. During development, profound changes in these parameters occurred that correlated with improved detection rates and reaction times. In particular, neural synchrony in the beta and gamma band increased until early adolescence (12–14 years) that was followed by a reduction in phase-synchro- nisation and amplitude of high-frequency oscillations during late adolescence (15–17 years). In 18–21 year olds, high-frequency oscillations showed a significant increase relative to late adolescent participants that was accom- panied by a reorganisation in the topography of phase- synchrony patterns in the beta band as well as by an increase in theta phase-synchrony between frontal and parietal electrodes. Accordingly, the development of induced oscillations and their synchronisation from late adolescence to early adulthood reflect a critical develop- mental period that is associated with a rearrangement of functional networks and with an increase of the temporal precision and spatial focusing of neuronal interactions.

Changes in neural synchrony have also been demon- strated in auditory processing during development. Muller et al. [34] assessed differences in oscillatory activity between 0 and 12 Hz in young children (9–11 years), older children (11–13 years), young adults (18–25 years) and older adults (64–75 years) during an auditory oddball task. Differences in the synchronisation and amplitude of oscillations in EEG data were most prominent for comparisons between chil- dren and young adults and for the processing of attended and deviant stimuli. Children were characterised by reduced synchronisation in local circuits over fronto-central electrodes at delta and theta frequencies as well as by reduced long-range synchronisation. Reduced local and long-range synchronisation was accompanied, however, by a relative increase in the power of

evoked and induced oscillations in children in the same frequencies, indicating that, as development progresses, low frequency activity is characterised by a shift to more precisely synchronised oscillations during adolescence. Similar results were reported by Yordanova et al. in the alpha band [35].

Changes in neural synchrony during development are also present in the motor system in which beta band oscillations are associated with the preparation and execu- tion of motor commands [36]. Synchrony of spinal inputs to motorneurons can be investigated by measuring the cov- ariation of signals from electromygraphic (EMG) record- ings over abductor muscles. Farmer et al. [37] analysed the coherence of EMG-signals in the 1 to 45 Hz frequency range during development in a sample of 50 participants (4–59 years). Pronounced developmental changes in beta band coherence were found between 7–9 and 12–14 years, with adolescent participants showing elevated levels of beta band coherence relative to children.

In addition to the increase in the synchrony of EMG signals, there is evidence that long-range synchronisation of oscillations between the primary motor cortex and muscles undergoes significant changes during develop- ment. James et al. [38] examined EEG recordings over primary motor cortex and EMG data from the contralateral wrist extensor muscle in a sample of 48 participants (0–58 years). In the youngest age groups (0–3 and 4–10 years) coherence values between EEG and EMG signals were randomly distributed across different frequencies indicat- ing that the drive from corticospinal pathways to motor-neurons is not oscillatory. By contrast, significant coherence values were found in adolescent participants between 12 and 17 years that showed, however, a less pronounced clustering in the beta band than in adult participants. Accordingly, these findings indicate that coherence between motor cortex and muscles increases during adolescence and is accompanied by a reduction in variance of frequencies at which such interactions occur.

2.6 Neural synchrony during development: relationship to anatomy and physiology

Our review highlights ongoing modifications of cortical circuits during childhood and adolescence that are reflected in the frequency and synchronisation of oscillatory activity. Following the emergence of gamma band oscillations during infancy [24,25], continued development of neural synchrony is observed whereby oscillations shift to higher frequencies and synchronisation becomes more precise

[29,30,33,34,38]. One fact highlighted in the cur- rent review is that this development is not complete until early adulthood and that neural synchrony continues to mature throughout the adolescent period that represents a critical phase of brain maturation. However, several issues remain to be addressed for future research (Box 2).

The maturation of neural synchrony during adolescence is compatible with the development of cognitive functions during this period that depend on neural synchrony, such as working memory and executive processes [39] as well as with concurrent changes in anatomy and physiology [40] (Figure 3.3).
This is supported by several studies showing that the myelination of long axonal fibres increases during adolescence and results in enhanced long-range connectivity.

Specifically, late development of gamma band oscillations is compatible with recent data indicating important changes in the GABAergic neurotransmission during adolescence. Hashimoto et al. [17] (Figure 3.3c) showed a predominance of GABA a2 subunits in the monkey dorsolateral prefrontal cortex (DLPFC) during early development whereas in adult animals a1 subunits are more expressed. This was accompanied by marked changes in the kinetics of GABA transmission, including a significant reduction in the duration of miniature IPSPs in pyramidal neurons. The shift in a subunit expression could provide a direct correlate of the observed increase in both amplitude and frequency of gamma band oscillations during adolescence because a1 subunits predominate at synapses of parvalbumin (PV) -positive basket cells (BCs) [41] that are crucially involved in the generation of gamma band oscillations [42].

The decrease in the slow-wave oscillations (delta, theta) has been related to synapting pruning [43]. According to this view, the higher number of synapses during childhood could explain the excess of delta and theta oscillations as well as the increase in metabolic rate that then become reduced during adolescence leading to reduced slow- activity and decreased energy consumption.

In addition to the changes in the amplitude of oscillations, changes in the precision of synchrony have been observed that can be related to continued anatomical changes. The development of white matter that continues until early adulthood [19,44] (Figure 3.3a) probably contributes to the maturation of long-range synchronisation between cortical regions by increasing the precision and frequency with which neural oscillations can be propagated (Figure 3.3b).

Figure 3.

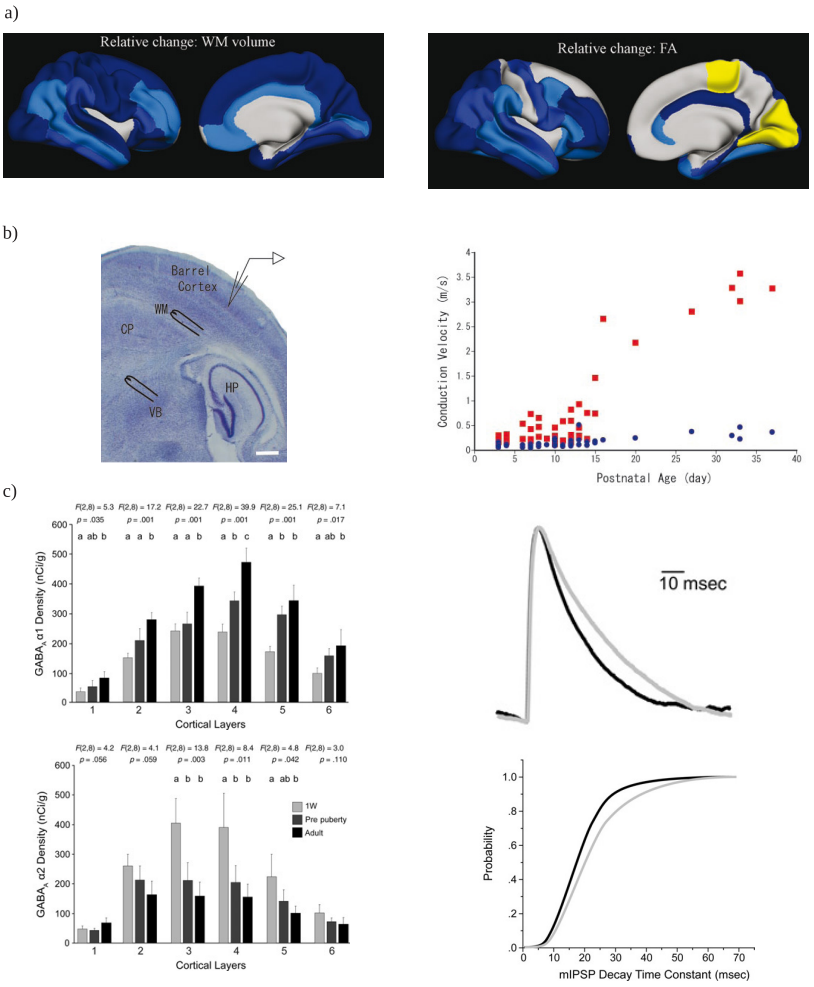

Figure 2.3: **Changes in Physiology and Anatomy During Adolescence (a)** Relative magnitude of developmental changes over the age span from 8 to 30 years in white matter. WM volume (left panel) and Fractional Anistropy (FA) (right panel) are colour coded and projected onto the surface of a semi-inflated average template brain. Diffusion measures are derived from voxels in underlying WM regions that overlapped with major tracts. Increases in volume of 15% or more were observed in most regions over the age span studied. The largest relative increase was observed for deep WM, which increased by 58% from 8 to 30 years. For FA, there were increases of 20% or more in regions on the lateral side of the occipital, parietal and frontal lobes, as well as in the cingulum, the parahippocampus, and the inferior temporal lobe. There were also moderate increases medially in the parietal and occipital lobes (adapted from [68]). **(b)** The relationship between myelination and conduction velocity (CV). Left panel: A photomicrograph of a thalamocortical slice, Nissl stained, representing the experimental procedure. Stimulation and recording sites are schematically illustrated. HP, hippocampus; CP, caudate putamen (Bar, 500 mm). Right panel: The CV of two portions of thalamocortical axons, calculated by the latencies and distances between the stimulated ventrobasal nucleus of the thalamus and white matter (CV VB-WM). CV VB-WM (red squares) was calculated from the distance between VB and WM divided by the latency difference between VB and WM stimulation. CV WM (blue circles) was obtained by the simple calculation using distance between stimulated (WM) and recorded sites, divided by the latency evoked by WM stimulation. As can be seen, both CVWM and CVVB-WM increase strongly with age extending into postnatal week 5 (adapted from [44]).
(c) Cortical layer comparisons of gamma-aminobutyric acid (GABA) A receptor-subunit a1 and in 1-week old, prepuberty, and adult groups of monkeys. Left panel: The means (SD) of GABA A receptor a 1 subunit expression levels in each age group were plotted across cortical layers. Layers 2–3 showed a prominent increase during adolescence, whereas layer 5 showed a significant increase in the preadolescent period. Right panel: Cumulative probability distribution curves of the mIPSP decay time constant in prepubertal (grey) and postpubertal (black) animals. The left shift of the curve from prepubertal to postpubertal animals indicates a higher fraction of shorter mIPSPs in postpubertal animals compared with prepubertal animals. Bar graph summarising the differences between age groups (Student's t test, *p = 0.05, n = 11 cells for each group). Because the decay time of IPSPs is a critical factor for the dominant frequency of oscillations within a network [13], these data together with the changes in a1 subunit expression provide one mechanism for the late maturation of high-frequency oscillations in EEG-data [as reported in 33] (adapted from [17]).

This is supported by several studies showing that the mye- lination of long axonal fibres increases during adolescence and results in enhanced long-range connectivity.

The data on the development of high-frequency oscil- lations and their synchronisation during adolescence are furthermore consistent with and extend findings on age- related changes in fMRI-activity patterns in a variety of cognitive tasks [45] and during the resting-state [46]. These studies revealed a developmental pattern whereby brain areas crucial for task performance become increas- ingly activated [47]. Activation of frontal and parietal regions was found to be more prominent and focused in adult participants than in children and adolescents during tasks involving working memory, executive controls and visual processing [48–50]. As the amplitude of the BOLD- signal is closely and positively correlated with the entrain- ment of neurons into synchronised gamma band oscil- lations [51], the fMRI data are fully compatible with the conclusions drawn from the present review that the ability of cortical networks to engage in precisely synchronised high-frequency oscillations increases during development and is a hallmark of maturity.

2.7 Neural Synchrony during Development: Implications for Psychopathology

In addition to the role of neural synchrony during normal brain maturation, the reviewed data have also important implications for the understanding of neuropsychiatric disorders, such as autism spectrum disorders (ASDs) and schizophrenia, which are associated with abnormal neural synchrony and aberrant neurodevelopment [52,53]. Considering the important role of neural synchrony in the shaping of cortical circuits at different developmental periods, we hypothesise that in ASDs abnormal brain maturation during early prenatal and postnatal periods results in cortical circuits that are unable to support the expression of high-frequency oscillations during infancy. These impaired oscillations might in turn reduce the temporal precision of coordinated firing patterns and thereby disturb activity-dependent circuit selection during further development. In schizophrenia, by contrast, clinical symptoms manifest typically during the transition from late adolescence to adulthood. As high-frequency oscillations and their synchronisation increase strongly during late adolescence and are associated with a reorganisation of cortical networks, we propose that in schizophrenia cortical circuits are unable to support the neural coding regime that emerges during late adolescence that relies on temporally more precise and spatially more

focused synchronisation patterns. This then leads to a breakdown of coordinated neural activity and the emergence of psychosis and cognitive dysfunctions.

2.8 Concluding Remarks

We have reviewed evidence on developmental changes in neural synchrony during childhood and adolescence that highlights the relationship between brain maturation and changes in the frequency, amplitude and synchronisation of neural oscillations. These data indicate that, in addition to providing a mechanism for the coordination of distrib- uted neural responses that underlies cognitive and percep- tual functions, neural synchrony is closely related to the development of cortical circuits. This is indicated by the relationship between the emergence of specific patterns of oscillatory activity and certain cognitive functions and by the correlation between the appearance of certain brain disorders at different developmental periods and electro- graphic signs of abnormal temporal coordination. Accord- ingly, such data support the view that neural synchrony is not epiphenomenal but plays a role in the functions of cortical networks. Future research should further address the role of neural synchrony during brain development by directly investigating relationships with the underlying anatomical and physiological changes as well as by using novel techniques that allow a more precise characteris- ation of development changes in neural synchrony.

2.9 Questions for Future Research

- What is the relationship between changes in hormone levels and the maturation of neural synchrony in cortical networks during adolescence?

- Are there sex differences in the maturation of neural synchrony during adolescence?

- During adolescence developmental changes in neural synchrony exceed those reflected in cognitive parameters. What is the precise relationship to cognitive development?

- What is the adaptive function of late brain maturation reflected by electrographic variables?

- The strength of oscillations and precision of synchrony increases until adulthood. Are there changes in neural synchrony during old age? If so, are they related to the emergence of cognitive deficits?

- Is there a relationship between the development of neural synchrony and changes in event-related potentials (ERPs)?

2.10 Glossary

Neural synchrony can be measured non-invasively with Electro and - Magentoencephalography (EEG/MEG) that sample ongoing electrical brain activity, which oscillates at various frequencies, through electrodes or sensors placed over the whole scalp.

Time-frequency analysis: The first step in order to measure amplitude and synchrony of oscillations in EEG and MEG data is the transformation of the electrophysiological signal into the frequency domain. This can be achieved by several time-frequency techniques [for a review of different methods see 63]. These methods involve Fourier analysis which describes the decomposition of a time series into sinusoidal functions and thereby allows the estimation of the signal at a given frequency.

Evoked vs. Induced Oscillations: Amplitude measures of oscillations can be further differentiated into evoked and induced components. Evoked oscillations show a constant phase and latency relationship to the onset of an external event and therefore can be recovered from the average evoked potentials. Typically, evoked oscillations occur with a latency of 50-150 ms. In contrast, induced oscillations are time not locked to the onset of a stimulus and occur with a temporal jitter across trials. For the extraction of induced oscillations, analysis needs to be performed on a single-trial basis because averaging across trials would cancel any oscillatory patterns.

Neural Synchrony in EEG/MEG Data: One way to estimate the synchrony of oscillations in EEG/MEG data is the analysis of phase relationships. Phase relationships can be examined by testing the stability of phases across trials (phase-locking) over a single electrode or between pairs of electrodes [64]. These two approaches yield estimates of the precision of local and long-range synchrony, respectively. Importantly, measures of phase-locking provide estimates of synchrony independent of the amplitude of oscillations. This is in contrast to measures of coherence where phase and amplitude are intertwined.

2.11 Acknowledgements

This work was supported by the Max Planck Society and the BMBF (Grant: 01GWS055) (P.J. Uhlhaas, W. Singer). ER was supported by the Hertie-Stiftung through the Frankfurt Institute of Advanced Studies and through grant FONDECYT 1070846 and a joint collaboration grant CONICYT/DAAD.

2.12 References

1 Buzsaki, G. and Draguhn, A. (2004) Neuronal oscillations in cortical networks. Science 304, 1926–1929
2 Fries, P. (2009) Neuronal gamma-band synchronization as a fundamental process in cortical computation. Annu. Rev. Neurosci. 32, 209–224
3 Singer, W. (1995) Development and plasticity of cortical processing architectures. Science 270, 758–764
4 Hebb, D.O. (1949) The organization of behavior: A neuropsychological theory, Wiley
5 Ben-Ari, Y. (2001) Developing networks play a similar melody. Trends Neurosci. 24, 353–360
6 Khazipov, R. and Luhmann, H.J. (2006) Early patterns of electrical activity in the developing cerebral cortex of humans and rodents. Trends Neurosci. 29, 414–418
7 Markram, H. et al. (1997) Regulation of synaptic efficacy by coincidence of postsynaptic APs and EPSPs. Science 275, 213–215
8 Huerta, P.T. and Lisman, J.E. (1993) Heightened synaptic plasticity of hippocampal CA1 neurons during a cholinergically induced rhythmic state. Nature 364, 723–725
9 Wespatat, V. et al. (2004) Phase sensitivity of synaptic modifications in oscillating cells of rat visual cortex. J. Neurosci. 24, 9067–9075
10 Engel, A.K. et al. (1991) Interhemispheric synchronization of oscillatory neuronal responses in cat visual cortex. Science 252, 1177–1179
11 Lowel, S. and Singer, W. (1992) Selection of intrinsic horizontal connections in the visual cortex by correlated neuronal activity. Science 255, 209–212
12 Cobb, S.R. et al. (1995) Synchronization of neuronal activity in hippocampus by individual GABAergic interneurons. Nature 378, 75–78
13 Wang, X.J. and Buzsaki, G. (1996) Gamma oscillation by synaptic inhibition in a hippocampal interneuronal network model. J. Neurosci. 16, 6402–6413
14 Draguhn, A. et al. (1998) Electrical coupling underlies high-frequency oscillations in the hippocampus in vitro. Nature 394, 189–192
15 Hestrin, S. and Galarreta, M. (2005) Electrical synapses define networks of neocortical GABAergic neurons. Trends Neurosci. 28, 304–309
16 Montoro, R.J. and Yuste, R. (2004) Gap junctions in developing neocortex: a review. Brain Res. Brain Res. Rev. 47, 216–226
17 Hashimoto, T. et al. (2009) Protracted developmental trajectories of GABA(A) receptor alpha1 and alpha2 Subunit expression in primate prefrontal cortex. Biol. Psychiatry 65, 1015–1023
18 Doischer, D. et al. (2008) Postnatal differentiation of basket cells from slow to fast signaling devices. J. Neurosci. 28, 12956–12968
19 Ashtari, M. et al. (2007) White matter development during late adolescence in healthy males: A cross-sectional diffusion tensor imaging study. Neuroimage 35, 501–510
20 Perrin, J.S. et al. (2009) Sex differences in the growth of white matter during adolescence. Neuroimage 45, 1055–1066
21 Niedermeyer, E. and Da Silva, F.L., (2005) Maturation of the EEG: Development of Waking and Sleep Patterns. In: Electroencephalography: Basic Principles, Clinical Applications, and Related Fields, Lippincott Williams & Wilkins
22 Whitford, T.J. et al. (2007) Brain maturation in adolescence: concurrent changes in neuroanatomy and neurophysiology. Hum. Brain Mapp. 28, 228–237
23 Campbell, I.G. and Feinberg, I. (2009) Longitudinal trajectories of non- rapid eye movement delta and theta EEG as indicators of adolescent brain maturation. Proc. Natl. Acad. Sci. U S A 106, 5177–5180
24 Takano, T. and Ogawa, T. (1998) Characterization of developmental changes in EEG-gamma band activity during childhood using the autoregressive model. Acta Paediatr. Jpn 40, 446–452
25 Benasich, A.A. et al. (2008) Early cognitive and language skills are linked to resting frontal gamma power across the first 3 years. Behav. Brain Res. 195, 215–222

26 Thatcher, R.W. et al. (2008) Development of cortical connections as measured by EEG coherence and phase delays. Hum. Brain Mapp. 12, 1400–1415
27 Srinivasan, R. (1999) Spatial structure of the human alpha rhythm: global correlation in adults and local correlation in children. Clin. Neurophysiol. 110, 1351–1362
28 Galambos, R. et al. (1981) A 40-Hz auditory potential recorded from the human scalp. Proc. Natl. Acad. Sci. U S A 78, 2643–2647
29 Rojas, D.C. et al. (2006) Development of the 40 Hz steady state auditory evoked magnetic field from ages 5 to 52. Clin. Neurophysiol. 117, 110– 117
30 Poulsen, C. et al. (2009) Age-related changes in transient and oscillatory brain responses to auditory stimulation during early adolescence. Dev. Sci. 12, 220–235
31 Csibra, G. et al. (2000) Gamma oscillations and object processing in the infant brain. Science 290, 1582–1585
32 Werkle-Bergner, M. et al. (2009) EEG gamma-band synchronization in visual coding from childhood to old age: Evidence from evoked power and inter-trial phase locking. Clin. Neurophysiology 120, 1291–1302
33 Uhlhaas, P.J. et al. (2009) The development of neural synchrony reflects late maturation and restructuring functional networks in humans. Proc. Natl. Acad. Sci. U. S. A. 106, 9866–9871
34 Muller, V. et al. (2009) Lifespan differences in cortical dynamics of auditory perception. Dev. Sci. 12, 839–853
35 Yordanova, J.Y. et al. (1996) Developmental changes in the alpha response system. Electroencephalogr. Clin. Neurophysiol. 99, 527– 538
36 Kilner, J.M. et al. (2000) Human cortical muscle coherence is directly related to specific motor parameters. J. Neurosci. 20, 8838–8845
37 Farmer, S.F. et al. (2007) Changes in EMG coherence between long and short thumb abductor muscles during human development. J. Physiol. 579, 389–402
38 James, L.M. et al. (2008) On the development of human corticospinal oscillations: age-related changes in EEG–EMG coherence and cumulant. Eur. J. Neurosci. 27, 3369–3379
39 Luna, B. et al. (2004) Maturation of cognitive processes from late childhood to adulthood. Child Dev. 75, 1357–1372
40 Toga, A.W. et al. (2006) Mapping brain maturation. Trends Neurosci. 29, 148–159
41 Klausberger, T. et al. (2002) Cell type- and input-specific differences in the number and subtypes of synaptic GABA(A) receptors in the hippocampus. J. Neurosci. 22, 2513–2521
42 Sohal, V.S. et al. (2009) Parvalbumin neurons and gamma rhythms enhance cortical circuit performance. Nature 459, 698–702
43 Feinberg, I. and Campbell, I.G. (2010) Sleep EEG changes during adolescence: An index of a fundamental brain reorganization. Brain Cogn. 72, 56–65
44 Salami, M. et al. (2003) Change of conduction velocity by regional myelination yields constant latency irrespective of distance between thalamus and cortex. Proc. Natl. Acad. Sci. U. S. A. 100, 6174–6179
45 Casey, B.J. et al. (2008) The adolescent brain. Ann. N. Y. Acad. Sci. 1124, 111–126
46 Supekar, K. et al. (2009) Development of large-scale functional brain networks in children. PLoS Biol. 7, e1000157
47 Durston, S. et al. (2006) A shift from diffuse to focal cortical activity with development. Dev. Sci. 9, 1–8
48 Crone, E.A. et al. (2006) Neurocognitive development of the ability to manipulate information in working memory. Proc. Natl. Acad. Sci. U. S. A. 103, 9315–9320
49 Rubia, K. et al. (2007) Linear age-correlated functional development of right inferior fronto-striato-cerebellar networks during response inhibition and anterior cingulate during error-related processes. Hum. Brain Mapp. 28, 1163–1177
50 Golarai, G. et al. (2007) Differential development of high-level visual cortex correlates with category-specific recognition memory. Nat. Neurosci. 10, 512–522
51 Niessing, J. et al. (2005) Hemodynamic signals correlate tightly with synchronized gamma oscillations. Science 309, 948–951
52 Uhlhaas, P.J. and Singer. W. (2010) Abnormal oscillations and synchrony in schizophrenia. Nat. Rev. Neurosci.
53 Uhlhaas, P.J. and Singer, W. (2007) What do disturbances in neural synchrony tell us about autism. Biol. Psychiatry 62, 190–191
54 Gray, C.M. et al. (1989) Oscillatory responses in cat visual cortex exhibit inter-columnar synchronization which reflects global stimulus properties. Nature 338, 334–337
55 Womelsdorf, T. et al. (2007) Modulation of neuronal interactions through neuronal synchronization. Science 316, 1609–1612
56 Herculano-Houzel, S. et al. (1999) Precisely synchronized oscillatory firing patterns require electroencephalographic activation. J. Neurosci. 19, 3992–4010
57 Gray, C.M. and Singer, W. (1989) Stimulus-specific neuronal oscillations in orientation columns of cat visual cortex. Proc. Natl. Acad. Sci. U. S. A. 86, 1698–1702
58 Fries, P. et al. (2001) Modulation of oscillatory neuronal synchronization by selective visual attention.

Science 291, 1560–1563
59 Uhlhaas, P.J. et al. (2009) Neural synchrony in cortical networks: history, concept and current status. Front. Integr. Neurosci. 3, 17
60 Kreiter, A.K. and Singer, W. (1996) Stimulus-dependent synchronization of neuronal responses in the visual cortex of the awake macaque monkey. J. Neurosci. 16, 2381–2396
61 Klimesch, W. et al. (2007) EEG alpha oscillations: the inhibition-timing hypothesis. Brain Res. Rev. 53, 63–88
62 Palva, S. and Palva, J.M. (2007) New vistas for alpha-frequency band oscillations. Trends Neurosci. 30, 150–158
63 Buzsaki, G. (2005) Theta rhythm of navigation: link between path integration and landmark navigation, episodic and semantic memory. Hippocampus 15, 827–840
64 von Stein, A. et al. (2000) Top-down processing mediated by interareal synchronization. Proc. Natl. Acad. Sci. U. S. A. 97, 14748–14753
65 Kopell, N. et al. (2000) Gamma rhythms and beta rhythms have different synchronization properties. Proc. Natl. Acad. Sci. U. S. A. 97, 1867–1872
66 Gogtay, N. et al. (2004) Dynamic mapping of human cortical development during childhood through early adulthood. Proc. Natl. Acad. Sci. U. S. A. 101, 8174–8179
67 Mu, Y. and Poo, M.M. (2006) Spike timing-dependent LTP/LTD mediates visual experience-dependent plasticity in a developing retinotectal system. Neuron 50, 115–125
68 Tamnes, C.K. et al. (2010) Brain maturation in adolescence and young adulthood: regional age-related changes in cortical thickness and white matter volume and microstructure. Cereb. Cortex doi:10.1093/cercor/bhp118
69 van Vugt, M.K. et al. (2007) Comparison of spectral analysis methods for characterizing brain oscillations. J. Neurosci. Methods 162, 49–63
70 Lachaux, J.P. et al. (1999) Measuring phase synchrony in brain signals. Hum. Brain Mapp. 8, 194–208

3

Gamma-Band Activity in Human Prefrontal Cortex Codes for the Number of Relevant Items Maintained in Working Memory

As published in: Frederic Roux, Harald Mohr, Michael Wibral, Wolf Singer and Peter Uhlhaas (2012): Gamma-Band Activity in Human Prefrontal Cortex Codes for the Number of Relevant Items Maintained in Working Memory. Journal of Neuroscience; 32(36):12411-20.

3.1 Abstract

Previous studies in human and animal electrophysiology have provided consistent evidence for a relationship between neural oscillations in different frequency-bands and the maintenance of information in working memory (WM). While the amplitude and cross-frequency coupling of neural oscillations have been shown to be modulated by the number of items retained during WM, inter-areal phase synchronization has been associated with the integration of distributed activity during WM maintenance. Together these findings provided important insights into the oscillatory dynamics of cortical networks during WM. However, little is known about the cortical regions and frequencies which underlie the specific maintenance of behaviourally relevant information in WM. In the current study, we addressed this question with magneto-encephalography (MEG) and a delayed sample to match (DSM) task involving distractors in 25 human participants. Using spectral analysis and beamforming, we found a WM-load related increase in the gamma band (60-80 Hz) which was localized to the right intra-parietal lobule (IPL) and left Brodmann area 9 (BA 9). WM-load related changes were also detected at alpha frequencies (10-14 Hz) in Brodmann area 6 (BA6), but did not covary with the number of relevant WM-items. Finally, we decoded gamma-band source activity with a linear discriminant analysis (LDA) and found that gamma-band activity in left BA9 predicted the number of target items maintained in WM. While the present data show that WM maintenance involves activity in the alpha and gamma-band, our results highlight the contribution of gamma-band delay activity in prefrontal cortex (PFC) for the maintenance of behaviourally relevant items.

3.2 Introduction

Working memory (WM) is a fundamental cognitive function that permits the maintenance of sensory information over a short period of time (Baddeley, 2003). Theoretical work suggests that temporally correlated activity in recurrent cell assemblies may sustain sensory information in the absence of external input (Hebb, 1949). In addition, synchronous fluctuations of neural activity have been suggested to bind the activity of cortical cell assemblies (Buzsáki and Draguhn, 2004). Accordingly, neural oscillations have been proposed as a mechanism to maintain the neural representations of sensory information during WM (Jensen et al., 2007). Support for this hypothesis was first provided by WM studies in humans (Tallon-Baudry et al., 1998) and non-human primates (Pesaran et al., 2002), which reported a sustained increase of oscillatory activity in the gamma frequency-range during the memory period of delayed response tasks. Subsequently, a large body of evidence has documented a parametric relationship between the amplitude of oscillatory activity at theta , alpha-, beta- and gamma-frequencies and the number of WM-items memorized during memory scanning tasks (Jensen and Tesche, 2002; Howard et al., 2003; Onton et al., 2005; Meltzer et al., 2008), visuo-spatial WM (Busch and Herrmann, 2003; Sauseng et al., 2005, 2009; Palva et al., 2011) and auditory WM (Leiberg et al., 2006).

Delay activity in the theta- (Jensen and Tesche, 2002; Meltzer et al., 2008) and gamma-bands (Howard et al., 2003; Meltzer et al., 2008; Palva et al., 2011) have both been associated with the active maintenance of sensory representations during WM. In contrast, modulations of spectral power at alpha frequencies have been assigned different roles. While some studies have related delay activity in the alpha-band with the functional inhibition of task-irrelevant brain areas (Jensen et al., 2002a; Jokisch and Jensen, 2007; Medendorp et al., 2007; Sauseng et al., 2009; Van Der Werf et al., 2010), others have linked alpha-band activity directly to processes underlying WM maintenance (Busch and Herrmann, 2003; Herrmann et al., 2004; Sauseng et al., 2005; Leiberg et al., 2006; Palva et al., 2011). In addition to the contribution of individual frequency bands, theoretical and empirical studies have implicated the coupling between oscillations frequencies as a mechanism for WM-maintenance. Specifically, theta-nested gamma-band oscillations have been proposed to sequentially code the order of WM items (Lisman and Idiart, 1995) which is supported by intracranial EEG (iEEG) recordings (Axmacher et al., 2010) as well as by scalp-recorded EEG/MEG-data (Sauseng et al., 2009; Fuentemilla et al., 2010).

More recently, EEG and MEG studies have mapped the oscillatory networks during WM retention. In these studies, gamma-band delay activity was localized to core regions of the WM network, previously identified by fMRI (Wager and Smith, 2003), including occipital, parietal, somato-sensory, prefrontal and frontal areas (Jokisch and Jensen, 2007; Medendorp et al., 2007; Haegens et al., 2010; Van Der Werf et al., 2010; Palva et al., 2011) and was found to correlate with individual WM capacity, i.e. the maximal number of items that can be held in WM (Palva et al., 2011). Similarly, source modeling approaches to alpha-band delay activity have reported networks directly involved into WM-maintenance (Palva et al., 2011), while other studies showed modulations of alpha-band activity outside the WM-network (Jokisch and Jensen, 2007; Medendorp et al., 2007; Haegens et al., 2010; Van Der Werf et al., 2010). Finally, inter-areal phase synchrony at alpha-, beta- and gamma-frequencies has been reported to be prominently involved into the maintenance of neural object representations (Palva et al., 2010).

Together these findings provide important evidence for the functional relationship between neural oscillations in different frequency ranges and the maintenance of information during WM. However, it is currently unclear which cortical networks and frequencies contribute to the maintenance of behaviourally relevant WM-information. This question is important because the storage capacity of WM is highly limited (Cowan, 2001) and inter-individual differences in WM-capacity critically depend on the ability to separate behaviourally relevant from irrelevant information (Vogel et al., 2005).

To examine this question, we recored MEG-data during the delay period of a visuo-spatial DSM-task with distractors which made it possible to identify delay activity that was specific to the maintenance of behaviourally relevant items (Figure 4.1). We employed spectral analysis as well as a beamforming approach to identify the cortical sources of delay activity in different frequency-bands. A decoding approach was employed to assess the contribution of delay activity in parietal and prefrontal areas to the maintenance of behaviourally relevant v. irrelevant information.

3.3 Methods

Participants and visual-spatial WM task. MEG recordings were collected from twenty five (10 females; age range: 18-32 years) adult participants with normal or corrected to normal vision. Written, informed consent was obtained prior to the begin of the experiment and all experimental procedures were in agreement with the guidelines of the university's ethics committee. Participants performed a delayed match to sample task (Figure 4.1).

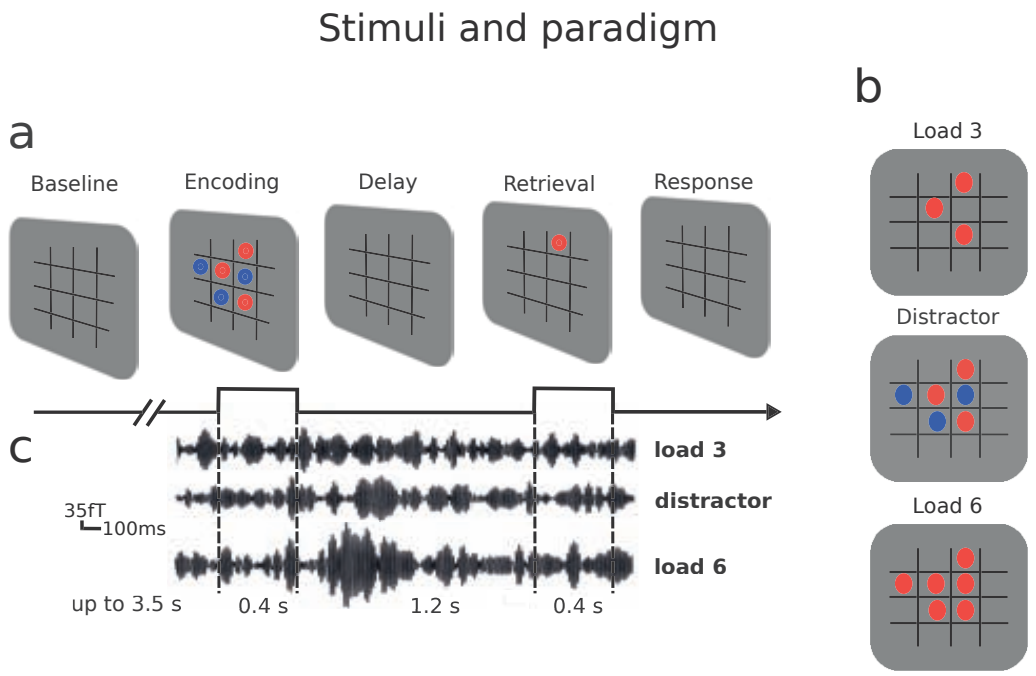

Figure 3.1: **The visuo-spatial working memory task. (a)** Example of a trial with distractors during the encoding. On one third of the trials, participants were shown three red discs together with three blue discs (distractors) and participants were asked to memorize the positions of the red discs only and to ignore the positions of the blue discs. In the remaining trials, distractors were absent and either three or six red discs were presented. After a maintenance phase of 1.2 s, a test item was presented at a position identical (match) or different (non-match) to the sample array. **(b)** Example of the memory arrays for the three conditions: load 3, distractor and load 6. **(c)** Sample traces of bandpass (60-80 Hz) filtered MEG signals during the load three, distractor and load six conditions from one single subject. The recording comprises the baseline, encoding, delay and retrieval periods. Note the enhanced oscillations in the gamma-frequency in the delay phase of the load 6 condition.

The sample stimulus consisted of either three red discs (load 3), three red and three blue discs (distractors) or six red discs (load 6) which were presented for 0.4 s. This was followed by a maintenance phase of 1.2 s and the test stimulus (0.4 s), a single item whose position was either identical or different from the positions of the items in the sample stimulus. The prestimulus period varied between 3.5 s and 1.5 s to prevent temporal expectation. Participants performed 150 trials per condition and the order of trials was randomized across conditions. Participants pressed one of two buttons to indicate whether the position of the

test item was a match or a non-match and were instructed to memorize only the positions of red discs and to ignore blue discs. Hand assignment was counterbalanced across participants and behavioural responses were recorded using a fiber-optic response device (Lumitouch, Photon Control Inc., Burnaby, BC, Canada). After responding, participants had the possibility to blink for 1 s before the next trial started.

MEG data acquisition and preprocessing. MEG signals were recorded continuously using a 275-channel whole-head system (Omega 2005, VSM MedTech Ltd., BC, Canada) in a synthetic third order axial gradiometer configuration. MEG signals were sampled at 1.2 kHz and bandpass filtered at 0.01 - 600 Hz. The electro-oculogramm was recorded in order to monitor horizontal and vertical eye movements. Prior to and after each run, the subject's head position relative to the gradiometer array was measured using three fiducial coils (one coil over the nasion and two coils at 1 cm distance from the left and right tragus). Inter-individual deviations of head orientations from the mean remained below 8° (range for x coordinates : -0.86 to 0.85 cm; range for y coordinates : -1 to 0.88 cm; range for z coordinates :-1.64 to 1.74 cm). MEG signals were preprocessed and analyzed using Matlab 2008b (The MathWorks) and the open source Matlab toolbox fieldtrip (http://www.ru.nl/fcdonders/fieldtrip/). Preprocessing included bandpass filtering of the MEG recordings (butterworth filter 4th order) between 0.1 and 250 Hz as well as detrending and subtraction of the DC-offset. The continuous recording was segmented into data epochs including the baseline (1.5 s), the encoding (0.4 s), the maintenance (1.2 s) as well as the recognition (0.4 s) phase of the task (3.5 s per trial). Data epochs for match and non-match trials were pooled together and only trials with correct responses were considered for further analyses. An automatic artefact detection and rejection algorithm from the fieldtrip toolbox was used to exclude epochs contaminated by eye blinks, muscle activity or sensor jump artefacts. The average number of trials per condition across participants included for analysis was 87 out of 150 trials (58%) (SD = 23 (15%)).

Structural MRI data acquisition. Structural MRIs were obtained with a 3-T Siemens Allegra scanner device (Siemens, Erlangen, Germany) using the standard CP birdcage head-coil and a T1 sequence. Three participants met an exclusion criterion for MRI scans and were not included for source-analyses.

Estimation of spectral power and statistical analysis. All spectral quantities were estimated using multi-tapers as implemented in the Matlab based open source toolbox Chronux (Mitra, PP., Bokil, H., 2008) (http://chronux.org/). The power spectrum of MEG delay activity was estimated using a 1.2 s window (from 0.4 to 1.6s) with a spectral concentration of 4 Hz using 4 Slepian data tapers for frequencies below 20 Hz and with a spectral concentration of 10 Hz using 10 Slepian data tapers for frequencies above 20 Hz. All spectral quantities of delay activity were normalized by the spectrum of baseline activity and expressed in values of relative change according to:

$$\mathrm{Norm(f)} = (\mathrm{St(f)} - \mathrm{Sb(f)})/\mathrm{Sb(f)}$$

where St(f) corresponds to the spectrum of delay activity and Sb(f) corresponds to the spectrum of baseline activity. Time-frequency representations of delay activity were calculated using a 500 ms window that was stepped by 50 ms between estimates through the trial with the time index aligned to the flushleft of the analysis window. Trials were aligned in time to the onset of the sample stimulus. In analogy to the normalization of the power spectrum, time-frequency representations were normalized by the time-frequency representations of baseline activity according to:

$$\mathrm{Norm(t,f)} = (\mathrm{St(t,f)} - \mathrm{Sb(tf)})/\mathrm{Sb(t,f)}$$

where St(t,f) and Sb(t,f) correspond to the time-frequency representation of task and baseline activity, respectively. Normalized spectral quantities of delay activity were tested for significant task-effects using a cluster-based randomization procedure implemented in the fieldtrip toolbox (Oostenveld et al., 2011). Task specific modulations of spectral power in both frequency bands were assessed using a one way analysis of variance (ANOVA) for repeated measures. This approach is sensitive to a main effect of the experimental conditions reflecting differences in the means between the load 3, distractor and load 6 conditions across participants. The alpha level chosen for statistical significance at sensor level was alpha = 0.025 (corrected) and the alpha level chosen for statistical significance at source level was alpha = 0.001 (uncorrected). All

subsequent steps in the statistical analysis were computed using the MATLAB statistics toolbox. The first 200 ms of the delay period were not considered for post-hoc comparisons of delay activity in order to exclude encoding related activity captured by half the length of the sliding window. A Bonferroni-correction was applied to post-hoc comparisons (two-sided dependent t-test) to adjust the alpha-level for multiple comparisons. To examine relationships between spectral power, RTs and WM-capacity, we selected sensors characterized by significant differences in delay activity across experimental conditions. Power-values in the alpha- (10-14 Hz) and gamma- (60-80 Hz) frequency range were then correlated with RTs and WM-capacity (K).

Beamforming. A frequency domain beamformer (Gross et al., 2001) was used to localize the sources of oscillatory activity in the alpha and gamma frequency bands. The cross-spectral density (CSD) matrices of each participant were computed for flushleft frequencies at 12 +/-2 Hz (alpha) using 3 Slepian data tapers and at 70 +/- 10 Hz (gamma) using 19 Slepian data tapers based on common filters. Common filters were computed for trials pooled across conditions on 2s time windows including 1s of the baseline period (from -1.6 to -0.6s) and 1s of the maintenance phase (from 0.6 to 1.6s). The beamformer was then computed for baseline and delay time segments of 1s for each condition separately with a regularization parameter of lambda = 1% . Post-stimulus activation effects were normalized with baseline activity according to:

Norm(x,y,z) = (Bt(x,y,z) – Bb(x,y,z)) ./Bb(x,y,z)

where Bt(x,y,z) corresponds to the beamformer of the delay phase and Bb(x,y,z) corresponds to the beamformer of baseline activity. Normalized source activity was tested for significant task-effects using the cluster-based randomization procedure described earlier. The alpha level chosen for statistical significance of task-effects in source space was alpha = 0.001 (uncorrected).

Computation of source grids. The forward solution for each participant was estimated from individual head models using a common dipole grid in MNI space which was warped onto the anatomy of each participant and a realistic single-shell volume conductor model (Nolte, 2003). Cortical segmentation and surface reconstruction were performed using SPM2 (http://www.fil.ion.ucl.ac.uk/spm) as well as spatial alignment of structural MRIs and functional maps. We computed between-subjects cluster based randomization test-statistics (Maris and Oostenveld, 2007) to measure

task-effects across conditions for each grid point and each frequency band. Only the peak voxels were selected for the subsequent reconstruction of virtual channels.

Computation of virtual channels. For each frequency band, the sensor-level data were band-pass filtered using a 4th-order zero-phase forward-reverse digital Butterworth filter, and source-level time courses of these band-limited signals were reconstructed using the real-valued frequency specific beamformer coefficients. The dominant dipole direction of the time courses was then extracted using eigenvalue decomposition (EVD), and spectral power for each frequency band was computed from band-limited time-frequency representation using multi-taper.

Single trial decoding of gamma-band source activity. 60-80 Hz single trial source activity was decoded from the integral of the power time course in this frequency band during the memory period (from 0.6 to 1.6 s) using linear discriminant analysis (Duda et al., 2002). The discriminant function was trained on a random selection of trials (90%), while the remaining trials (10%) were used to asses the classification hit rate. This procedure was repeated 1000 times and the probability of a correct classification was expressed as the average classification hit rate across iterations. To assess the statistical significance of the classification results, we computed d-prime values for the decoding of load 3 and load 6 trials for each participant. We computed d-prime as previously proposed (Stanislaw and Todorov, 1999) as:

$$d' = z(P(Y|s)) - z(P(Y|n))$$

with z(P(Y|s)) being the z-score of the hit rate, and z(P(Y|n)) being the z-score of the false alarm rate. We defined the hit rate as the proportion of correctly classified trials and the false alarm rate as the proportion of trials that were falsely classified. Thus for load 3, the hit rate was computed as the proportion of correctly decoded load 3 trials and the false alarm rate as the proportion of load 6 trials that were falsely classified as load 3 and vice versa. This approach was applied to the results of the single trial decoding for gamma-band delay activity in the IPL and BA9 for each participant.

3.4 Results

Behavioral Performances. The hit rate and reaction times were analysed for the three different conditions (Table 1). There was a significant difference in the hit rates ($\chi^2(2,77) = 21.9$, $p < 0.0001$, kruskal-wallis one-way ANOVA). Post-hoc comparisons revealed a decrease in the hit rate between load 3 and load 6 ($z = 4.19$, $p < 0.0001$, post-hoc Mann-Withney U-test ; corrected) as well as between load 6 and the distractor condition ($z = 3.83$, $p < 0.001$, post-hoc Mann-Withney U-test; corrected). No differences were found for hit rates in the load 3 and distractor conditions ($z = 0.44$, $p > 0.05$, post-hoc Mann-Withney U-test; corrected). Furthermore, no differences were found for reaction times ($F(2,77) = 0.9$, $p > 0.05$, one-way ANOVA). Delay activity revealed a peak in

	Conditions		
Behavioral measure	Load 3	Distractor	Load 6
Hit Rate (%)	95.7 (5.4)	95.4 (4.5)	86.1 (11.2)
Reaction times (ms)	653.9 (154.4)	663.6 (151.3)	710 (163.5)

Table 3.1: Means and standard deviations (in parentheses) for behavioural performances.

the alpha (10-14 Hz) and gamma (60-80 Hz) frequency-ranges. In both frequency bands, activity was significantly elevated above baseline ($p < 0.001$; corrected; t-test; Figure 4.2a-b) and modulated across task conditions ($p < 0.025$; corrected; ANOVA). Delay activity between 0.6 and 1.6 s showed a significant increase of gamma-band power during load 6 as compared to both load 3 and the distractor condition ($P<0.001$; corrected; post-hoc t-test; Figure 4.3a-b) while there was no difference between the distractor condition and load 3 ($p > 0.05$; post-hoc t-test).

Spectral power at sensor level. Delay activity revealed a peak in the alpha (10-14 Hz) and gamma (60-80 Hz) frequency-ranges. In both frequency bands, activity was significantly elevated above baseline ($p < 0.001$; corrected; t-test; Figure 4.2a-b) and modulated across task conditions ($p < 0.025$; corrected; ANOVA). Delay activity between 0.6 and 1.6 s showed a significant increase of gamma-band power during load 6 as compared to both load 3 and the distractor condition ($P<0.001$; corrected; post-hoc t-test; Figure 4.3a-b) while there was no difference between the distractor condition and load 3 ($p > 0.05$; post-hoc t-test).

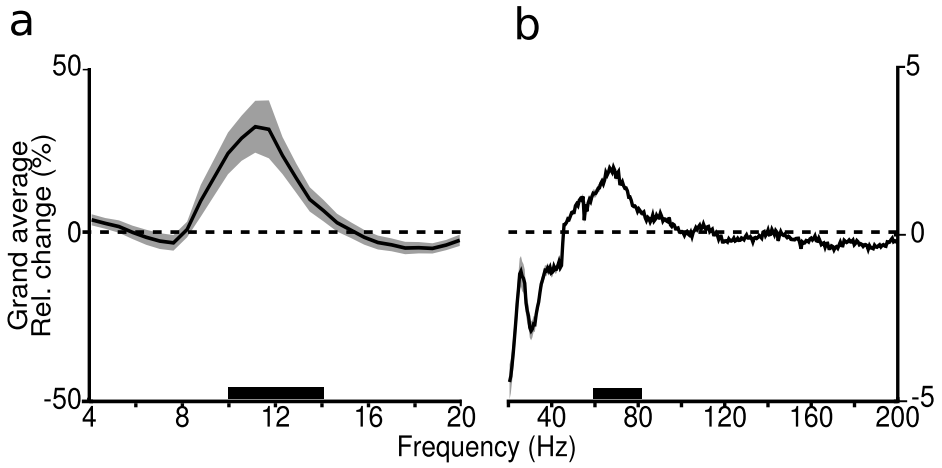

Figure 3.2: **MEG power spectrum of delay activity (a)**, Power spectrum for frequencies from 4 to 20 Hz. **(b)**, Power spectrum for frequencies from 20 to 200 Hz. x-axis represents frequency and y-axis represents power. Spectral power is expressed in percent change relative to baseline activity. The solid horizontal black lines mark the frequency bands considered for analysis. The shaded area around the curve corresponds to SEM.

The increase in gamma-band power between load 3 and load 6 was correlated with WM capacity ($r = 0.48$, $p < 0.05$), i.e. the maximal number of items each individual could hold in WM (Rouder et al., 2011). In addition, there was a significant relationship between the increase in gamma-band power between load 3 and load 6 and the difference in reaction times between both conditions ($r = -0.46$, $p < 0.05$). A similar correlation was found for the increase in gamma-band power between load 6 and the distractor condition and WM capacity (Figure 4.4a-b; Table 2). Gamma-band delay activity in each condition alone, however, did not correlate with reaction times (load 3, $r = 0.22$ $p > 0.05$; distractor, $r = 0.3$, $p > 0.05$; load6, $r = -0.03$; $p > 0.05$).

Alpha-band delay activity was characterized by a different relationship with WM load and reaction times (Figure 4.4a, Table 3). While spectral power was increased in load 6 and the distractor condition relative to load 3 ($p < 0.01$; corrected; post-hoc t-test; Figure 4.5b), there was no difference between load 6 and the distractor condition ($p > 0.05$; post-hoc t-test). Alpha-band power in the distractor ($r = 0.46$, $p < 0.05$) and load 6 ($r = 0.47$, $p < 0.05$) conditions showed a positive correlation with reaction times (Figure 4.4c-d) but there was no relationship between the increase in alpha-band delay activity between load 3 and load 6 nor between the distractor condition and load 6 and individual WM capacity (Table 2).

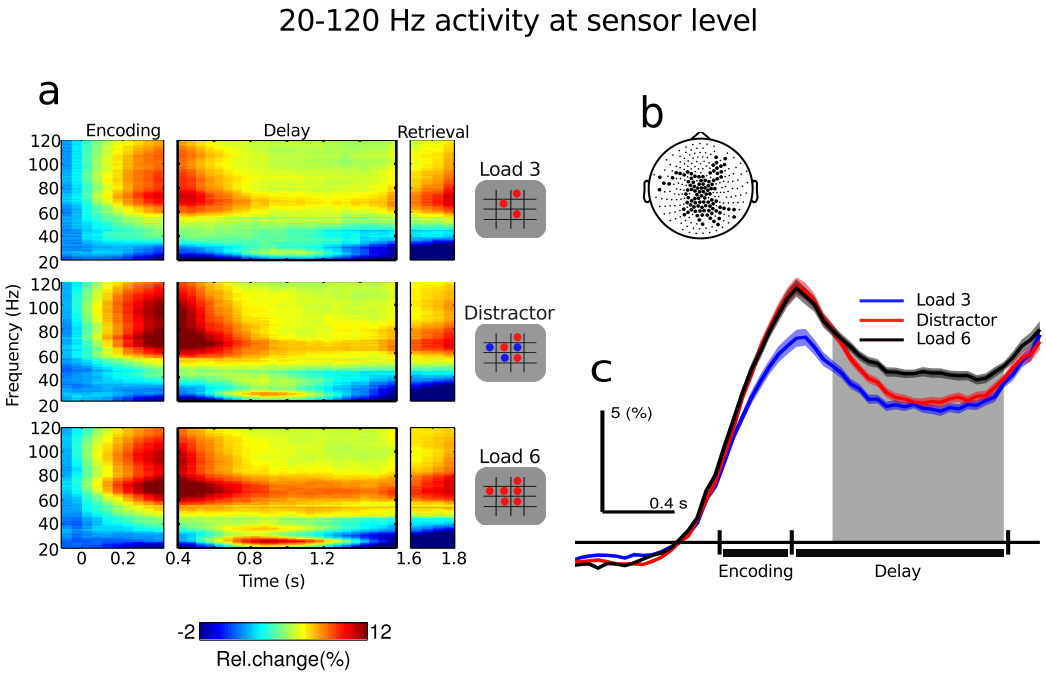

Figure 3.3: **MEG spectrograms for 20 –120 Hz activity. (a)**, Two-dimensional plots of the spectrograms for each condition. Note the transient increase of 10 –14 Hz harmonic activity in the 20 –28 Hz range. x-axis represents time and y-axis represents frequency. Spectral power is expressed in percent change relative (Rel. change) to baseline activity. **(b)**, Gamma-band activity was significantly modulated by task conditions in 100 (38%) sensors ($p < 0.025$; corrected; ANOVA). **(c)**, 60 – 80 Hz activity averaged across trials. The shaded area around the traces corresponds to the SEM. The light gray region marks the temporal interval of significant differences between conditions ($p < 0.001$; corrected; post hoc t test). MEG power spectrum of delay activity.

We did not observe significant changes relative to baseline in the theta (4-7 Hz)- and beta-bands (15-30 Hz ; Figure 4.2a-b) except for a transient increase of beta oscillations (20-28 Hz) from 0.75 to 1.2 s (Figure 4.3a). This beta activity was positively correlated with alpha-band oscillations across conditions and participants (average correlation coefficient r = 0.55, SD = 0.3). Thus 20-28Hz delay activity likely reflects harmonics of oscillations in the 10-14 Hz range.

Spectral power at source level. Task-related differences in gamma-band power ($P<0.001$; uncorrected; ANOVA) were localized to left BA 9 (MNI coordinates: -2, 52, 40) and right IPL (MNI coordinates: 30, -48, 32). Gamma-band power in BA 9 was increased during the load 6 condition as compared to the distractor and load 3 conditions ($p < 0.001$; corrected; post-hoc t-test; Figure 4.6a-b). However, there was no difference between load 3 and the distractor condition ($p > 0.05$; post-hoc t-test). In the IPL, gamma-band power was enhanced in the load 6 and distractor conditions relative to load 3 ($p < 0.001$; corrected; post-hoc t-test; Figure 4.6c-d) but reached similar amplitudes in the load 6 and the distractor condition ($p > 0.05$; post-hoc t-test). Task effects

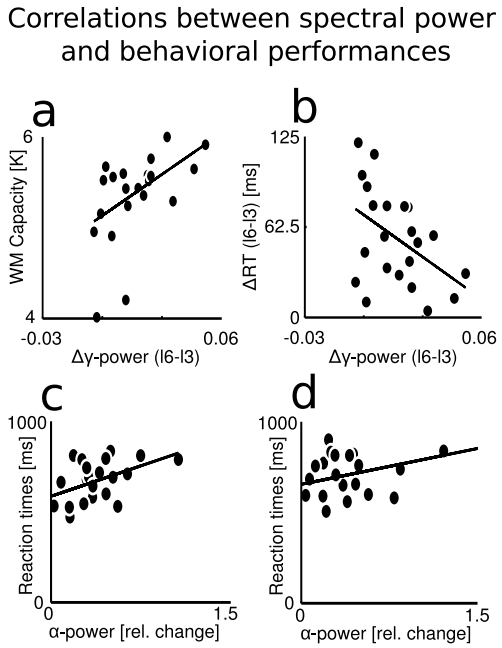

Figure 3.4: **Relationship between spectral power and behavioural performances. (a)**, Linear regression between the increase of gamma band (60 – 80 Hz) delay activity from load 6 relative to load 3 and WM capacity. **(b)**, Linear regression between the increase of 60 – 80 Hz delay activity from load 6 relative to load 3 and the increase in reaction times from load 6 to load 3. **(c)**, Linear regression between alpha-band (10 –14 Hz) delay activity and reaction times in the distractor condition. **(d)**, Linear regression between 10 and 14 Hz delay activity and reaction times in the load 6 condition. rel. change, Relative change.

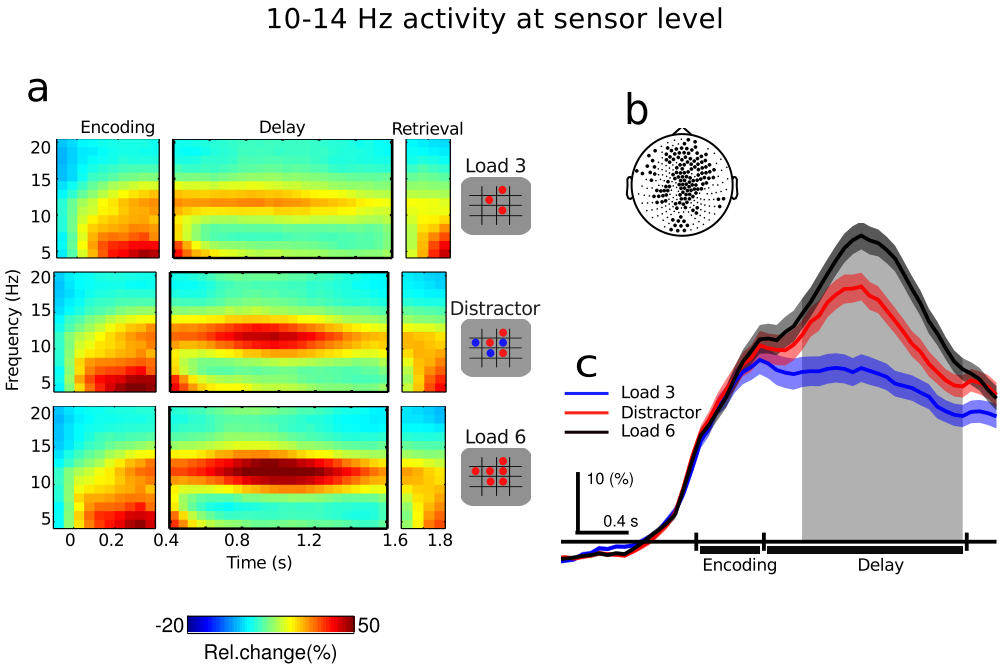

Figure 3.5: **MEG spectrograms for 6-20 Hz activity (same convention as in Figure 4.2). (a)** Two dimensional plots of the spectrograms for each condition. X-axis: time; Y-axis: frequency. Spectral power is expressed in percent change relative to baseline activity. **(b)** Alpha-band power was significantly modulated across task conditions in 137 (58%) sensors ($p < 0.025$; corrected; ANOVA). **(c)** 10-14 Hz activity averaged across trials ($p < 0.01$; corrected; post-hoc t-test).

($p < 0.001$; uncorrected; ANOVA) in the alpha-band were localized to BA 6 (MNI coordinates: 42, 10, 58; Figure 4.6e) which contributes to premotor cortex. Alpha power in BA 6 increased in the load 6 and distractor conditions relative to load 3 ($p < 0.001$; corrected; post-hoc t-test). As for gamma-band power in the IPL, alpha-band activity in BA 6 did not differ between load 6 and the distractor condition ($p > 0.05$; post-hoc t-test; Figure 4.6e).

Differences in delay activity	**Maximal WM capacity (K)**	**Reaction time increase (ms)**
Load 6 - Load 3		
10-14 Hz	-0.39	0.27
60-80 Hz	-0.49*	-0.46*
Load 6 - distractor		
10-14 Hz	-0.26	0.18
60-80 Hz	0.3	-0.31

Table 3.2: Pearson product moment correlation between spectral power in the alpha and gamma-bands at sensor level and WM performances. * signifies p <0.05.

Reaction times	**10-14 Hz**	**60-80 Hz**
Load 3	0.39	0.22
Distractor	0.46*	0.3
Load 6	0.47*	-0.03

Table 3.3: Pearson product moment correlation between spectral power in the alpha and gamma-bands at sensor level and reaction times. * signifies p <0.05.

Predicting WM load from single trial 60-80 Hz source activity

To identify the cortical area whose activation predicts the number of items maintained in WM, LDA was applied to 60-80 Hz activity during behaviourally successful trials in BA 9 and IPL. We first decoded gamma activity from load 3 and load 6 trials and then applied the same classifier to gamma-band activity during distractor trials in order to estimate the probability of distractor trials being classified as load 3 and load 6 across trials for each participant. Assuming that 60-80 Hz oscillations reflect the maintenance of behaviourally relevant items in WM, we predicted that gamma-band activity during behaviourally successful trials with distractors should have a higher probability to be classified as load 3 than as load 6.

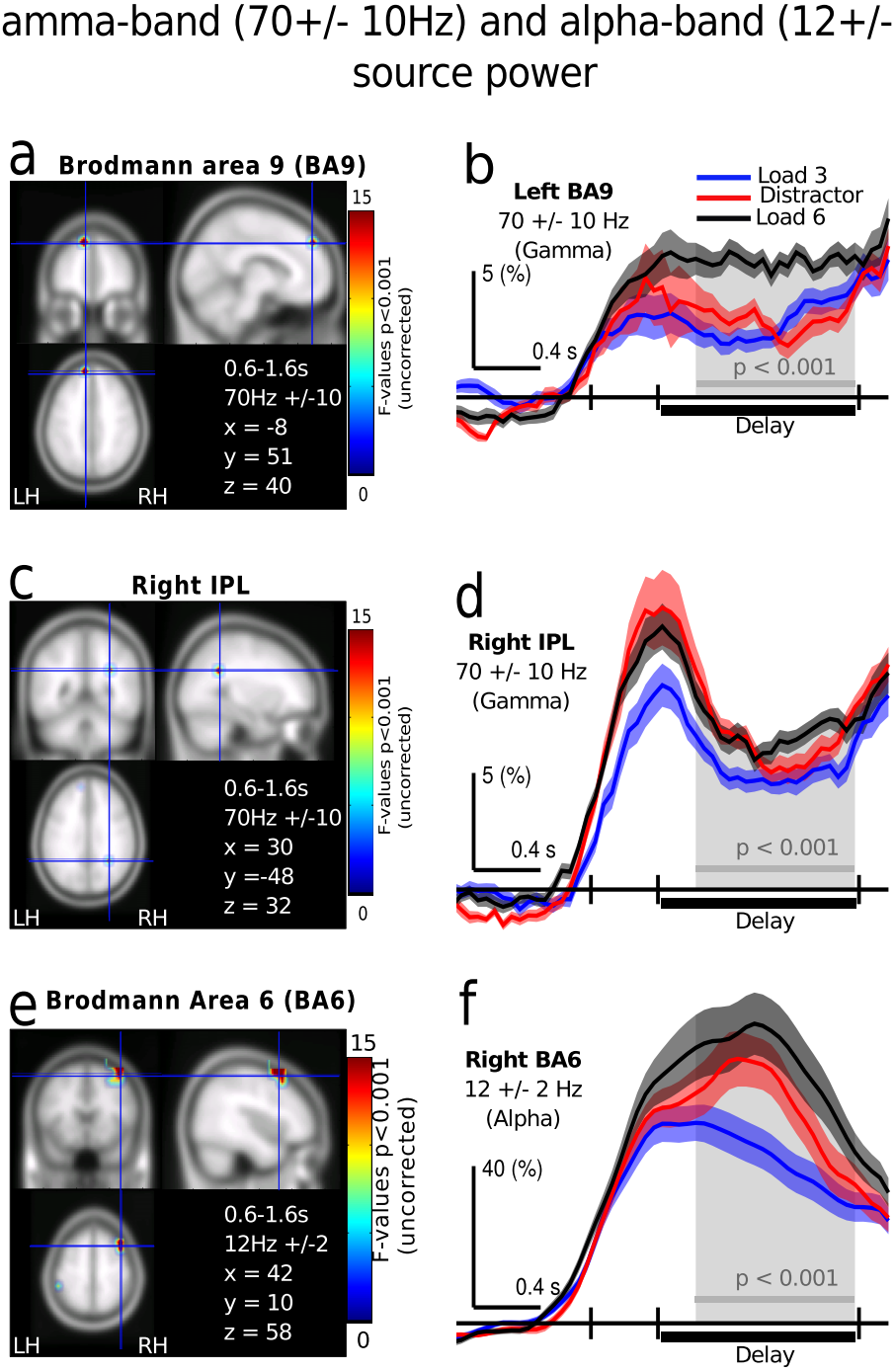

Figure 3.6: **Delay activity at cortical source level.** Images of the differences in 60-80 Hz activity (0.6 to 1.6 s) across task conditions during the delay period for the left BA 9 **(a)** and intraparietal lobule (IPL) **(b)**. Effects are separately shown for the two brain regions and are displayed on axial, sagital and coronal sectional views of the MNI template brain. The locations of BA 9 and IPL are marked for orientation. All functional maps display dependent F-values thresholded at $p < 0.001$ (uncorrected). Time course of 60-80 Hz activity for peak voxels averaged across trials in BA 9 **(c)** and IPL **(d)**. The light gray region corresponds to the temporal interval of significant differences between conditions ($p < 0.001$; corrected; post-hoc t-test). **(b)** In BA 9, there was a significant increase of 60-80 Hz activity from 0.6 to 1.6 s during load 6 as compared to the load 3 and distractor conditions, while activity during load 3 and the distractor was similar. **(d)** In contrast, in the IPL 60-80 Hz delay activity was increased during load 6 and the distractor as compared to load 3 and did not differ between the distractor and load 6 condition. **(e)** Statistical map of the differences in 10-14 Hz activity (0.6 to 1.6 s) across task conditions during the delay period for Brodmann area 6 (BA6). **(f)** Time course of 10-14 Hz source activity averaged across trials for BA 6 . Source activity in the 10-14 Hz range was significantly elevated during the delay (0.6 to 1.6 s) in the distractor and load 6 conditions as compared to load 3, and remained similar in the distractor and load 6 conditions.

The average probability of a correct assignment of load 3 trials was 59 % (SD across participants = 10%) in BA 9 and 56 % (SD across participants = 10%) in the IPL. Load 6 trials were correctly decoded with an average probability of 55 % (SD across participants = 8%) in BA 9 and of 57 % (SD across participants = 9%) in the IPL (Figure 4.7a). The decoding performance reported in the present study corresponds to performance levels reported by classification approaches in functional magnetic resonance imaging (fMRI) data (Knops et al., 2009). Decoding performance for gamma-band source activity in the IPL was not significantly different from zero across participants for load 3 ($t(21) = 1.6$, $p > 0.05$). However, decoding of delay activity for load 6 trials in the IPL was significant ($t(21) = 3.35$, $p < 0.01$). In BA9, the distribution of d' values was significantly different from zero across participants in both conditions (load 3: $t(21) = 3.29$, $p < 0.01$; load 6: $t(21) = 3.1$, $p < 0.01$).

To test the hypothesis that 60-80 Hz oscillations are correlated with the maintenance of behaviourally relevant WM items we predicted class membership (load 3 vs. load 6) for distractor trials using the same discriminant function as for the classification of load 3 and load 6 trials. We found that gamma-band activity in BA 9 predicted the amount of behaviourally relevant information maintained in WM with 17 out of 22 (77%) participants showing a probability of distractor trials being classified as load 3 greater than chance ($p < 0.01$; corrected; two-sided Binomial-Test). In IPL, distractor trials were classified as load 3 trials in only 10 (45%) out of 22 participants ($p = > 0.05$; two-sided Binomial Test). The mean classification probability for distractor trials in the IPL to be classified as load 3 was 49 % (SD: 15 %), whereas in BA9 the mean probability of distractor trials to be classified as load 3 was 59 % (SD: 19%). Furthermore, the probability of distractor trials to be classified as load 3 was significantly higher in BA 9 as compared to the IPL ($P < 0.01$, two-sided t-test). These results suggest that the number of behaviourally relevant items maintained in WM can be decoded from 60-80 Hz source power in BA 9 (Figure 4.7b).

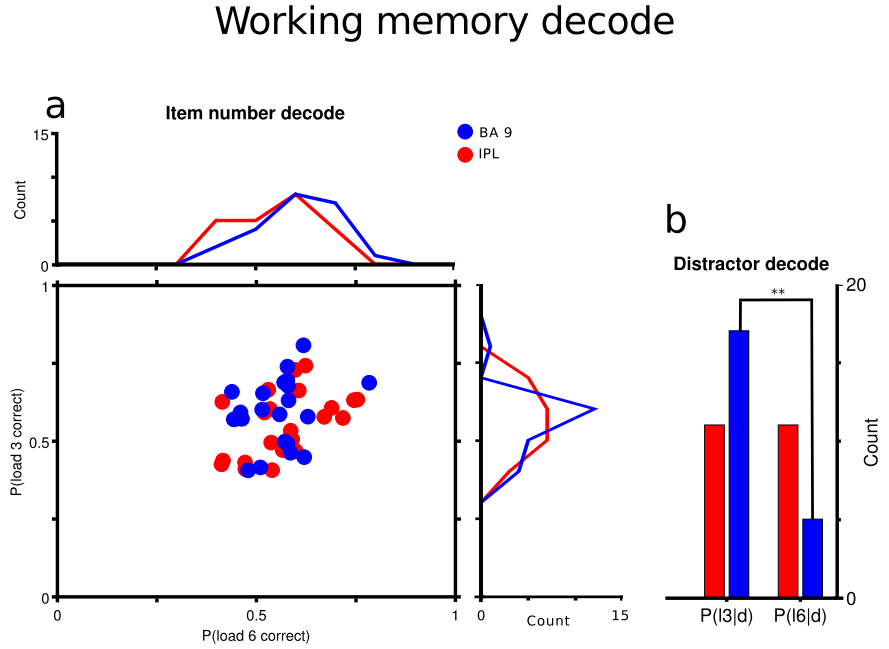

Figure 3.7: **Single trial decoding of 60-80 Hz delay activity. (a)** Each dot represents classification performance in BA 9 (blue) and IPL (red) for each participant. Horizontal axis is the probability that a trial corresponding to load six is decoded correctly. Vertical axis is the probability that a trial corresponding to load three is decoded correctly. Line plots show the histograms of participant counts for the decode in each condition. **(a)** Decoding of distractor trials for 60-80 Hz delay activity in BA 9 (blue) and IPL (red). Vertical axis is the count of participants for which single trial gamma-band source activity in the distractor condition was decoded as load three or as load six. Delay activity in BA 9 corresponding to distractor trials was decoded as load 3 with a probability of p = 0.77 (P < 0.025; corrected; two-sided Binomial-test), while in the IPL distractor trials had equal probability (p = 0.5) to be decoded as load three or load 6 (P = n. s.; two-sided Binomial-test).

3.5 Discussion

WM-Delay Activity of Alpha and Gamma-Band Oscillations at Sensor Level. In line with previous studies (Tallon-Baudry et al., 1998; Pesaran et al., 2002; Howard et al., 2003; Jokisch and Jensen, 2007; Meltzer et al., 2008; Haegens et al., 2010; Van Der Werf et al., 2010), we report an increase of oscillatory activity in the gamma frequency-band during the retention phase. Furthermore, 60-80 Hz delay activity was observed to increase with WM-load, which is consistent with data obtained from intra-cortical recordings in humans (Howard et al., 2003).

Interestingly, when only three out of six presented items were relevant, the analysis of gamma-band activity revealed a correspondence between the oscillation amplitude and the number of target items. This relationship was not found for spectral power in the alpha-band because a similar amplitude increase occurred between the distractor condition and load 6, suggesting that only 60-80 Hz delay activity is sensitive to the number of relevant WM-items. Furthermore,

correlations with RTs and WM-capacity suggest that gamma-band activity had a facilitatory effect on WM-performance.

This relationship was not found for alpha-band activity. Consistent with previous studies (Jensen et al., 2002b; Meltzer et al., 2008; Sauseng et al., 2009; Palva et al., 2011), alpha-band oscillations were modulated by WM-load because 10-14 Hz activity increased between load 3 and load 6 but correlated negatively with RTs. Together with previous evidence which has interpreted alpha-band activity over motor areas in human EEG-data as the inhibition of motor areas (Pfurtscheller et al., 1997) and studies showing that alpha-band delay activity increases over task-irrelevant brain regions (Pfurtscheller et al., 1997; Worden et al., 2000; Jokisch and Jensen, 2007; Medendorp et al., 2007; Sauseng et al., 2009; Haegens et al., 2010), our data suggest that alpha-band oscillations are not involved in the active maintenance of WM-representations. Instead, a more likely function of increased 10-14 activity could be the inhibition of cortical areas involved into the preparation or execution of motor actions. This interpretation is consistent with reports of focally increased 11-13 Hz activity during the inhibition of motor memory traces (Hummel et al., 2002) and the association between increased alpha-band power and slower behavioural responses in the current study.

Alpha and Gamma-Band WM-Networks. Further support for the distinct contributions of alpha- and gamma-band oscillations towards the maintenance of relevant WM-representations was obtained through the identification of the underlying cortical sources. Previous MEG studies have reported a WM-load specific strengthening of oscillatory delay activity in prefrontal and parietal areas which correlated with individual WM capacity (Palva et al., 2011), suggesting that activity in these brain areas is implicated in the maintenance of WM representations. In agreement with these findings, we report WM-related changes of gamma-band source activity in left BA 9 and the right IPL.

In both cortical regions we observed an increase of gamma-band delay activity with WM-load. However, the analysis of source activity revealed that the correspondence between oscillation amplitude and the number of target items was specific to activity in BA 9. This was confirmed by a decoding approach applied to single trial delay activity at source level which showed that 60-80 Hz activity in BA 9 co-varied with the number of relevant items, which was not the case in the IPL.

Our results thus suggest a specific contribution of gamma-band activity in left BA 9 towards the maintenance of relevant items in visuo-spatial WM. This conclusion is consistent with electrophysiological recordings in non-human primates (Rainer et al., 1998), lesion studies in humans (du Boisgueheneuc et al., 2006) and non-human primates (Funahashi et al., 1993) as well as the specific effect of disrupting WM-maintenance through transcranial magnetic stimulation (TMS) in PFC (Feredoes et al., 2011), which highlight the importance of left PFC for the maintenance of behaviourally relevant WM representations.

In the alpha-band, task effects were localized to right BA 6, a region comprising the premotor cortex and the supplementary motor area (SMA) which has been shown to be critically involved in the planning and inhibition of motor plans (Sumner et al., 2007). These results further support the interpretation of 10-14 Hz delay activity as a mechanism to protect memory traces from interfering preparatory motor activity.

Relationship to Previous Neurophysiological WM-theories and Empirical Findings. Previous work suggests that successful WM maintenance involves a distributed network of cortical areas (Miller and Desimone, 1994; Palva et al., 2010, 2011). In line with these findings, we report delay activity at alpha- and gamma-band frequencies in parietal and frontal regions. However, our data suggests that only gamma-band activity in BA 9 contributes towards the maintenance of behaviourally relevant WM-items.

WM-delay activity at gamma and alpha-band frequencies in distinct nodes of the WM-network in our study can be integrated with recent data from invasive and non-invasive electrophysiological recordings. Thus, gamma-band activity in parietal cortices could be related to topographic maps which code for the spatial memories of saccades (Blatt et al., 1990; Ben Hamed et al., 2001). This is suggested by the fact that gamma-band activity in IPL was modulated by the number of stimuli presented in the memory array but not by the number of relevant items, which suggests that the modulation of 60-80 Hz activity reflects a scanning and maintenance of the spatial position of possible WM-locations.

Accordingly, gamma-band activity in IPL may reflect the activity of memory fields (Funahashi et al., 1989) which have been suggested to synchronize at gamma-frequencies in order to strengthen their input on downstream targets in the occulomotor network (Van Der Werf et al., 2010). Based on this hypothesis, we propose that the coupling between PFC-IPL through coherent oscillations (Fries, 2005) may serve as a link for the read out of behaviourally relevant stimuli positions. This interpretation is consistent with memory fields in the PFC which have been reported to be critically implicated in the control of memory guided occulomotor responses during WM (Funahashi et al., 1993) and with our findings that fluctuations of gamma-band activity in PFC allowed the decoding of the number behaviourally relevant items.

The interpretation of gamma-band delay activity as the maintenance and readout of spatial maps coding for WM-locations is further supported by the localization of alpha-band delay activity in BA 6. TMS stimulation of SMA has been observed to impair the ability to reproduce memorized gaze positions (Müri et al., 1995) and neurons in pre-SMA have been implicated in the organization of occulomotor sequences (Isoda and Tanji, 2004). From this perspective, alpha-band oscillations in SMA in our study could be involved in the inhibition of occulomotor movements as these could interfere with WM-locations maintained in parietal cortex. The distinct roles of alpha- and gamma-band oscillations in the present study suggest that these findings may be specific to visuo-spatial WM and may not apply to other WM-paradigms. This could be one explanation for the absence of significant task-effects in the theta-band in our study which has been prominently implicated in neurophysiological WM theories (Lisman, 2010). Previous studies which have reported a relationship between WM-load and the modulation of theta-band oscillations have investigated WM-delay activity during tasks that typically require the maintenance of sequential WM representations, i.e. Sternberg tasks (Jensen and Tesche, 2002).

Methodological Limitations of Source Localization. The pattern of lateralization of both alpha- and gamma-band activity can be considered consistent with previous studies which have emphasized the role of the left PFC for the maintenance of relevant items in WM (Rainer et al., 1998; du Boisgueheneuc et al., 2006). In addition right IPL activity has been shown to be critical for visuo-spatial WM (Yamanaka et al., 2010) while the lateralization of activation foci to the right hemisphere occurs with increasing executive demands which could account for increased alpha-band delay activity in BA 6 (Wager and Smith, 2003).

We would like to note, however, that we cannot completely exclude the possibility that the pattern of source-localizations may have been affected by the constrains of the spatial beamformer employed in the current study. Although the estimation of neural source signals using inverse modeling reduces the cross-talk between sensors at the scalp surface, the output of spatial beamformers can suffer from signal cancellation and cross-talk effects which can affect the identification of sources (Gross et al., 2001).

3.6 Conclusions

The aim of the current study was to identify the frequencies and cortical regions which contribute to the maintenance of behaviourally relevant WM representations. The present findings provide novel evidence for a frequency and anatomically specific relationship between 60-80 Hz activity in left BA 9 and the maintenance of relevant WM representations. In addition, the current study provides evidence for spectral changes at alpha and gamma-band frequencies in parietal and premotor cortex. However, delay activity in these areas was not found to be implicated into the maintenance of relevant WM-items.

Our findings also highlight that MEG source-data can be used to predict the amount of behaviourally relevant information maintained in WM from single-trial fluctuations of gamma-band oscillations in PFC. Studies with fMRI have shown that fluctuations in the BOLD signal can decode the content of WM from delay activity in early visual areas (Harrison and Tong, 2009). The present results suggest that MEG source-data can be used as well to predict the content of WM, suggesting that non-invasively recorded brain oscillations allow functional links between oscillatory activity and cognitive processes.

In future studies, it will be interesting to investigate coherence between oscillations in the IPL and BA 9 to test whether the readout of relevant information is mechanistically implemented through gamma-band synchronization between memory fields in parietal and prefrontal areas. In addition, decoding approaches applied to eye position data in combination with spectral measures of delay activity in parietal and prefrontal cortex may help to further clarify the mechanistic function of gamma-band activity in the IPL and BA 9.

Finally, we believe that the current findings are also important for future research investigating the pathophysiology of neuropsychiatric disorders, such as schizophrenia. Aberrant PFC activity has been linked to recall deficits in working memory (Goldberg et al., 1989), a core deficiency in schizophrenia. In addition, there is evidence that gamma-band activity is impaired in patients with schizophrenia (Uhlhaas and Singer, 2010), suggesting a possible contribution of dysfunctional gamma-band oscillations in PFC towards WM impairments in the disorder.

3.7 Acknowledgements

This work was supported by the Max-Planck society and the LOEWE Grant 'Neuronale Koordination Forschungsschwerpunkt Frankfurt'.

3.8 References

Axmacher, N., Henseler, M.M., Jensen, O., Weinreich, I., Elger, C.E., and Fell, J. (2010). Cross-frequency coupling supports multi-item working memory in the human hippocampus. Proc. Natl. Acad. Sci. U.S.A. 107, 3228–3233.

Baddeley, A. (2003). Working memory: looking back and looking forward. Nat Rev Neurosci 4, 829–839.

Ben Hamed, S., Duhamel, J.R., Bremmer, F., and Graf, W. (2001). Representation of the visual field in the lateral intraparietal area of macaque monkeys: a quantitative receptive field analysis. Exp Brain Res 140, 127–144.

Blatt, G.J., Andersen, R.A., and Stoner, G.R. (1990). Visual receptive field organization and cortico-cortical connections of the lateral intraparietal area (area LIP) in the macaque. J. Comp. Neurol 299, 421–445.

du Boisgueheneuc, F., Levy, R., Volle, E., Seassau, M., Duffau, H., Kinkingnehun, S., Samson, Y., Zhang, S., and Dubois, B. (2006). Functions of the left superior frontal gyrus in humans: a lesion study. Brain 129, 3315–3328.

Busch, N.A., and Herrmann, C.S. (2003). Object-load and feature-load modulate EEG in a short-term memory task. Neuroreport 14, 1721– 1724.

Buzsáki, G., and Draguhn, A. (2004). Neuronal oscillations in cortical networks. Science 304, 1926–1929.
Cowan, N. (2001). The magical number 4 in short-term memory: a reconsideration of mental storage capacity. Behav Brain Sci 24, 87– 114; discussion 114–185.
Van Der Werf, J., Jensen, O., Fries, P., and Medendorp, W.P. (2010). Neuronal synchronization in human posterior parietal cortex during reach planning. J. Neurosci. 30, 1402–1412.
Duda, R.O., Hart, P.E., and Stork, D.G. (2002). Pattern classification (Wiley: Wiley-Interscience).
Feredoes, E., Heinen, K., Weiskopf, N., Ruff, C., and Driver, J. (2011). Causal evidence for frontal involvement in memory target maintenance by posterior brain areas during distracter interference of visual working memory. Proc. Natl. Acad. Sci. U.S.A. 108, 17510– 17515.
Fries, P. (2005). A mechanism for cognitive dynamics: neuronal communication through neuronal coherence. Trends Cogn. Sci. (Regul. Ed.) 9, 474–480.
Fuentemilla, L., Penny, W.D., Cashdollar, N., Bunzeck, N., and Düzel, E. (2010). Theta-coupled periodic replay in working memory. Curr. Biol 20, 606–612.
Funahashi, S., Bruce, C.J., and Goldman-Rakic, P.S. (1989). Mnemonic coding of visual space in the monkey's dorsolateral prefrontal cortex. J. Neurophysiol 61, 331–349.
Funahashi, S., Bruce, C.J., and Goldman-Rakic, P.S. (1993). Dorsolateral prefrontal lesions and oculomotor delayed-response performance: evidence for mnemonic "scotomas."J. Neurosci 13, 1479–1497.
Goldberg, T.E., Weinberger, D.R., Pliskin, N.H., Berman, K.F., and Podd, M.H. (1989). Recall memory deficit in schizophrenia. A possible manifestation of prefrontal dysfunction. Schizophr. Res. 2, 251–257.
Gross, J., Kujala, J., Hamalainen, M., Timmermann, L., Schnitzler, A., and Salmelin, R. (2001). Dynamic imaging of coherent sources: Studying neural interactions in the human brain. Proc. Natl. Acad. Sci. U.S.A 98, 694–699.
Haegens, S., Osipova, D., Oostenveld, R., and Jensen, O. (2010). Somatosensory working memory performance in humans depends on both engagement and disengagement of regions in a distributed network. Human Brain Mapping 31, 26–35.
Harrison, S.A., and Tong, F. (2009). Decoding reveals the contents of visual working memory in early visual areas. Nature 458, 632–635.
Hebb (1949). The organization of behavior. (New York: Wiley).
Herrmann, C.S., Senkowski, D., and Röttger, S. (2004). Phase-locking and amplitude modulations of EEG alpha: Two measures reflect different cognitive processes in a working memory task. Exp Psychol 51, 311–318.
Howard, M.W., Rizzuto, D.S., Caplan, J.B., Madsen, J.R., Lisman, J., Aschenbrenner-Scheibe, R., Schulze-Bonhage, A., and Kahana, M.J. (2003). Gamma Oscillations Correlate with Working Memory Load in Humans. Cerebral Cortex 13, 1369 –1374.
Hummel, F., Andres, F., Altenmüller, E., Dichgans, J., and Gerloff, C. (2002). Inhibitory Control of Acquired Motor Programmes in the Human Brain. Brain 125, 404–420.
Isoda, M., and Tanji, J. (2004). Participation of the primate presupplementary motor area in sequencing multiple saccades. J. Neurophysiol. 92, 653–659.
Jensen, O., Gelfand, J., Kounios, J., and Lisman, J.E. (2002a). Oscillations in the alpha band (9-12 Hz) increase with memory load during retention in a short-term memory task. Cereb. Cortex 12, 877–882.
Jensen, O., Gelfand, J., Kounios, J., and Lisman, J.E. (2002b). Oscillations in the alpha band (9-12 Hz) increase with memory load during retention in a short-term memory task. Cereb. Cortex 12, 877–882.
Jensen, O., Kaiser, J., and Lachaux, J.-P. (2007). Human gamma-frequency oscillations associated with attention and memory. Trends Neurosci 30, 317–324.
Jensen, O., and Tesche, C.D. (2002). Frontal theta activity in humans increases with memory load in a working memory task. Eur. J. Neurosci 15, 1395–1399.
Jokisch, D., and Jensen, O. (2007). Modulation of Gamma and Alpha Activity During a Working Memory Task Engaging the Dorsal or Ventral Stream. J. Neurosci. 27, 3244–3251.
Knops, A., Thirion, B., Hubbard, E.M., Michel, V., and Dehaene, S. (2009). Recruitment of an area involved in eye movements during mental arithmetic. Science 324, 1583–1585.
Leiberg, S., Lutzenberger, W., and Kaiser, J. (2006). Effects of memory load on cortical oscillatory activity during auditory pattern working memory. Brain Res. 1120, 131–140.
Lisman, J. (2010). Working memory: the importance of theta and gamma oscillations. Curr. Biol 20, R490–492.
Lisman, J.E., and Idiart, M.A. (1995). Storage of 7 +/- 2 short-term memories in oscillatory subcycles. Science 267, 1512–1515.
Maris, E., and Oostenveld, R. (2007). Nonparametric statistical testing of EEG- and MEG-data. J. Neurosci. Methods 164, 177–190.
Medendorp, W.P., Kramer, G.F.I., Jensen, O., Oostenveld, R., Schoffelen, J.- M., and Fries, P. (2007). Oscillatory activity in human parietal and occipital cortex shows hemispheric lateralization and memory effects in a delayed double-step saccade task. Cereb. Cortex 17, 2364–2374.
Meltzer, J.A., Zaveri, H.P., Goncharova, I.I., Distasio, M.M., Papademetris, X., Spencer, S.S.,

Spencer, D.D., and Constable, R.T. (2008). Effects of working memory load on oscillatory power in human intracranial EEG. Cereb. Cortex 18, 1843–1855.
Miller, E.K., and Desimone, R. (1994). Parallel neuronal mechanisms for short-term memory. Science 263, 520–522.
Mitra, PP., Bokil, H. (2008). Observed Brain Dynamics (New York: Oxford University Press).
Müri, R.M., Rivaud, S., Vermersch, A.I., Léger, J.M., and Pierrot-Deseilligny, C. (1995). Effects of transcranial magnetic stimulation over the region of the supplementary motor area during sequences of memory-guided saccades. Exp Brain Res 104, 163–166.
Nolte, G. (2003). The magnetic lead field theorem in the quasi-static approximation and its use for magnetoencephalography forward calculation in realistic volume conductors. Phys. Med. Biol. 48, 3637–3652.
Onton, J., Delorme, A., and Makeig, S. (2005). Frontal midline EEG dynamics during working memory. Neuroimage 27, 341–356.
Oostenveld, R., Fries, P., Maris, E., and Schoffelen, J.-M. (2011). FieldTrip: Open source software for advanced analysis of MEG, EEG, and invasive electrophysiological data. Comput Intell Neurosci 2011, 156869.
Palva, J.M., Monto, S., Kulashekhar, S., and Palva, S. (2010). Neuronal synchrony reveals working memory networks and predicts individual memory capacity. Proc. Natl. Acad. Sci. U.S.A. 107, 7580–7585.
Palva, S., Kulashekhar, S., Hämäläinen, M., and Palva, J.M. (2011). Localization of cortical phase and amplitude dynamics during visual working memory encoding and retention. J. Neurosci. 31, 5013– 5025.
Pesaran, B., Pezaris, J.S., Sahani, M., Mitra, P.P., and Andersen, R.A. (2002). Temporal structure in neuronal activity during working memory in macaque parietal cortex. Nat Neurosci 5, 805–811.
Pfurtscheller, G., Neuper, C., Andrew, C., and Edlinger, G. (1997). Foot and hand area mu rhythms. Int J Psychophysiol 26, 121–135.
Rainer, G., Asaad, W.F., and Miller, E.K. (1998). Selective representation of relevant information by neurons in the primate prefrontal cortex. Nature 393, 577–579.
Rouder, J.N., Morey, R.D., Morey, C.C., and Cowan, N. (2011). How to measure working memory capacity in the change detection paradigm. Psychon Bull Rev 18, 324–330.
Sauseng, P., Klimesch, W., Doppelmayr, M., Pecherstorfer, T., Freunberger, R., and Hanslmayr, S. (2005). EEG alpha synchronization and functional coupling during top-down processing in a working memory task. Hum Brain Mapp 26, 148–155.
Sauseng, P., Klimesch, W., Heise, K.F., Gruber, W.R., Holz, E., Karim, A.A., Glennon, M., Gerloff, C., Birbaumer, N., and Hummel, F.C. (2009). Brain oscillatory substrates of visual short-term memory capacity. Curr. Biol 19, 1846–1852.
Stanislaw, H., and Todorov, N. (1999). Calculation of signal detection theory measures. Behav Res Methods Instrum Comput 31, 137–149.
Sumner, P., Nachev, P., Morris, P., Peters, A.M., Jackson, S.R., Kennard, C., and Husain, M. (2007). Human medial frontal cortex mediates unconscious inhibition of voluntary action. Neuron 54, 697–711.
Tallon-Baudry, C., Bertrand, O., Peronnet, F., and Pernier, J. (1998). Induced gamma-band activity during the delay of a visual short-term memory task in humans. J. Neurosci 18, 4244–4254.
Uhlhaas, P.J., and Singer, W. (2010). Abnormal neural oscillations and synchrony in schizophrenia. Nat. Rev. Neurosci 11, 100–113.
Vogel, E.K., McCollough, A.W., and Machizawa, M.G. (2005). Neural measures reveal individual differences in controlling access to working memory. Nature 438, 500–503.
Wager, T.D., and Smith, E.E. (2003). Neuroimaging studies of working memory: a meta-analysis. Cogn Affect Behav Neurosci 3, 255–274.
Worden, M.S., Foxe, J.J., Wang, N., and Simpson, G.V. (2000). Anticipatory biasing of visuospatial attention indexed by retinotopically specific alpha-band electroencephalography increases over occipital cortex. J. Neurosci. 20, RC63.
Yamanaka, K., Yamagata, B., Tomioka, H., Kawasaki, S., and Mimura, M. (2010). Transcranial magnetic stimulation of the parietal cortex facilitates spatial working memory: near-infrared spectroscopy study. Cereb. Cortex 20, 1037–1045.

4

The Phase of Thalamic Alpha Activity Entrains Cortical Gamma-Band Activity in Parietal Cortex: Evidence from Resting State MEG Recordings

As submitted in: Frederic Roux, Michael Wibral, Wolf Singer, Jaan Aru, and Peter Uhlhaas (2012): The Phase of Thalamic Alpha Activity Entrains Cortical Gamma-Band Activity in Parietal Cortex: Evidence from Resting State MEG Recordings. Journal of Neuroscience.

4.1 Abstract

Recent findings have implicated thalamic alpha oscillations in the phasic modulation of cortical activity. However, the precise relationship between thalamic alpha oscillations and neocortical activity remain unclear. Here we show in a large sample of healthy participants (n = 45) using beamforming and measures of phase amplitude coupling that the amplitude of gamma-band activity in posterior medial parietal cortex is modulated by the phase of thalamic alpha oscillations during eyes close resting state. In addition, our findings show that gamma-band activity in visual cortex was not modulated by thalamic alpha oscillations but coupled to the phase of strong local alpha activity. To overcome the limitations of electromagnetic source localization we estimated conduction delays using transfer entropy and found non-spurious information transfer from thalamus to cortex. The present findings provide novel evidence for a phase coupling between cortical gamma-band activity and thalamic alpha oscillations which highlight the role of phasic inhibition in the coordination cortical activity.

4.2 Introduction

A growing body of evidence implicates rhythmic activity in the alpha-band (8-13Hz) as a core feature of cortical communication (Jensen and Mazaheri, 2010) and cognition (VanRullen and Koch, 2003). This is supported by evidence demonstrating that the phase of the alpha cycle modulates neural firing (Haegens et al., 2011), perceptual detection rates (Varela et al., 1981; Dugué et al., 2011) and brain metabolism (Scheeringa et al., 2011), suggesting that alpha-band oscillations exert critical influence on the excitability level of neocortical networks and on the timing of neuronal responses (Klimesch et al., 2007; Jensen and Mazaheri, 2010).

One brain region which could be crucially involved in this process is the thalamus, a key structure involved in the generation of alpha oscillations (Da Silva et al., 1973; Jahnsen and Llinás, 1984; Bollimunta et al., 2011). Recent data show that alpha-band rhythms generated in the thalamus are linked with the temporal coordination of spiking activity in thalamo-cortical (TC) circuits (Lorincz et al., 2009; Vijayan and Kopell, 2012), providing important support for the inhibition-timing hypothesis that alpha oscillations control the output of cortical networks via phasic inhibition (Klimesch et al., 2007).

Moreover there is emerging evidence that information transfer from thalamus to cortex is mediated via TC synchronization at alpha frequencies (Saalmann et al., 2012), raising the possibility that TC alpha activity may also contribute to the modulation of cortical gamma-band activity. However, evidence for this relationship is so far lacking.

To investigate this question, we recorded resting state activity in a large sample (N=45) of healthy participants with magnetoencephalogaphy (MEG). We focused on interactions between alpha (8-13Hz) and gamma (30-70Hz) activity because previous work has indicated that activity in the gamma-band reflects active neuronal processing (Fries et al., 2007) and is modulated by the phase of task related and spontaneous alpha oscillations (Chorlian et al., 2006; Osipova et al., 2008; Cohen et al., 2009; Voytek et al., 2010; Foster and Parvizi, 2012; Saalmann et al., 2012; Spaak et al., 2012; Yanagisawa et al., 2012). Using a whole brain analysis as well as seed region based analysis of phase-amplitude coupling (PAC) at source-level, we examined the temporal framing of neocortical gamma-band activity by the phase of cortical and thalamic alpha oscillations. Finally, we tested the physiological validity of our findings using transfer entropy (TE) to control for spurious TC interactions resulting from volume conduction.

4.3 Methods

MEG Data Acquisition and Preprocessing. 4 minutes of eyes closed spontaneous MEG-activity were recorded (sampling rate: 1.2 KHz, low-pass filter: 600 Hz) using a whole-head MEG system with 275 axial gradiometers (Omega 2005, VSM MedTech Ltd., BC, Canada) from n = 45 healthy adult participants which were aged between 18 and 27 years old [mean age: 20.5 years ; SD: 2; 24 females]. The study was approved by the ethics committee of the Goethe University Frankfurt, and written informed consent was obtained from participants prior to the recording. The vertical and horizontal electro-oculogram (EOG) was recorded to monitor eye movements for artifacts. Partial artifact rejection was performed by rejecting segments of the trials containing eye-blinks, muscle and SQUID artifacts. On average, 163 s ± 53 s of artifact free data underwent subsequent analysis. In addition, independent component analysis (ICA) (Bell and Sejnowski, 1995) was used to remove cardiac activity and eye movements.

Structural MRI Data Acquisition. Structural MRIs were obtained with a 3-T Siemens Allegra scanner device (Siemens, Erlangen, Germany) using the standard CP birdcage head-coil and a T1 sequence. Eleven participants met an exclusion criterion for MRI scans and were not included for source-analyses.

Data Analysis

Source Localization. A linearly constrained minimum variance (LCMV) beamformer algorithm (Sekihara et al., 2004) was used to generate maps of source activity in a spatial grid of 4590 points with a resolution of 1 cm. Co-registration with MNI coordinates was based on three fiducial coils placed on the nasion and the left and right pre-auricular ridges. The forward solution for each participant was estimated from individual head models using a common dipole grid in MNI space which was warped onto the anatomy of each participant and a realistic single-shell volume conductor model (Nolte, 2003). Virtual electrodes were estimated for each grid location by calculating the beamformer weights from the sensor covariance matrix and multiplying the bandpass filtered sensor signals with the beamformer weights.

Spectral Analysis. Spectral power was estimated for MEG signals at sensor level at frequencies between 1 and 100 Hz, using multi-taper spectral analysis. The spectrogram for MEG sensor signals was computed from windows of 10 s which were displaced in time at 1 s steps and a spectral concentration of 1.5 Hz per frequency bin using 29 slepian tapers.

Cross-Frequency Coupling

Alpha-Gamma Phase-Amplitude Coupling. Phase-amplitude coupling (PAC) was estimated following previously described approaches (Sauseng et al., 2009; Miller et al., 2010). In brief, a phase time series $\Phi(t)$ is estimated for every sample of an MEG sensor or source time series x(t) using Morlet wavelets (Tallon-Baudry and Bertrand, 1999) and $\Phi(t)$ is sorted into values ranging from $-\pi$ to π (rad). We estimated $\Phi(t)$ for frequencies ranging from 1 to 15 Hz to be able to detect possible PAC effects occurring between gamma-band amplitude and slower rhythms. The amplitude of gamma-band activity $\gamma(t)$ was obtained by first band-pass filtering x(t) between 30 and 70 Hz using a 4th order butterworth filter. Next we applied the Hilbert transform to x(t) to obtain a complex time series h(t), and $\gamma(t)$ was estimated from the absolute value of h(t). Finally, $\gamma(t)$ was log transformed before the z-score was computed by demeaning and dividing $\gamma(t)$ by the standard deviation. To prevent artifacts arising from aliasing, the cutoff for the upper limit of frequencies at which $\Phi(t)$ was estimated was set to 15 Hz, so that the upper frequency limit used to estimate $\Phi(t)$ and the lower frequency bound used for the estimation of $\gamma(t)$ were separated by a factor of two. Finally, the samples of $\gamma(t)$ were aligned in time with the samples of the sorted phase time series $\Phi(t)$ and averaged over 51 equally wide phase bins. This resulted in a phase-amplitude distribution for every frequency between 1 and 15 Hz.

Modulation Index. In order to map the alpha-gamma PAC in source space we computed the Modulation Index (MI) from alpha-gamma phase-amplitude distributions computed from virtual channel activity. The MI is an adaptation of the Kullback-Leibler divergence (Kullback and Leibler, 1951) and measures the distance of an empirical amplitude distribution over phase bins from the uniform distribution. The assumption underlying this metric is that MI values reflect the degree of PAC between two frequency bands. Therefore, grid points with high MI values reflect a higher degree of PAC as compared to grid points with lower MI values (see (Tort et al., 2010) for more details).

Thalamo-Cortical Information Transfer

Thalamo-Cortical Alpha-Gamma Phase-Amplitude Coupling. Similarly, TC alpha-gamma coupling was estimated by computing phase time series at alpha frequencies (8-13 Hz) using two spatial filters located in the left (x = -10, y = -20, z = 10) and right (x = 10, y = -20, z= 10) thalamus. Our approach is thus similar to the methodology employed by previous MEG studies which have successfully measured thalamo-cortical synchronization with a sensitivity of 2cm around thalamic regions (Lou et al., 2010). MI values were then calculated from

the distribution of gamma-band amplitude with respect to the thalamic alpha phase for each point within the grid.

Transfer Entropy. Because phase estimates in source space can be biased by the limited spatial resolution of electromagnetic source imaging, we measured TC conduction delays using delay sensitive TE (Schreiber, 2000) to control for spurious TC information transfer. TE was computed based on the reconstructed state-space. Reconstruction parameters were optimized using Ragwitz' criterion to ensure optimal self prediction. Delay sensitive TE was computed from thalamus to cortex with individual embedding parameters for each participant and connection.

Thalamo-Cortical Phase Synchronization. Phase synchronization between thalamus and cortex was measured by means of the phase locking value (PLV) (Lachaux et al., 1999) for phase time series obtained using Morlet wavelets for frequencies between 1 and 100 Hz.

Statistical Analysis

Statistical Significance at Sensor Level. At MEG sensor level, the statistical significance of the estimated PAC was assessed by randomly shifting the phase time series in time by at least 5001 points with respect to the time course of gamma-band amplitude for every MEG channel and frequency between 1 and 15 Hz. The mean average gamma-band amplitude was then recalculated as a function of phase for the shifted amplitude time series. This procedure was repeated 200 times in order to obtain the average shifted PAC. A non-parametric permutation based Monte-Carlo approach was used to estimate the significance of the empirical PAC between cortical rhythms in the 1-15 Hz range and gamma-band amplitude as compared to the average shifted data. In short, this approach consists in calculating dependent t-values for each frequency and phase bin and every channel to measure the consistency of the difference between the empirical and shifted data across participants and comparing these t-values to a distribution of t-values calculated from randomly recomposed empirical and shifted datasets. A cluster-algorithm based approach was then used to correct for multiple comparisons (Maris and Oostenveld, 2007). The threshold for the clustering entry level and for statistical significance of the clusters was $p < 0.01$ (corrected).

Statistical Significance of Phase-Amplitude Coupling at Source Level. To assess the statistical significance of alpha-gamma coupling at source level we

compared empirical MI values to MI values estimated from shifted data using the same permutation based Monte-Carlo approach that was used to assess the statistical significance of alpha-gamma PAC at sensor level. At the source level dependent t-values were calculated to contrast the MI values estimated from empirical data against MI values estimated from shifted data for each grid point in source space. These t-values hence measure the consistency of the difference between empirical and shifted MI values across participants. The threshold for the clustering entry level and statistical significance of the clusters was $p < 0.01$ (corrected).

Statistical Significance of Transfer Entropy. We used permutation testing ($n = 5*10^6$ permutations) (Lindner et al., 2011) to compare the empirical TE values against values obtained from surrogate data sets. Surrogate data was generated by shifting the source time series (thalamus) with respect to the target time series (cortex). For each participant, results where thresholded at a level of $p < 0.05$ (uncorrected). Second level group level statistics for the presence of links were then performed using one-sided binomial tests (binomial-distribution) with a significance level of $p < 0.05$ (Bonferroni corrected). In addition, we carried out a shift test to reject false positive transfer entropy due to volume conduction effects (Lindner et al., 2011).

Analysis software

All analyses were performed using custom MATLAB scripts as well as open source MATLAB toolboxes (fieldtrip: http://www.fieldtrip.fcdonders.nl/; chronux: http://www.chronux.org/; SPM2: http://www.fil.ion.ucl.ac.uk/spm/ ; TRENTOOL: http://www.trentool.de/).

4.4 Results

Spectral Estimates at Sensor Level. We observed a peak of spectral power at 10 Hz in the grand average power spectrum as well as in the distribution of peak frequencies (Fig. 5.1A-B). In addition, we found a negative correlation between spectral power in the 8-13 Hz and 30-70 Hz frequency ranges which was significant in 36 of 45 (80%) participants (mean Pearson correlation coefficient -0.38; SD = 0.24; $P < 0.05$; $P < 0.0001$; Binomial-test; two-sided; Fig. 5.1C-D).

Phase-Amplitude Coupling at Sensor Level. Time-frequency representations of epochs which were phase aligned with the occipital alpha rhythm revealed a strong phasic entrainment of spectral power in the 30-70 Hz

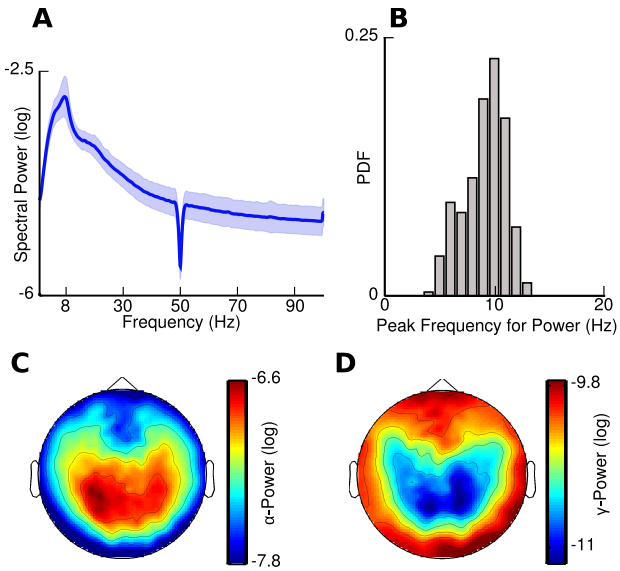

Figure 4.1: **Spectral power at sensor level. A,B:** Grand average power spectrum (A) of resting state activity and probability density function (PDF) of peak frequencies (B) showing strong activity in the alpha-band. **C,D:** Topographies of log transformed (C) alpha- (8-13H) and (D) gamma-band (30-70Hz) power.

frequency range (Fig. 5.1A). This was confirmed by the topography of statistical t-values which revealed two peaks of significant PAC over left and right occipital channels (Fig. 5.2B). In addition, phase-frequency representations of statistical t-values revealed that the amplitude of 30-70Hz activity was significantly modulated by the phase of frequencies in the alpha range (8-15Hz) and that gamma-band activity was either in phase or anti-phase with the alpha cycle over left or right sensors respectively ($P < 0.01$; t-test;two-sided; corrected; Fig. 5.2B-C).

Cortical Sources of Alpha-Gamma Phase-Amplitude Coupling. Similarly to our results at sensor level, we observed two spatially separated clusters of modulation index (MI) values in the left and right occipital regions comprising Brodmann area 18 (BA 18) and the cuneus (Fig. 5.3A; Table 1). The peak of the histogram of mean gamma-band amplitude values over local alpha phase bins was shifted towards the descending phase of the alpha cycle ($\pi/2$ rad) and there was a trend towards a positive correlation between the phase bins at which occipital gamma-band amplitudes were highest across both hemispheres ($r = 0.29$; $P = 0.06$; Fisher's correlation coefficient for circular data; Fig. 5.3B-E).

Thalamic Sources of Alpha-Gamma Phase-Amplitude Coupling. Based on prior findings which have highlighted the importance of thalamic oscillations for the phasic control of spiking activity in TC circuits (Lorincz et al., 2009; Vijayan and Kopell, 2012), we estimated the phase of thalamic alpha activity from two virtual electrodes in the thalamus and examined the coupling of brain wide gamma-band activity to the phase of the thalamic alpha rhythm. This

approach revealed that TC alpha-gamma PAC was significant in posterior medial parietal areas, comprising the left and right precuneus as well as the right posterior cingulate area ($P < 0.01$; t-test; two-sided; corrected; Fig. 5.4A-B; Table 2). Moreover, the histogram of mean gamma-band amplitude values was flushlefted at the peak of the thalamic alpha phase (0 rad), and there was a positive and significant correlation between phase bins at which cortical gamma-band activity reached maxima in both hemispheres ($r = 0.36$; $P < 0.05$; Fisher's correlation coefficient for circular data; Fig. 5.4C-F). Furthermore, alpha power in the posterior medial parietal cortex was greatly reduced as compared to alpha power in the visual cortex ($P < 0.001$; two-sided t-test).

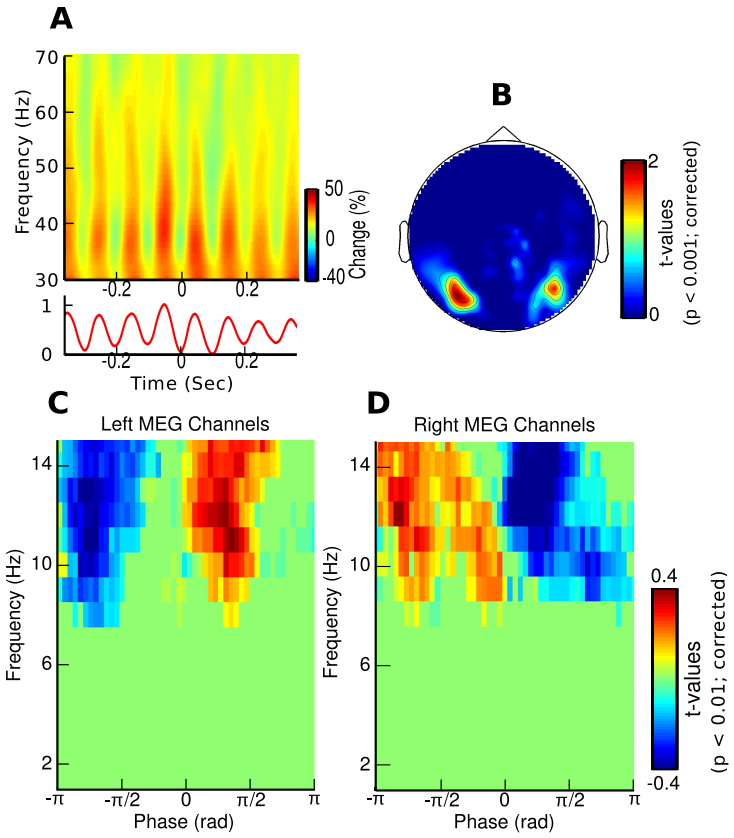

Figure 4.2: **Alpha-gamma PAC at sensor level. A:** Time-frequency representation of epochs phase aligned with occipital alpha activity. **B:** Topography of statistical t-values averaged over significant frequencies ($P < 0.01$; dependent t-test; two-sided; corrected) for the comparison of alpha-gamma PAC with shifted data at sensor level. **C,D:** Average phase-frequency maps of statistical t-values for MEG sensors showing significant PAC for different alpha phases. The pseudo colors indicate increased (warm colors) and decreased (cold colors) gamma-band activity as compared to shifted data.

Thalamo-Cortical Information Transfer. We observed that phase synchronization between the thalamus and the cortical regions which showed significant coupling with the phase of thalamic alpha activity was particularly enhanced at alpha frequencies (Fig. 5.4E). To control that thalamic phase estimates were not confounded by the limited resolution of electromagnetic source localization, we estimated conduction latencies from thalamus to cortex using TE analysis and found non-spurious TC information transfer as well as

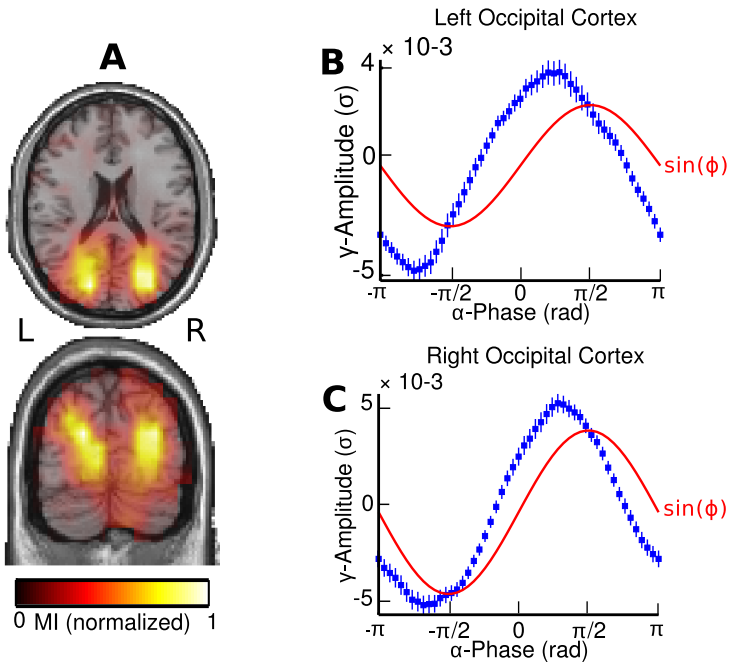

Figure 4.3: **Alpha-gamma PAC at source level. A:** Source maps of normalized MI values displayed on axial and coronal sections of the MNI template brain. The map shows two clusters of MI values in the left and right visual cortex, indicating enhanced local PAC in the visual cortex. **B,C:** Cortical gamma-band amplitude as a function of local alpha phase averaged over grid points in the left (B) and right (C) visual cortex. Error bars represent standard error of mean (SEM); red line represents the fit of a sinusoidal function ($\sin(\phi)$) to the data.

physiologically realistic conduction delays (range: 12.5-19.8 ms; mean: 15.8 ms; standard deviation: 2.4 ms; binomial test, $P < 0.01$; FDR corrected; Fig. 5.4F).

4.5 Discussion

The goal of the present study was to examine the relationship between thalamic alpha oscillations and neocortical gamma-band activity in resting-state MEG recordings. The thalamus has been involved in the regulation of information transmission to the cortex via the modulation of response magnitude, firing mode, and synchrony of neurons (Saalmann and Kastner, 2009), but it remains unclear how the thalamus coordinates the output of cortical networks. Alpha oscillations are a prominent feature of electrophysiological resting state recordings in humans and have been linked with phasic inhibition (Klimesch et al., 2007), which has been suggested as an effective mechanism to regulate the output of cortical networks (Jensen and Mazaheri, 2010).

Consistent with previous work examining interactions between alpha- and gamma-band oscillations (Chorlian et al., 2006; Osipova et al., 2008; Cohen et al., 2009; Voytek et al., 2010; Foster and Parvizi, 2012; Saalmann et al., 2012; Spaak et al., 2012; Yanagisawa et al., 2012), we observed that local gamma-band activity was coupled to the phase of the alpha-band rhythm which was most

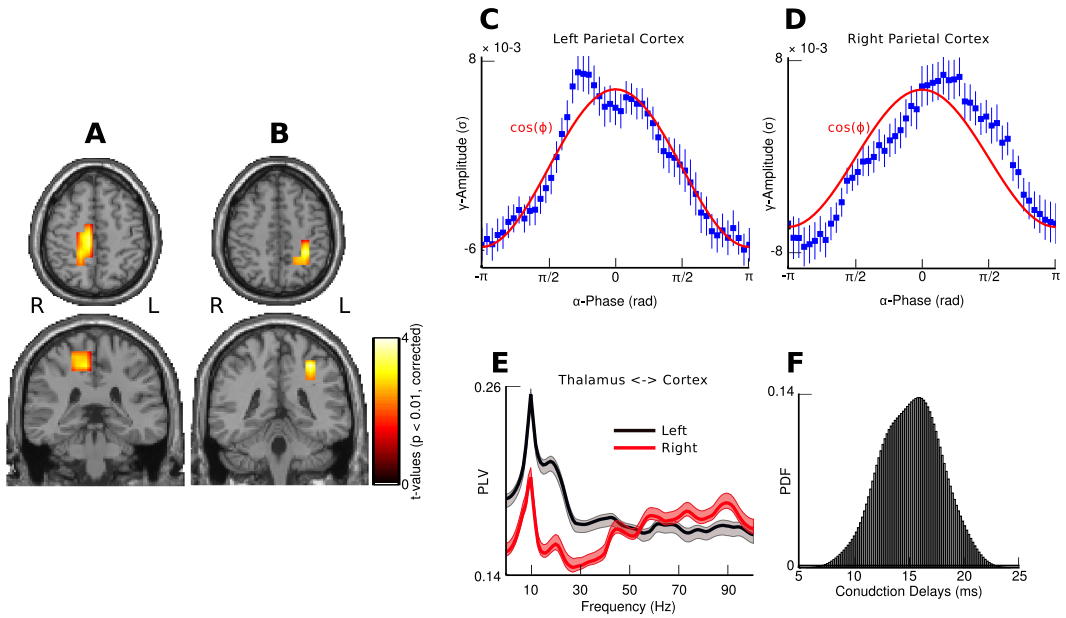

Figure 4.4: **Thalamo-cortical PAC. A,B:** Statistical source maps of t-values (P<0.01; dependent t-test; two-sided; corrected) for the comparison of thalamo-cortical alpha-gamma PAC with shifted data for seed regions in the left (A) and right (B) thalamus. **C,D:** Cortical gamma-band amplitude as a function of thalamic alpha phase averaged over grid points in the left (C) and right (D) posterior medial parietal cortex. Error bars represent SEM, and the red line represent the fit of a cosine function ($\cos(\phi)$) to the data. **E:** Phase synchronization between the thalamus and posterior medial parietal areas in the left (black) and right (red) hemisphere for frequencies from 1 to 100 Hz. Phase synchronization was measured by means of the phase locking value (PLV). H: PDF of thalamo-cortical conduction delays as measure by TE (mean: 15.8 ms; SD: 2.4 ms).

pronounced over the visual cortex, suggesting that fluctuations of broad-band gamma-band activity are linked to the phase of the alpha cycle. Moreover, source-space wide testing of PAC revealed that fluctuations of gamma-band activity in the visual cortex were greatest near the trough of local alpha activity.

In contrast, TC alpha-gamma coupling became significant only in posterior medial parietal cortex where cortical gamma-band activity was greatest at the peak of the thalamic alpha rhythm. Importantly, TE analysis revealed significant and directed information transfer from the thalamus to posterior-medial parietal cortex with TC conduction latencies of 15 ms which are in agreement with previously reported thalamo-cortical delays (Ribary et al., 1991; Alloway et al., 1993). Thus, the results of the TE analysis show that the present results reflect physiological meaningful information transfer and not simple volume conduction and highlight the crucial role of thalamic alpha oscillations in the phasic control over neocortical gamma-band activity.

TC-Synchronizationa and Phasic Inhibition. Our data are in line with experimental studies and theoretical models of TC alpha oscillations which highlight the crucial role of thalamic activity on neocortical networks. Specifically, data from electrophysiological in vitro recordings and computational models of TC circuits show that during strong phasic inhibition the spiking of

relay-mode neurons and pyramidal cells will occur near the trough of the alpha cycle, whereas during weaker inhibition spiking activity will be coupled to the peak of the alpha cycle (Lorincz et al., 2009; Vijayan and Kopell, 2012). In agreement with these findings, one possible implication of our data is that the differential temporal framing of cortical gamma-band activity reflects differences in the strength of phasic inhibition in TC networks (Figure 5.5).

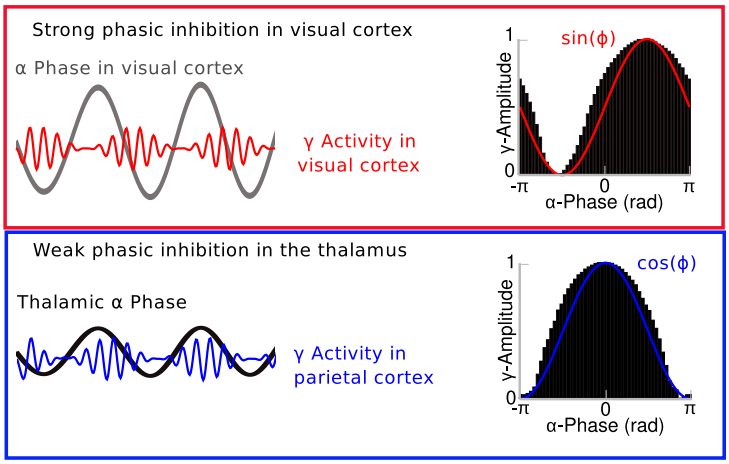

Figure 4.5: **Cartoon illustrating the possible implication of differential alpha-gamma coupling (synthetic data shown for illustration).** The cartoon is based on the present findings and results reported by Lörincz et al. (2009) and Vijayan and Kopell (2012). **Upper panel:** Strong input (burst mode) to inhibitory interneurons in the thalamus will result in the occurrence of cortical gamma-band activity near the trough of cortical alpha oscillations. Accordingly, cortical gamma-band activity will occur during strong TC inhibition, thereby reducing the probability of signal propagation to other areas. **Lower panel:** Weak inputs (single spike mode) to thalamic interneurons will result in the occurrence of cortical gamma-band activity near the peak of thalamic alpha oscillations, ie during reduced inhibition. As a result, the output of an area may become more efficient in driving other regions. Note that when gamma-band activity occurs near the trough of the alpha cylce the phase-amplitude distribution will have the shape of a $\sin(\phi)$ function, whereas the occurrence of gamma-band activity near the peak of alpha will resemble a $\cos(\phi)$ function (synthetic data).

We observed that gamma-band power in posterior medial parietal cortex was greatest at the peak of thalamic alpha activity, while in the visual cortex gamma-band was strongest near the trough of the alpha cycle. This differential coupling could reflect a selective routing of gamma-band activity in TC networks engaged in self-referential processes and that the thalamus exerts a directed influence on the precuneus and the posterior cingulate cortex, two brain regions that have important anatomical connections with the dorsal part and the higher associative nuclei of the thalamus (Morgane et al., 2005; Cavanna and Trimble, 2006) and which form central hubs in the default mode resting state network (DMN) (Gusnard et al., 2001; Raichle et al., 2001; Raichle and Snyder, 2007).

In contrast, phase-relationships between alpha-band oscillations and gamma-band activity in visual regions occurred at the trough of the alpha-cycle suggesting a reduction in excitability levels in visual regions during the absence of visual input. Thus, the differential entrainment of neocortical gamma-band

activity through the phase of thalamic and local alpha-band oscillations is likely to support the emergence of state-dependent networks through the modulation of cortical excitability (Fig. 5.5) whereby networks that are engaged in the processing of activity in the absence of sensory input are enhanced while activity in sensory regions is reduced. This hypothesis is supported by fMRI- and combined EEG/fMRI-studies which demonstrate that during eyes closed resting state alpha power in the visual cortex is associated with a decrease of functional connectivity between the visual cortex and the thalamus (Scheeringa et al., 2012) while functional connectivity between the thalamus and the posterior medial parietal cortex is enhanced (Gur et al., 1995).

4.6 Conclusions

In summary, our data provide novel evidence for a central role of thalamic alpha-band oscillations in the coordination of neocortical networks as well as in the occurrence of cross-frequency coupling between alpha and gamma-band activity. Our data address both of these central issues through showing for the first time that the phase of thalamic alpha-band oscillations entrains cortical gamma-band activity. Accordingly, these findings support the hypothesis that phasic inhibition in thalamo-cortical circuits may importantly contribute to coordinate neocortical activity.

Importantly, the present findings highlight that large scale interactions in brain wide networks can be measured using non-invasive recording techniques such as MEG despite the limited spatial resolution of electromagnetic source localization. The present approach may thus provide important insights on the role of the thalamus in the context of task-related MEG/EEG recordings.

In addition to understanding normal brain functioning, it is likely that our findings are relevant for psychiatric disorders, such as schizophrenia and attention deficit hyperactivity disorders (ADHD). In both diseases, dysfunctional TC-interactions play an important role (O'Donnell and Grace, 1998; Pinault, 2011; Li et al., 2012). Such an impairment may result in the loss of the ability to amplify or suppress relevant and irrelevant streams of information, a core deficit observed in both disorders (Butler et al., 2005; Doyle, 2006).

4.7 Acknowledgements

This work was supported by the Max-Planck society, the LOEWE Grant 'Neuronale Koordination Forschungsschwerpunkt Frankfurt' and the Basque

Center on Cognition, Brain, and Language Cognition (BCBL).

4.8 References

Alloway KD, Johnson MJ, Wallace MB (1993) Thalamocortical interactions in the somatosensory system: interpretations of latency and cross-correlation analyses. J Neurophysiol 70:892–908.

Bell AJ, Sejnowski TJ (1995) An information-maximization approach to blind separation and blind deconvolution. Neural Comput 7:1129–1159.

Bollimunta A, Mo J, Schroeder CE, Ding M (2011) Neuronal mechanisms and attentional modulation of corticothalamic α oscillations. J Neurosci 31:4935–4943.

Butler PD, Zemon V, Schechter I, Saperstein AM, Hoptman MJ, Lim KO, Revheim N, Silipo G, Javitt DC (2005) Early-stage visual processing and cortical amplification deficits in schizophrenia. Arch Gen Psychiatry 62:495–504.

Cavanna AE, Trimble MR (2006) The precuneus: a review of its functional anatomy and behavioural correlates. Brain 129:564–583.

Chorlian DB, Porjesz B, Begleiter H (2006) Amplitude modulation of gamma band oscillations at alpha frequency produced by photic driving. Int J Psychophysiol 61:262–278.

Cohen MX, Axmacher N, Lenartz D, Elger CE, Sturm V, Schlaepfer TE (2009) Good vibrations: cross-frequency coupling in the human nucleus accumbens during reward processing. J Cogn Neurosci 21:875–889.

Da Silva FH, Van Lierop TH, Schrijer CF, Van Leeuwen WS (1973) Organization of thalamic and cortical alpha rhythms: spectra and coherences. Electroencephalogr Clin Neurophysiol 35:627–639.

Doyle AE (2006) Executive functions in attention-deficit/hyperactivity disorder. J Clin Psychiatry 67 Suppl 8:21–26.

Dugué L, Marque P, VanRullen R (2011) The phase of ongoing oscillations mediates the causal relation between brain excitation and visual perception. J Neurosci 31:11889–11893.

Foster BL, Parvizi J (2012) Resting oscillations and cross-frequency coupling in the human posteromedial cortex. Neuroimage 60:384–391.

Fries P, Nikolić D, Singer W (2007) The gamma cycle. Trends Neurosci 30:309–316.

Gur RC, Mozley LH, Mozley PD, Resnick SM, Karp JS, Alavi A, Arnold SE, Gur RE (1995) Sex differences in regional cerebral glucose metabolism during a resting state. Science 267:528–531.

Gusnard DA, Raichle ME, Raichle ME (2001) Searching for a baseline: functional imaging and the resting human brain. Nat Rev Neurosci 2:685–694.

Haegens S, Nácher V, Luna R, Romo R, Jensen O (2011) α-Oscillations in the monkey sensorimotor network influence discrimination performance by rhythmical inhibition of neuronal spiking. Proc Natl Acad Sci USA 108:19377–19382.

Jahnsen H, Llinás R (1984) Ionic basis for the electro-responsiveness and oscillatory properties of guinea-pig thalamic neurones in vitro. J Physiol (Lond) 349:227–247.

Jensen O, Mazaheri A (2010) Shaping functional architecture by oscillatory alpha activity: gating by inhibition. Front Hum Neurosci 4:186.

Klimesch W, Sauseng P, Hanslmayr S (2007) EEG alpha oscillations: the inhibition-timing hypothesis. Brain Res Rev 53:63–88.

Kullback S, Leibler RA (1951) On Information and Sufficiency. The Annals of Mathematical Statistics 22:79–86.

Lachaux JP, Rodriguez E, Martinerie J, Varela FJ (1999) Measuring phase synchrony in brain signals. Hum Brain Mapp 8:194–208.

Lindner M, Vicente R, Priesemann V, Wibral M (2011) TRENTOOL: a Matlab open source toolbox to analyse information flow in time series data with transfer entropy. BMC Neurosci 12:119.

Li X, Sroubek A, Kelly MS, Lesser I, Sussman E, He Y, Branch C, Foxe JJ (2012) Atypical pulvinar-cortical pathways during sustained attention performance in children with attention-deficit/hyperactivity disorder. J Am Acad Child Adolesc Psychiatry 51:1197–1207.e4.

Lorincz ML, Kékesi KA, Juhász G, Crunelli V, Hughes SW (2009) Temporal framing of thalamic relay-mode firing by phasic inhibition during the alpha rhythm. Neuron 63:683–696.

Lou HC, Gross J, Biermann-Ruben K, Kjaer TW, Schnitzler A (2010) Coherence in consciousness: paralimbic gamma synchrony of self-reference links conscious experiences. Hum Brain Mapp 31:185–192.

Maris E, Oostenveld R (2007) Nonparametric statistical testing of EEG- and MEG-data. J Neurosci Methods 164:177–190.

Miller KJ, Hermes D, Honey CJ, Sharma M, Rao RPN, Den Nijs M, Fetz EE, Sejnowski TJ, Hebb AO, Ojemann JG, Makeig S, Leuthardt EC (2010) Dynamic modulation of local population activity by rhythm phase in human occipital cortex during a visual search task. Front Hum Neurosci 4:197.

Morgane PJ, Galler JR, Mokler DJ (2005) A review of systems and networks of the limbic forebrain/limbic midbrain. Prog Neurobiol 75:143–160.
Nolte G (2003) The magnetic lead field theorem in the quasi-static approximation and its use for magnetoencephalography forward calculation in realistic volume conductors. Phys Med Biol 48:3637–3652.
O'Donnell P, Grace AA (1998) Dysfunctions in multiple interrelated systems as the neurobiological bases of schizophrenic symptom clusters. Schizophr Bull 24:267–283.
Osipova D, Hermes D, Jensen O (2008) Gamma power is phase-locked to posterior alpha activity. PLoS ONE 3:e3990.
Pinault D (2011) Dysfunctional thalamus-related networks in schizophrenia. Schizophr Bull 37:238–243.
Raichle ME, MacLeod AM, Snyder AZ, Powers WJ, Gusnard DA, Shulman GL (2001) A default mode of brain function. Proc Natl Acad Sci USA 98:676–682.
Raichle ME, Snyder AZ (2007) A default mode of brain function: a brief history of an evolving idea. Neuroimage 37:1083–1090; discussion 1097–1099.
Ribary U, Ioannides AA, Singh KD, Hasson R, Bolton JP, Lado F, Mogilner A, Llinás R (1991) Magnetic field tomography of coherent thalamocortical 40-Hz oscillations in humans. Proc Natl Acad Sci USA 88:11037–11041.
Saalmann YB, Kastner S (2009) Gain control in the visual thalamus during perception and cognition. Curr Opin Neurobiol 19:408–414.
Saalmann YB, Pinsk MA, Wang L, Li X, Kastner S (2012) The pulvinar regulates information transmission between cortical areas based on attention demands. Science 337:753–756.
Sauseng P, Klimesch W, Heise KF, Gruber WR, Holz E, Karim AA, Glennon M, Gerloff C, Birbaumer N, Hummel FC (2009) Brain oscillatory substrates of visual short-term memory capacity. Curr Biol 19:1846–1852.
Scheeringa R, Mazaheri A, Bojak I, Norris DG, Kleinschmidt A (2011) Modulation of visually evoked cortical FMRI responses by phase of ongoing occipital alpha oscillations. J Neurosci 31:3813–3820.
Scheeringa R, Petersson KM, Kleinschmidt A, Jensen O, Bastiaansen MC (2012) EEG alpha power modulation of fMRI resting state connectivity. Brain Connect.
Schreiber (2000) Measuring information transfer. Phys Rev Lett 85:461–464.
Sekihara K, Nagarajan SS, Poeppel D, Marantz A (2004) Asymptotic SNR of scalar and vector minimum-variance beamformers for neuromagnetic source reconstruction. IEEE Transactions on Biomedical Engineering 51:1726 –1734.
Spaak E, Bonnefond M, Maier A, Leopold D., Jensen O (2012) Layer-specific entrainment of gamma-band neural activity by the alpha rhythm in monkey visual cortex. Current Biology.
Tallon-Baudry, Bertrand (1999) Oscillatory gamma activity in humans and its role in object representation. Trends Cogn Sci (Regul Ed) 3:151–162.
Tort ABL, Komorowski R, Eichenbaum H, Kopell N (2010) Measuring phase-amplitude coupling between neuronal oscillations of different frequencies. J Neurophysiol 104:1195–1210.
VanRullen R, Koch C (2003) Is perception discrete or continuous? Trends Cogn Sci (Regul Ed) 7:207–213.
Varela FJ, Toro A, John ER, Schwartz EL (1981) Perceptual framing and cortical alpha rhythm. Neuropsychologia 19:675–686.
Vijayan S, Kopell NJ (2012) Thalamic model of awake alpha oscillations and implications for stimulus processing. Proc Natl Acad Sci USA.
Voytek B, Canolty RT, Shestyuk A, Crone NE, Parvizi J, Knight RT (2010) Shifts in gamma phase-amplitude coupling frequency from theta to alpha over posterior cortex during visual tasks. Front Hum Neurosci 4:191.
Yanagisawa T, Yamashita O, Hirata M, Kishima H, Saitoh Y, Goto T, Yoshimine T, Kamitani Y (2012) Regulation of motor representation by phase-amplitude coupling in the sensorimotor cortex. J Neurosci 32:15467–15475.

5

Age Related Changes of MEG Alpha and Gamma-Band Activity Reflect the Late Maturation of Distractor Inhibition during Working Memory Maintenance

In preparation for publication: Frederic Roux, Michael Wibral, Wolf Singer and Peter Uhlhaas: Age Related Changes of MEG Alpha and Gamma-Band Activity Reflect the Late Maturation of Distractor Inhibition during Working Memory Maintenance.

5.1 Abstract

The present study investigated the development of visuospatial working memory (WM) and the efficiency of distractor inhibition in adolescence. To this end, a sample of n = 97 participants (age range: 12-24 years) performed a WM task with manipulations of WM-load and task-irrelevant items (distractors), while behavioral performances and magneto-encephalographic (MEG) data were monitored. Compared to adults, WM-capacity in adolescent participants was reduced and reaction times (RTs) and error rates were increased. In adult participants, distracter-related gamma-band activity was indicative of higher WM-capacity. This relationship was not found in younger age groups, suggesting that adolescents were less efficient at inhibiting distractors during WM maintenance. Accordingly, these findings point towards the immaturity of large-scale functional networks that support WM maintenance in adolescence.

5.2 Introduction

Working memory (WM) is highly prone to interferences from distracting information (Dempster and Brainderd, 1995). Thus, one factor that may crucially account for individual differences in WM capacity is the ability to prevent distractors from interfering with the maintenance of WM representations (Awh and Vogel, 2008). Indeed, previous research has shown that the modulation of distractor-related brain activity is highly predictive of WM capacity (Vogel et al., 2005; McNab and Klingberg, 2008; Jost et al., 2011), suggesting that individuals with higher WM-capacity are very efficient at inhibiting distractor-related activity.

WM and distractor inhibition are cognitive functions associated with prefrontal circuits (Butters and Pandya, 1969; Butters et al., 1971; Knight et al., 1981; Funahashi et al., 1993; Chao and Knight, 1995; Goldman-Rakic, 1995; Miller and Cohen, 2001; Fuster, 2008; Voytek et al., 2012; Noudoost and Moore, 2013). In addition, the selection and maintenance of task-relevant WM information involve subcortical, primary sensory and parietal regions (Miller and Desimone, 1994; Todd and Marois, 2004; McNab and Klingberg, 2008; Edin et al., 2009; Harrison and Tong, 2009).

Behavioral, anatomical and functional imaging studies have also examined the developmental changes in distractor-inhibition and associated WM-capacity. Evidence from classical developmental studies shows that the ability to ignore task-irrelevant information follows a protracted development which extends well beyond adolescence (Pascual-Leone, 1970; Lane and Pearson, 1982; Schiff and Knopf, 1985; Diamond and Doar, 1989; Dempster, 1992; Harnishfeger and Bjorklund, 1994; Harnishfeger, 1995; Ridderinkhof et al., 1997). Moreover, neuroimaging studies have linked age-related changes in the functional recruitment of parietal and prefrontal networks with developmental changes in WM capacity and the ability to inhibit distractors during adolescence (Bunge et al., 2002; Durston et al., 2002; Luna et al., 2004; Crone et al., 2006; Diamond, 2006). Accordingly, these findings suggest that the late maturation of prefrontal and parietal regions supports the development of the ability to manipulate information in WM during adolescence (Klingberg et al., 2002; Casey et al., 2005; Bunge and Wright, 2007).

A relatively unexplored question, however, is the contribution of neural oscillations in the maturation of distractor inhibition during WM. Studies with electro- (EEG) and magneto-enecephalography (MEG) indicate that rhythmic fluctuations of activity may provide important insights into normal and pathological brain development (for a review see Uhlhaas et al., 2010).Emerging evidence highlights the possibility that both low- and high-frequency oscillations follow a protracted development until adulthood (Uhlhaas et al., 2009; Werkle-Bergner et al., 2012) which are accompanied by important modifications in underlying neurotransmitter-systems (Tseng and O'Donnell, 2005; Hashimoto et al., 2009).

To examine the link between distractor-inhibition, WM and neural oscillations, we recorded the MEG activity of ninety seven healthy participants (55 females; age range: 12-27 years) while they performed a visual-spatial working memory task (VSWM) which involved the maintenance of spatial positions of WM-items as well as the suppression of irrelevant WM information (Fig. 6.1). We focused on power in the gamma (60-80Hz) frequency range as our previous work has shown that 60-80 Hz activity is associated with the maintenance of behaviorally relevant WM items (Roux et al., 2012). Developmental changes were also investigated at alpha (10-14 Hz) frequencies, as recent findings have reported age-related changes in the amplitude and phase dynamics of EEG alpha activity during WM maintenance (Werkle-Bergner et al., 2012) and alpha-band activity has a crucial role for the inhibition of task-irrelevant activity (Jensen et al., 2012).

To investigate the functional role of alpha and gamma-band activity for distractor inhibition and WM-capacity, we first focused on the analysis of delay activity in adult participants (21-24 years) and examined the distractor related modulation of spectral power in the alpha and gamma frequency bands. In a second step, we examined whether developmental changes in alpha and gamma-band activity would account for age-related differences in WM-capacity.

5.3 Methods

Stimuli and Task. On each trial a sample stimulus was presented and participants were instructed to remember only the spatial positions of the red

items and to ignore blue items (Figure 6.1). In contrast to our first study (Roux et al., 2012), the number of WM-items was increased from 3 to 4 and from 6 to 8 WM-items in both WM-load conditions as pilot data had indicated stronger developmental effects for a WM-load of 8 items. The sample stimulus consisted of either four red items (load 4), four red and four blue items (Distractors), or eight red items (load 8) which were presented for 0.4 s. Participants reported whether the positions of the red items in the sample were a match or a mismatch by pressing one of two buttons. The prestimulus period varied between 3.5 s and 1.5 s to reduce temporal expectation. Participants performed 150 trials per condition and the order of trials was randomized across conditions. Hand assignment was counterbalanced across participants and behavioral responses were recorded using a fiber-optic response device (Lumitouch, Photon Control Inc., Burnaby, BC, Canada). After responding, participants had the possibility to blink for 1 s before the next trial started.

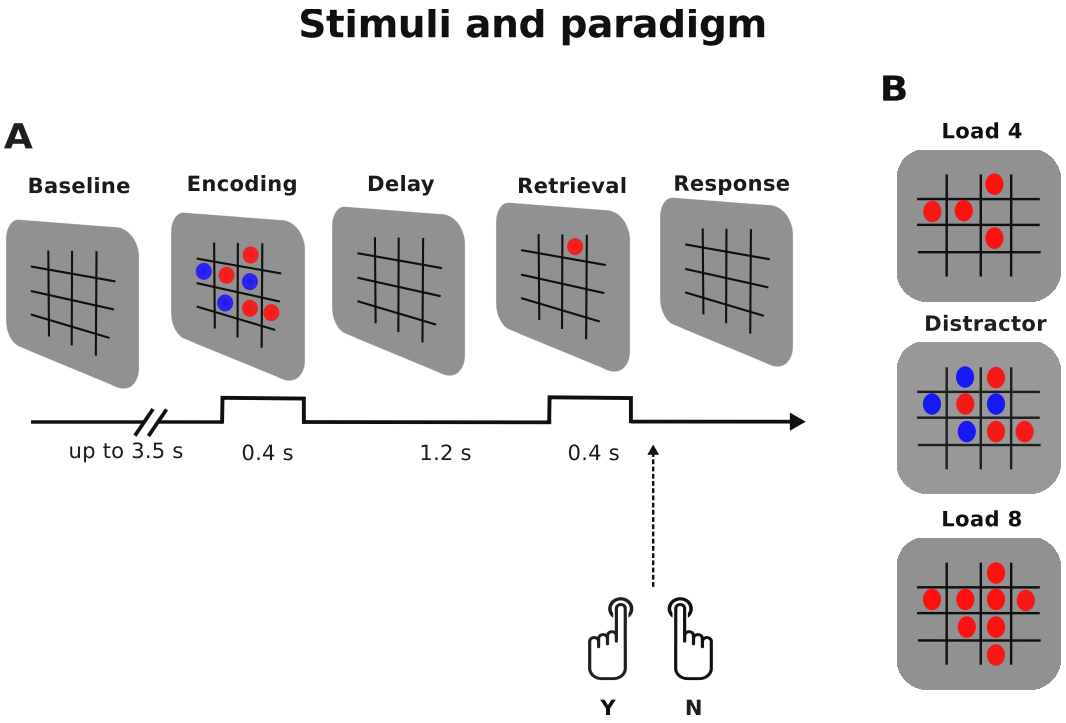

Figure 5.1: **The adapted Version of the Visual-Spatial Working-Memory task. A:** Example of a distractor trial. Each trial began with a jittered inter-trial interval (1.5-3.5 s) which was followed by the presentation of the memory array (0.4 s), the delay period (1.2 s), the retrieval phase (0.4 s) and a response interval (2 s). Participants were instructed to memorize the positions of the red items and to ignore blue items. During the retrieval phase participants pressed a button to indicate whether the sample item was a match or a mis-match. **B:** Examples of memory arrays presented during the load 4 (upper panel), distractor (middle panel) and load 8 (lower panel) conditions.

Participants. MEG recordings were collected from 97 right handed healthy participants (55 females; age range: 12-27 years; Fig. 4A) which were recruited from local high-schools and the Goethe University Frankfurt. All participants

had normal or corrected to normal vision and were screened for the presence of psychiatric disorders, neurological illnesses and substance abuse and assessed for performance on the Hamburg-Wechsler intelligence testing battery (HAWI-K/E) (Tewes, 1991; Petermann and Petermann, 2010). Written informed consent was obtained from all participants after the study procedures were described. For participants younger than 18 years, written consent was obtained from a parent or legal guardian. To assess age-related changes, participants were divided into four age groups (Fig. 6.4B): 12-14 years (early adolescence, n = 18, mean age: 13.27 years, 9 males), 15-17 years (late adolescence, n = 27, mean age: 16, 8 males), 18-20 years (young adults, n = 30, mean age: 18.9, 12 males), 21-27 years (adults, n = 22, mean age: 22.3 years, 13 males). The four groups did neither differ in sex distribution ($\chi^2(3,97) = 4.7$, P = 0.19), nor in head circumference ($\chi^2(3,97) = 5.66$, P = 0.12). The present study was approved by the ethics board of the Goethe-University Frankfurt.

Magneto-Encephalographic Recordings and Preprocessing. MEG signals were recorded continuously using a 275-channel whole-head system (Omega 2005, VSM MedTech Ltd., BC, Canada) in a synthetic third order axial gradiometer configuration. MEG signals were sampled at 1.2 kHz and bandpass filtered at 0.01 - 600 Hz. The vertical and horizontal electro-oculogramm were recorded in order to monitor eye movements. Continuous recordings were aligned in time to the onset of the sample stimulus and segmented into data epochs which included the baseline (1.5 s), the encoding (0.4 s), the maintenance (1.2 s) and the recognition (0.4 s) phase of the task (3.2 s per trial). Data epochs for match and non-match trials were pooled together and only trials with correct responses were considered for further analyses. An automatic artifact detection and rejection algorithm was used to exclude epochs contaminated by eye blinks, muscle activity or sensor jump artifacts. Further preprocessing of individual epochs included detrending as well as DC offset removal and down-sampling of the sampling rate to 300 Hz. Independent component analysis (ICA) was used to remove cardiac activity and eye movements. 17 of 275 channels were excluded from further analysis for technical reasons.

Behavioral Data. Detection rates and reaction time (RT) data were examined for differences between the four groups with a kruskall-wallis non-parametric analysis of variance. The threshold for statistical significance was alpha = 0.05. Correlations between behavioral performances and MEG activity were calculated with Spearman's non-parametric correlation coefficient. All posthoc comparisons

were carried out using the Wilcoxon rank sum test and a Bonferroni correction was used to adjust the alpha level for multiple comparisons.

Post-Hoc Non-Parametric Curve Fitting. The distribution of group means was modeled by the function y = sign(x-d)(1-exp(-((x-d)/s)^2)) which is a nonlinear monotonic function of the model parameters d (flushleft) and s (steepness) and where x is the independent variable (age group). The optimal model parameters were estimated by successively fitting the model to the data with different values for d and s and by measuring the corresponding error. The model parameters which produced the smallest error were then considered for our model (Fig. 6.4D, 6.4F, 6.4H).

Estimation of Spectral Quantities. Time-frequency representations (TFRs) of stimulus related activity were calculated using a sliding window that was stepped by 25 ms between estimates through the data epochs with the time index aligned to the flushleft of the analysis window. An adaptive hanning window (Oppenheim and Schafer, 1989) (length = 6 cycles per frequency) was used to compute TFRs for frequencies in the 6 to 30 Hz range whereas time-frequency representations for frequencies between 30 and 150 Hz were computed based on multi-taper spectral analysis (Thomson, 1982) using 9 Slepian data tapers and a fixed time window (length = 0.5 s) with a spectral concentration of 10 Hz. TFRs for low and high frequencies were normalized to a baseline by subtracting the average activity during the baseline from the whole time-frequency interval before dividing the difference by the average baseline activity. This normalization was computed on a frequency-by-frequency basis according to:

N(t,f) = (s(t,f) - sb(f))/sb(f)

where s(t,f) corresponds to the TFRs of the entire data epoch and sb(f) corresponds to the average baseline activity per frequency. For low (<30Hz) and high (>30Hz) frequencies a baseline interval from -1.2 to 0 s was chosen. All subsequent analyses were computed from delay activity averaged from 0.65 to 1.6 s. The first 250 ms of delay activity were not considered for analysis to avoid encoding related activity captured by half the width of the sliding window. Spectral quantities were computed on equal numbers of data epochs across conditions for each participant (average number of trials per condition: 81.3/150 trials, SD = 23.3). Importantly there were no differences in trial numbers across the four age groups ($\chi^2(3,97) = 3.04$, P = 0.38). In order to increase the signal amplitude above the underlying source, MEG fields were transformed into orthogonal horizontal and vertical planar gradients prior to TF-analysis.

Statistical Analysis of Spectral Quantities. All spectral quantities were examined for group differences using either the t-test or the F-test for independent samples. Furthermore, spectral quantities were examined for developmental changes using the non-linear model derived from the post-hoc analysis of behavioral data. The model was fitted to the distribution of individual values using regression analysis to examine whether it would allow to retrieve the pattern observed in the behavioral data. To validate the model, t-values were estimated successively for the empirical data as well as for randomized partitions of the data. To control the false positive rate the statistical analyses performed on spectral quantities were combined with a non-parametric monte-carlo based cluster-permutation approach with n = 4000 randomizations (Maris and Oostenveld, 2007). The threshold for clustering entry level and for statistical significance was alpha = 0.05 and the treshold for statistical significance was alpha = 0.05.

Analysis Software. Behavioral data and MEG signals were preprocessed and analyzed using custom routines written in Matlab 2008b and the open source Matlab-toolbox fieldtrip (Oostenveld et al., 2011) [http://www.ru.nl/fcdonders/fieldtrip/].

5.4 Results

WM-Capacity, Distractors Inhibition and Gamma-Band Modulation in Adults. Consistent with our previous findings (Roux et al., 2012), we observed a pronounced increase of activity in the gamma (60-80 Hz) frequency range across the entire delay period (0.65 to 1.6 s). Gamma-band activity during the delay phase was characterized by a sustained increase over occipital, parietal and central sensors (Fig. 6.2A,6.2C). In adult participants, however, gamma power did not differ between conditions [load 8 vs. load 4: P = 0.89; distractor vs. load 4: P = 0.74; load 8 vs. distractor: P = 0.92; t-test for dependent samples]. To further examine the link between WM-capacity and gamma-band activity, we examined 60-80 Hz spectral power in participants with low vs. high WM-capacity based on a median split of the adult sample (Fig. 6.2B,6.2D-E). Participants with high WM capacity showed WM-load related increase of 60-80 Hz activity [P < 0.05; t-test for independent samples] as well as a reduction of 60-80 Hz activity in the distractor condition as compared to the load 8 condition

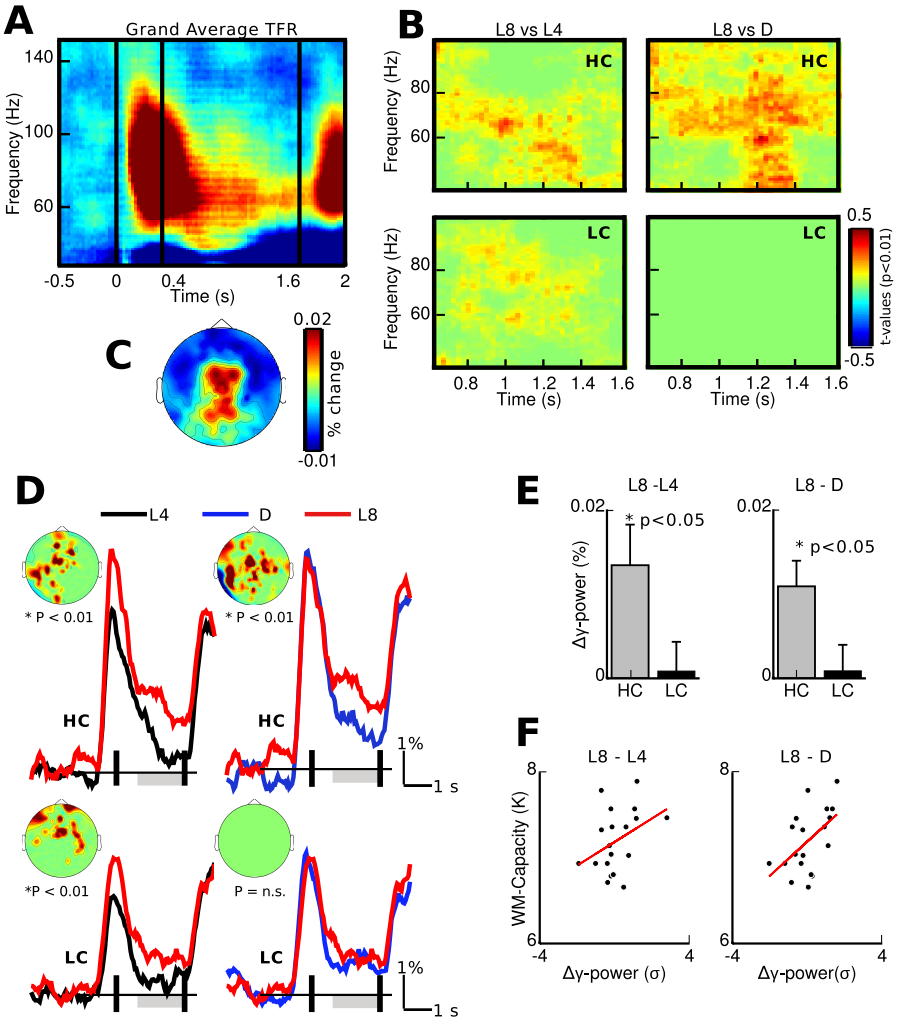

Figure 5.2: **Gamma-Activity and WM-Capacity in Adult Participants. A:** Grand average TFR of 40-100 Hz activity. X-axis: time (s), y-axis: frequency (Hz). Pseudo colors indicate relative change in power as compared to the baseline interval (%). **B:** Statistical maps for high-capacity (HC) and low-capacity (LC) participants. For both groups there was a significant increase of gamma-band activity during load 8 as compared to load 4. However, only the HC group showed a reduction of distractor-related gamma power as compared to load 8. X-axis: time (s), y-axis: frequency (Hz). Pseudo colors indicate statistical t-values tresholded for significance ($P < 0.05$; corrected). **C:** Grand average topography for 60-80 Hz delay activity. **D:** Time courses of 60-80 Hz activity and topographies of statistical t-values for the comparisons shown in B. In the HC group, gamma power was significantly enhanced in the load 8 condition as compared to both the load 4 and the distractor condition (left and right upper panel). In the LC group, gamma power was enhanced in load 8 as compared to load 4, but there was no difference between load 8 and the distractor condition. The gray bar indicates the temporal interval for which significant differences in distractor-related gamma-band activity were found. Color code: black = load 4; blue = distractor; red = load 8. **E:** Differences in gamma-band activity between load 8 and load 4 (left panel) and between load 8 and the distractor condition (right panel) for the LC and HC group. In the HC group, the modulation of gamma power was significantly enhanced as compared to the LC group ($P < 0.05$, t-test for independent samples). **F:** Relationship between WM-capacity and the modulation of gamma-band activity. Left panel: Modulation of gamma-band activity between load 8 and load 4 and WM-capacity. Right panel: Modulation of gamma-activity between load 8 and the distractor condition and WM-capacity.

[$P < 0.01$; t-test for independent samples]. By contrast, no significant difference in gamma power between the distractor condition and load 4 condition was present [$P = 0.67$; t-test for independent samples], indicating that the high capacity group was highly efficient at inhibiting the task-irrelevant stimuli during the maintenance phase. In the low capacity group, 60-80 Hz activity was modulated by WM-load [$P < 0.05$; t-test for independent samples] but there was no difference between the distractor condition and the load 8 condition [$P = 0.06$; t-test for independent samples], suggesting that participants were less efficient in preventing irrelevant items from accessing the limited WM space. To quantify the relationship between distractor inhibition and WM capacity more formally, we measured the degree to which each participant's WM capacity was correlated with the difference in gamma power between the load conditions 4 and 8 and with the difference in gamma power between the load 8 and the distractor conditions (Fig 2F). The correlation coefficients indicate that in both cases, the relative increase in gamma-power in the load 8 condition is associated with higher WM-capacity, although this effect was strongest for the difference between the distractor condition and load 8 [Spearman's $r = 0.5$; $P < 0.05$] as compared to the modulation of gamma-power between load 4 and load 8 [Spearman's $r = 0.4$, $P = 0.1$].

WM-Capacity, Distractors Inhibition and Alpha-Band Modulation in Adults. A sustained enhancement of spectral power was also found in the alpha-band (10-14 Hz) across conditions over temporal, central and frontal MEG channels (Fig. 6.3A,6.3C). Similar to the gamma-band, alpha power was differentially modulated for participants with low and high WM-capacity (Fig. 6.3B, 6.3D-E). In participants with high WM capacity, alpha power was significantly stronger in the distractor condition as compared to the load 4 and the load 8 conditions [distractor vs. load 8: $P < 0.05$; distractor vs. load 8: $P < 0.01$; t-test for dependent samples]. By contrast, in participants with low WM-capacity, alpha power was enhanced in the distractor condition as compared to load4 [distractor vs. load 4: $P < 0.05$; t-test for dependent samples], but there was no difference between the distractor condition and load 8 [distractor vs. load 8: $P = 0.13$; t-test for dependent samples]. Moreover, alpha power during the delay period was associated with faster RTs [load 4: $r = -0.49$, $P < 0.05$; distractor: $r = -0.35$, $P = 0.01$; load 8: $r = -0.47$, $P < 0.05$; Spearman's r; Fig. 3F]. However, we did not observe a significant relationship between alpha power during the delay phase and WM capacity [load 4: $r = -0.28$, $P = 0.23$; distractor: $r = -0.35$, $P = 0.13$; load 8: $r = -0.33$, $P = 0.15$; Spearman's r].

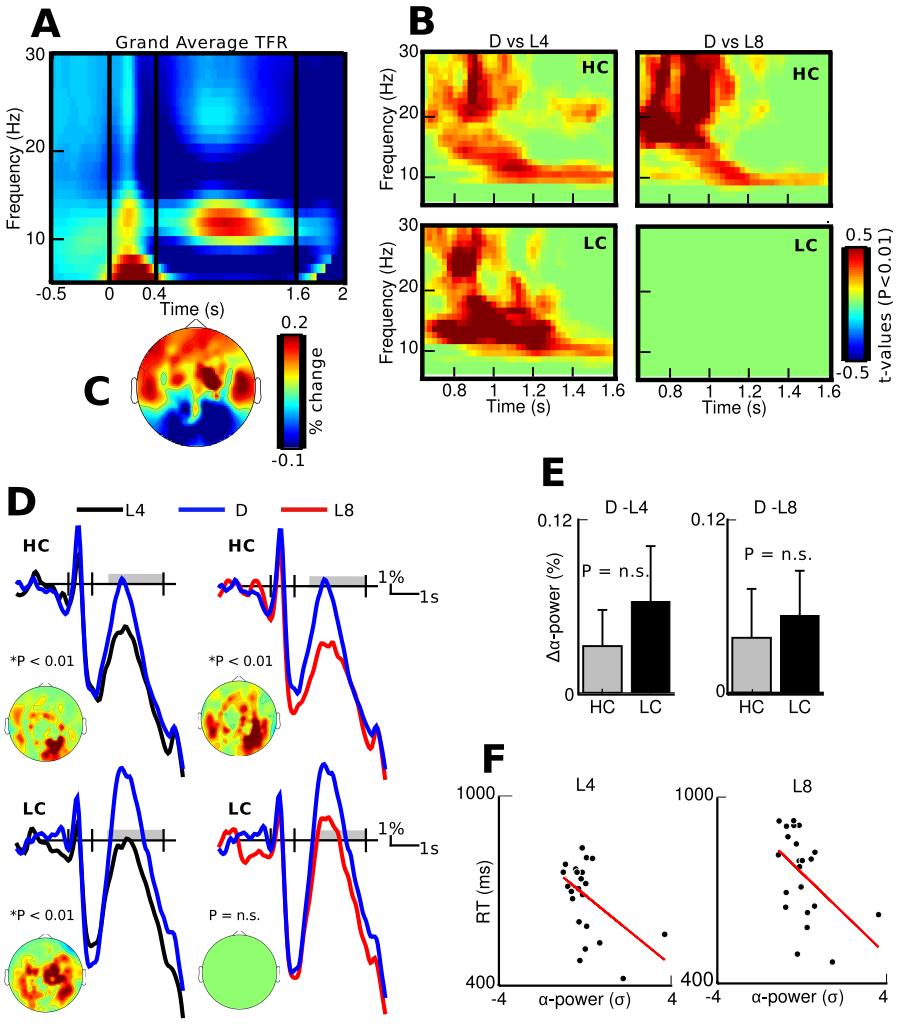

Figure 5.3: **Alpha-Activity and WM-Capacity in Adult Participants.** (same convention as Figure 4) **A:** Grand average TFR of 6-30 Hz activity. **B:** Statistical maps for high-capacity (HC) and low-capacity (LC) participants. For both groups there was a significant increase of alpha-band activity during the distractor condition as compared to load 4. However, only the HC group showed a enhanced alpha power as compared to load 8. **C:** Grand average topography for 10-14 Hz delay activity (0.65-1.6 s). **D:** Time courses of 10-14 Hz activity and topographies of statistical t-values for the comparisons shown in B. In the HC group, alpha power was significantly enhanced in the distractor condition as compared to both load 4 and load 8 (left and right upper panel). In the LC group, however, alpha power was enhanced during the distractor condition as compared to load 4, but there was no difference between the distractor and load 8. **E:** Differences in alpha-band activity between the distractor and load 4 (left panel) and between the distractor and load 8 (right panel) for the LC and HC group. There was no difference in the modulation of alpha-band activity between both groups ($P > 0.05$, t-test for independent samples). **F:** Relationship between faster RTs and alpha-band activity. Left panel: Alpha-band activity during load 4 and RTs. Right panel: Alpha-band activity during load 8 and RTs.

Behavioral Performances. No developmental changes were found in WM-capacity [WM-capacity: $\chi^2(3,89) = 5.93$, P = 0.1; Fig. 4C]. However, there was a trend towards statistical significance for the age-related decrease of RTs [$\chi^2(3, 89) = 7.15$, P = 0.06, Fig. 4E]. In addition, older participants showed a reduction of error rates as compared to younger participants [error rate: $\chi^2(3, 89) = 14.9$, $P < 0.05$; Posthoc rank sum test: adult > early adolescence; Fig. 4G].

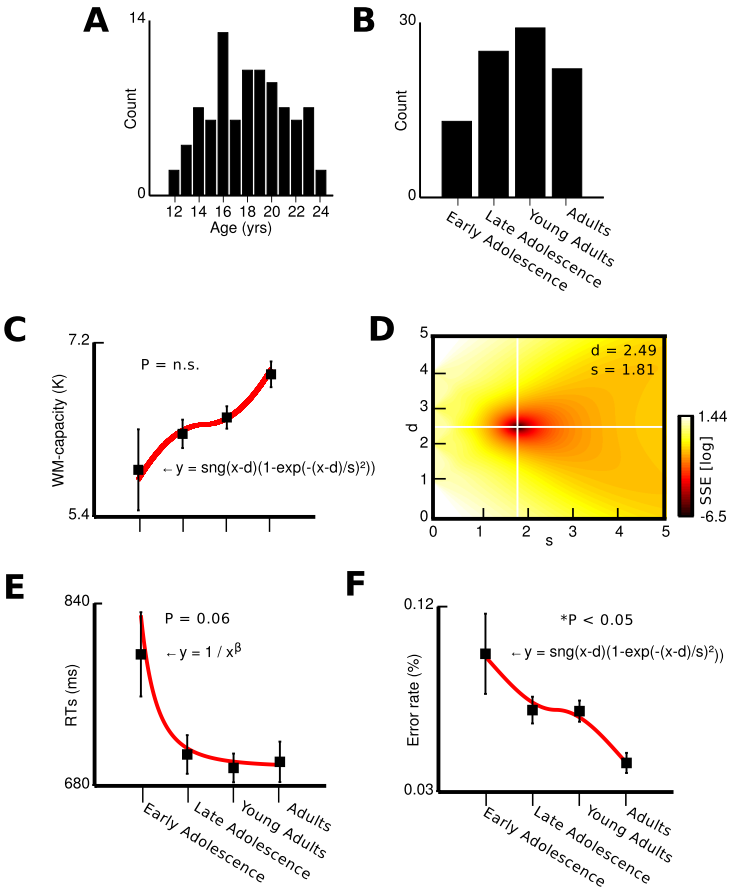

Figure 5.4: **Participants and Behavioral Performances. A:** Histogram of participants as a function of individual age (range: 12-14 years).**B:** Histogram of participants as a function of age group (group1: young adolescents, group2: late adolescents, group 3: young adults, group 4: adults). **C:** Development of WM-capacity across the different age groups. The red line corresponds to the fit as estimated by the non-linear model $y = sign(x-d)(1-exp(-(\frac{x-d}{s})^2))$. **D:** Post-hoc analysis of optimal model parameters. X-axis: steepness parameter (s). Y-axis: flushleft parameter (d). The pseudo-color code corresponds to the mean squared error (log scale). The lowest error was found for the parameter values d = 2.49 and s = 1.81.**E&F:** Age related changes in RTs and error rates.

Developmental Changes in WM-related Gamma-Band Activity. Age related changes for 40-100 Hz activity failed to reach statistical significance [WM-load 4: P = 0.25; distractor: P = 0.59; WM-load 8: P = 0.25; independent

F-test]. Subsequent analysis of non-linear developmental effects, however, revealed a significant age-related increase of gamma-band power over occipital and parietal channels in the distractor condition [$P < 0.05$; Fig. 5A-C,Fig. 6A-D]. Because there was a relationship in adult participants between WM-capacity and the modulation of gamma power in the distractor condition as compared to load 8, and because our previous findings show that single trial fluctuations of distractor-related gamma-band activity code for the number of relevant objects maintained in WM (Roux et al., 2012), we examined the stability of amplitude differences between the distractor and the load 8 condition in the 40-100 Hz frequency range over single trials. In adult participants, single trial gamma-power in the distractor condition was consistently reduced as compared to load 8 trials, whereas in adolescents this relationship was inversed: young adolescents showed consistently higher 40-100 Hz activity when exposed to distractors as compared to load 8 trials [$P < 0.05$; F-test for independent samples; Fig. 6E-G]. No age related differences were found in the modulation of gamma-band power between load 4 and load 8 trials [$P = 0.32$; two-tailed t-test for independent samples].

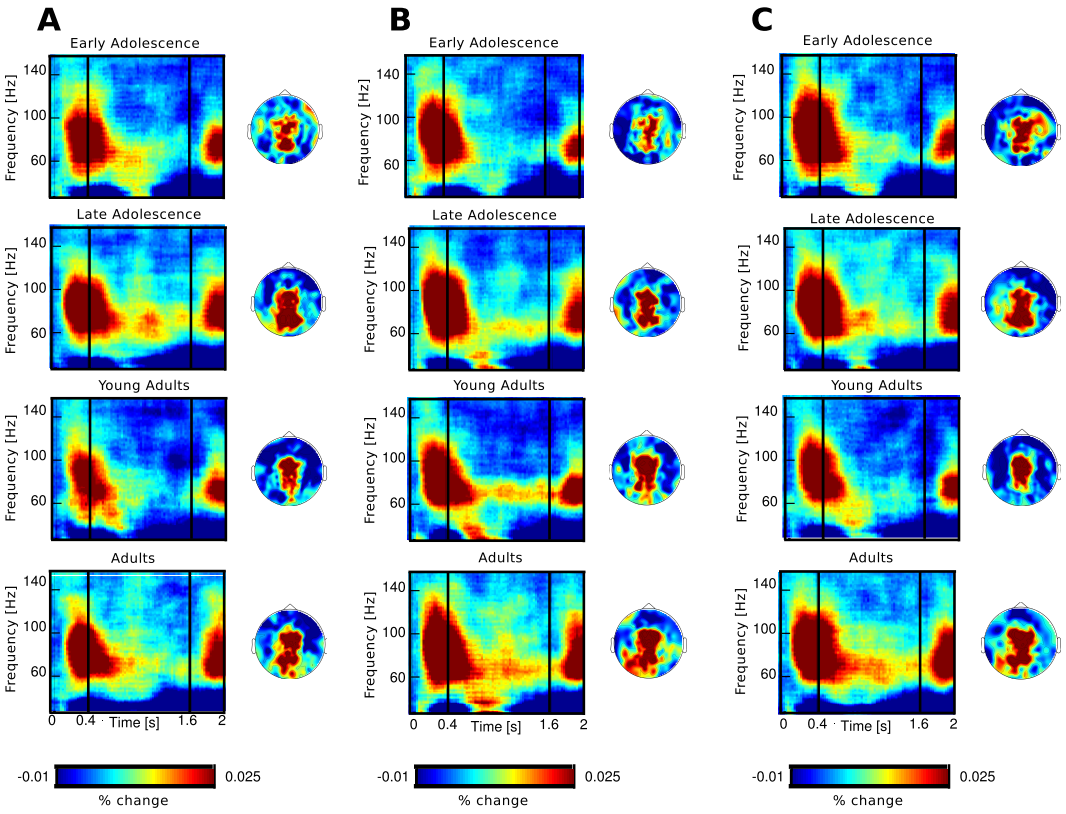

Figure 5.5: **High-Frequency (40-100 Hz) Activity during WM-Maintenance. A-C:** TFRs and topographies of high-frequency activity during load 4 (**A**), the distractor condition (**B**) and load 8 (**C**) for the young adolescent, late adolescent, young adult and adult age groups. X-axis: time (s), y-axis: frequency (Hz). Pseudo-colors indicate the percent change in power as compared to a baseline interval.

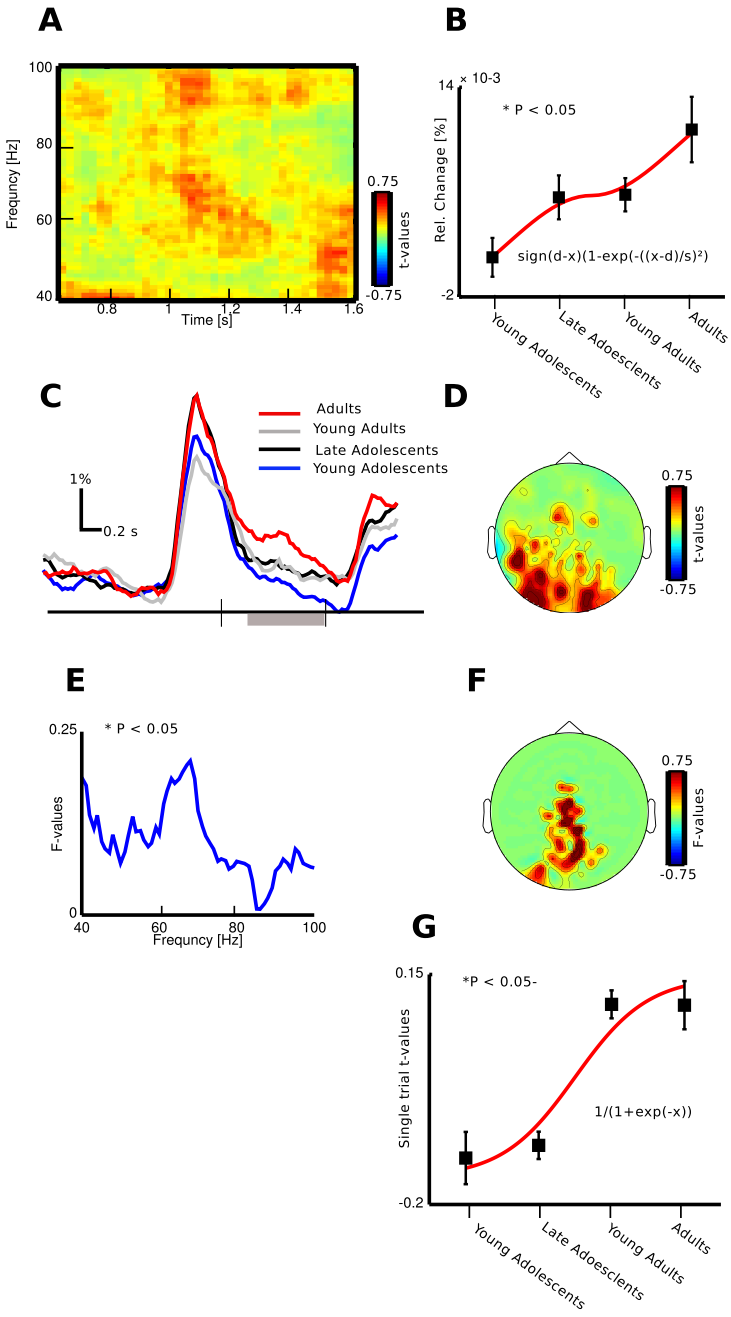

Figure 5.6: **Non-Linear Development of High-Frequency Activity during WM-Maintenance. A:** Statistical map of non-linear age-related changes in high-frequency activity during WM-maintenance. X-axis: time (s), y-axis: frequency (Hz). Pseudo-colors correspond to regression t-values thresholded for significance ($P<0.05$; corrected). **B:** Non-linear monotonic increase of 60-80 Hz activity across age groups. The red line corresponds to the fit provided by the non-linear model. **C:** Time courses of distractor-related gamma-band power for the young adolescent (blue), late adolescent (black), young adult (gray) and adult (red) participants. Gray bar indicates the temporal interval for which significant differences in distractor-related gamma-band activity were found. **D:** Topography of regession t-values tresholded for significance ($P < 0.05$; corrected). The topography shows strong developmental changes in distractor-related gamma-band power over occipital, parietal and central channels. **E:** Spectrum of statistical F-values tresholded for significance reflecting developmental changes across the four age groups in the stability of single-trial fluctuations of distractor-related high-frequency activity ($P < 0.05$; corrected). X-axis: frequency (Hz), y-axis: F-values ($P < 0.05$; corrected). **F:** Topography of statistical F-values tresholded for significance showing age-related changes in the stability of distractor-related single trial fluctuations of high-frequency delay activity ($P < 0.05$; corrected). **G:** Non-linear development in the stability of single trial fluctuations of distractor-related high-frequency activity. X-axis: age group, y-axis: single trial t-values. Note that the distribution of group means can be fitted with a sigmoid function ($y = 1/(1+\exp(-x))$), suggesting a developmental transition in the modulation of distractor-related high-frequency activity occurring between adolescence and adulthood.

Developmental Changes in WM-related Alpha-Band Activity. Similar to our results in the gamma-band, we did not observe any significant age-related differences of alpha power across the four age groups [WM-load4: P = 0.33; distractor: P = 0.16; WM-load4: P = 0.33; independent F-test]. However, a significant age-related increase of alpha-band activity was found when we assessed developmental changes based on the non-linear model (Fig. 6.7A-C, Fig. 6.8A-D). The analysis of 6-30 Hz power during the maintenance phase revealed that power in the 10-14 Hz range was significantly higher over temporal, central and frontal sensors in older participants as compared to younger participants [P $<$ 0.05; independent regression t-values].

5.5 Discussion

Summary: The present data provide novel evidence for late developmental changes in alpha and gamma-band activity related with the inhibition of task-irrelevant information during WM. Our data are consistent with previous findings showing that alpha and gamma-band oscillations have distinct functional roles during WM maintenance and replicate previous findings from our group (Jokisch and Jensen, 2007; Sauseng et al., 2009; Roux et al., 2012). In adult participants, WM delay activity was associated with a sustained enhancement of activity in the alpha and gamma-band frequency ranges during the delay period. Consistent with the role of gamma-band activity in the maintenance of WM representations (Tallon-Baudry et al., 1998; Pesaran et al., 2002; Howard et al., 2003; Jensen et al., 2007; Palva et al., 2011), we found an increase in gamma-band power between 0.65 and 1.6 s during the successful maintenance of information in WM.

An additional, novel observation is the relationship between gamma-band activity, distractor suppression and WM-capacity. In line with previous research (Vogel et al., 2005), higher WM capacity was associated with a more efficient suppression of task-irrelevant activity in the gamma-band during the distractor condition. A sustained enhancement of activity was also observed at lower frequencies in the alpha (10-14 Hz) frequency-range during the delay phase. Alpha power was strongest in response to distractors, confirming that alpha activity was not modulated by the number of task-relevant WM-items. The present findings are in agreement with recent evidence from MEG recordings,

suggesting that oscillatory activity in the alpha band may protect WM representations against interferences from distractors (Bonnefond and Jensen, 2012). More precisely, the data by Bonnefond et al. show a strong phase adjustment of oscillatory activity in the alpha band prior to distractor items, suggesting that the phase of alpha oscillations may serve as a mechanism to reduce neuronal excitability during distractor processing . Importantly, recent theoretical work suggests that such a mechanism may allow for the suppression of distractor related activity and the selective gating of task-relevant information through the modulation of gamma-band power (Jensen et al., 2012).

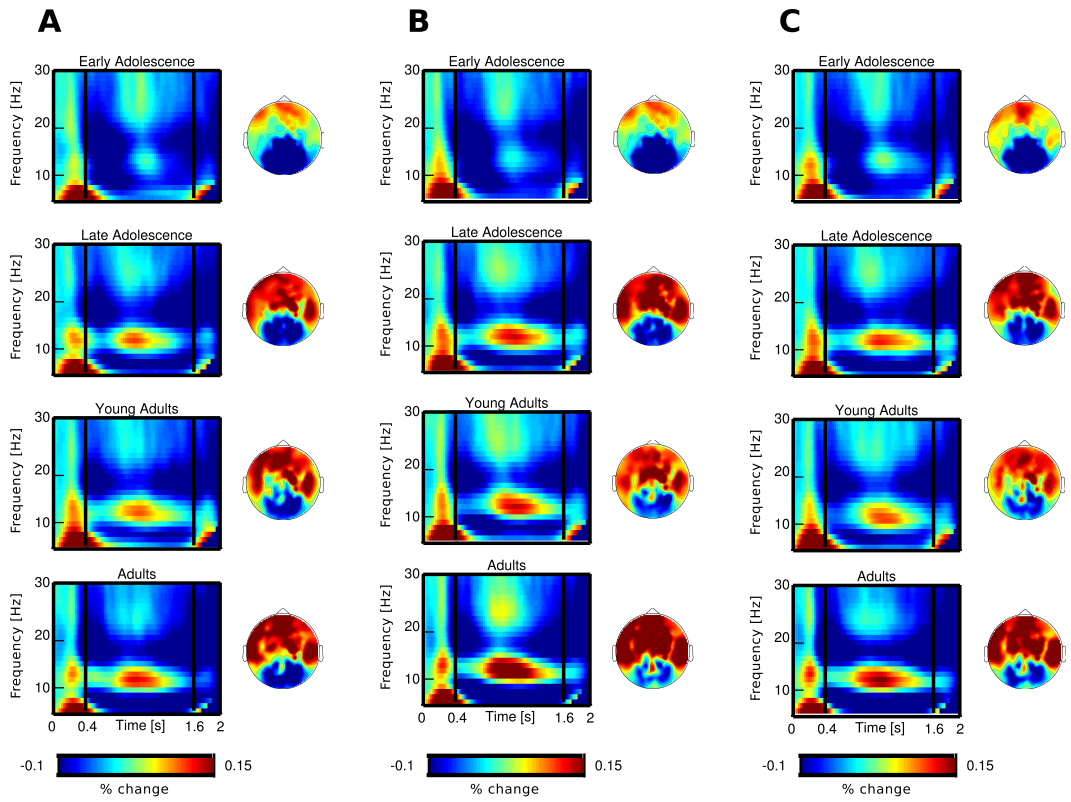

Figure 5.7: **Low-Frequency (6-30 Hz) Activity during WM-Maintenance. A-C:** TFRs and topographies of low-frequency activity during load 4 (**A**), the distractor condition (**B**) and load 8 (**C**) for the young adolescent, late adolescent, young adult and adult age groups. X-axis: time (s), y-axis: frequency (Hz). Pseudo-colors indicate the percent change in power as compared to a baseline interval.

Developmental changes of behavioral performances showed that adolescents were more susceptible to interferences from distractors as compared to adult participants. This was confirmed by the analysis of single-trial amplitude fluctuations in response to distractors and load 8 trials which revealed significant differences in the suppression of distractor-related gamma-band activity at the single trial level between adolescents and adult participants. In adult participants gamma-power was strongly enhanced when eight red items were presented as compared to distractors trials, suggesting that adult participants

were more efficient at inhibiting distractor-related gamma-band activity during the maintenance period. In adolescents, however, gamma-band power was found to be higher on distractor trials as compared to trials where eight red items were presented, suggesting that adolescents were not able to suppress the representation of task-irrelevant items during the delay period. Critically, age-related changes in behavioral performance as well as in alpha and gamma-band activity both followed a non-linear developmental trajectory.

Relationship to previous Research. The current findings support previous evidence showing that individual differences in WM capacity critically depend on the ability to suppress the representation of task-irrelevant information during WM maintenance (Vogel et al., 2005; Awh and Vogel, 2008; McNab and Klingberg, 2008). Furthermore, the present findings are compatible with and extend previous evidence showing that adolescents have a higher susceptibility towards interference from distractors as compared to adults (Olesen et al., 2007), suggesting that adolescents and adults differ in their ability to suppress distractor-related representations. This interpretation is in line with recent findings from EEG recordings, suggesting that age-related changes of alpha activity during WM maintenance reflect the development of inhibitory control (Sander et al., 2012) and with a growing body of evidence linking alpha oscillations with the phasic modulation of neuronal activity (Klimesch et al., 2007; Busch et al., 2009; Lorincz et al., 2009; Dugué et al., 2011; Haegens et al., 2011; Scheeringa et al., 2011; Vijayan and Kopell, 2012), and the inhibition of distractors (Bonnefond and Jensen, 2012; Jensen et al., 2012).

Putative mechanisms behind developmental changes. Converging evidence from developmental studies involving magnetic resonance imaging (MRI) indicate that the parietal cortex and the PFC undergo important maturational changes in gray and white matter volumes during adolescence and adulthood (Giedd et al., 1999; Klingberg et al., 1999; Sowell et al., 1999, 2003; Paus, 2005; Lenroot and Giedd, 2006; Hashimoto et al., 2009; Gogtay and Thompson, 2010; Raznahan et al., 2011; Lebel et al., 2012), which have been proposed to reflect the re-organization of functional networks implicated in the development of higher cognitive functions (Casey et al., 2005). In agreement with these data, the late development of WM-capacity has been associated with age-related differences in fractional anisotropy in the frontal lobe and parietal cortices (Nagy et al., 2004), suggesting that developmental changes in the white-matter organization of fronto-parietal fiber-tracts may contribute to the

development of WM capacity. Similarly, theoretical models suggest that the connectivity of fronto-parietal networks may critically account for the observed changes in brain activity associated with development of working memory (Edin et al., 2007). In addition, the generation of rhythmic fluctuations of activity is related to several different neurotransmitter systems. GABAergic neurons play a central role in the generation of oscillatory activity in the alpha and gamma frequency ranges (Traub et al., 2004; Lorincz et al., 2009; Buzsáki and Wang, 2012), whereas glutamate and acteylcholin seem to control their amplitude and duration (Rodriguez et al., 2004; Lörincz et al., 2008; Vijayan and Kopell, 2012). Recent evidence suggests that these neurotransmitter-systems undergo important changes during adolescence and development (Tseng and O'Donnell, 2005; Hashimoto et al., 2009; Janiesch et al., 2011).

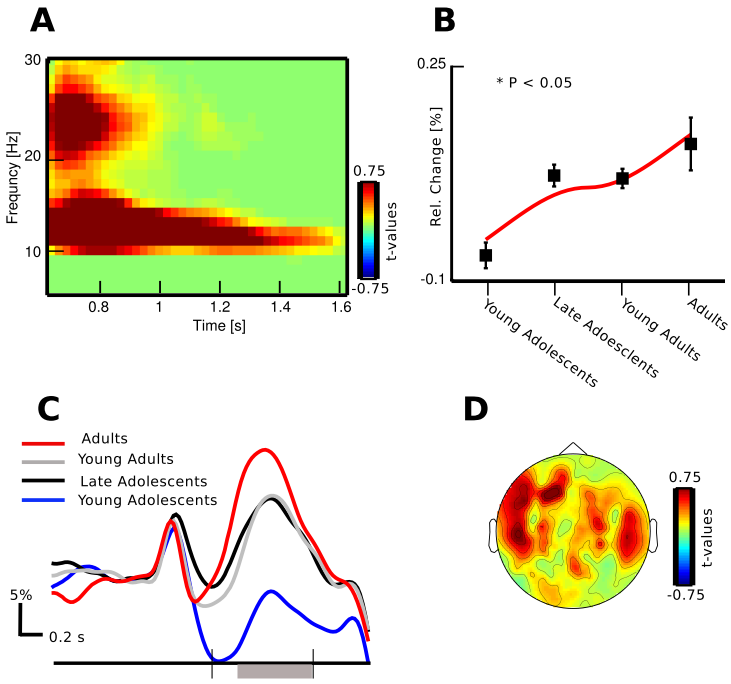

Figure 5.8: **Non-Linear Development of Low-Frequency Activity during WM-Maintenance. A:** Statistical map of non-linear age-related changes in low-frequency activity during WM-maintenance. X-axis: time (s), y-axis: frequency (Hz). Pseudo-colors correspond to regression t-values thresholded for significance (P<0.05; corrected). **B:** Non-linear but monotonic increase of 10-14 Hz activity across age groups. The red line corresponds to the fit provided by the non-linear model. **C:** Time courses of distractor-related 10-14 Hz activity for the young adolescent (blue), late adolescent (black), young adult (gray) and adult (red) participants. The gray bar indicates the temporal interval for which significant differences in distractor-related gamma-band activity were found. **D:** Topography of regression t-values tresholded for significance (P < 0.05; corrected). The topography shows strong developmental changes in distractor-related alpha-band power over temporal, central and frontal channels.

5.6 Further steps

Current theoretical models of distractor inhibition propose that alpha oscillations may support the suppression of task-irrelevant information through the phasic modulation of neural excitability levels (Jensen et al., 2012). This hypothesis is

supported by converging evidence showing that alpha oscillations modulate neural firing rates (Haegens et al., 2011), perceptual detection rates (Busch et al., 2009), neural metabolism (Scheeringa et al., 2011) as well as the amplitude of task-related gammma-band activity (Voytek et al., 2010; Spaak et al., 2012; Yanagisawa et al., 2012). In future studies it will therefore be important to clarify the contribution of alpha oscillations towards the development of distractor inhibition by examining how alpha oscillations modulate distractor-related gamma-band activity and to identify the sources involved into the generation of alpha-gamma coupling.

5.7 Conclusions

In summary, our findings show that the development of task-related alpha and gamma-band activity demonstrates that functional networks undergo important maturational processes during adolescence and adulthood. The present study replicates previous findings through demonstrating that distractor inhibition involves activity in the alpha and gamma frequency bands. In addition, our findings confirm existing results by showing that the ability to suppress distractors is not fully mature in adolescents.

5.8 Acknowledgements

This work was supported by the Max-Planck society, the LOEWE Grant 'Neuronale Koordination Forschungsschwerpunkt Frankfurt' and the Basque flushleft on Brain, Language and Cognition (BCBL).

5.9 References

Awh E, Vogel EK (2008) The bouncer in the brain. Nat Neurosci 11:5–6.
Bonnefond M, Jensen O (2012) Alpha Oscillations Serve to Protect Working Memory Maintenance against Anticipated Distracters. Current Biology.
Bunge SA, Dudukovic NM, Thomason ME, Vaidya CJ, Gabrieli JDE (2002) Immature frontal lobe contributions to cognitive control in children: evidence from fMRI. Neuron 33:301–311.
Bunge SA, Wright SB (2007) Neurodevelopmental changes in working memory and cognitive control. Curr Opin Neurobiol 17:243–250.
Busch NA, Dubois J, VanRullen R (2009) The phase of ongoing EEG oscillations predicts visual perception. J Neurosci 29:7869–7876.
Butters N, Pandya D (1969) Retention of delayed-alternation: effect of selective lesions of sulcus principalis. Science 165:1271–1273.
Butters N, Pandya D, Sanders K, Dye P (1971) Behavioral deficits in monkeys after selective lesions within the middle third of sulcus principalis. J Comp Physiol Psychol 76:8–14.
Buzsáki G, Wang X-J (2012) Mechanisms of gamma oscillations. Annu Rev Neurosci 35:203–225.
Casey BJ, Galvan A, Hare TA (2005) Changes in cerebral functional organization during cognitive development. Curr Opin Neurobiol 15:239–244.
Chao LL, Knight RT (1995) Human prefrontal lesions increase distractibility to irrelevant sensory inputs. Neuroreport 6:1605–1610.

Crone EA, Wendelken C, Donohue S, Van Leijenhorst L, Bunge SA (2006) Neurocognitive development of the ability to manipulate information in working memory. Proc Natl Acad Sci USA 103:9315–9320.
Dempster F, Brainderd C (1995) Interference and Inhibition in Cognition. Academic Pres.
Dempster FN (1992) The rise and fall of the inhibitory mechanism: Toward a unified theory of cognitive development and aging. Developmental Review 12:45–75.
Diamond A (2006) The early development of executive functions. In: Lifespan cognition: Mechanisms of change (Bialystok E, Craik F, eds), pp 70–95. New York: Oxford University Press.
Diamond A, Doar B (1989) The performance of human infants on a measure of frontal cortex function. Developmental Psychology 22:271–294.
Dugué L, Marque P, VanRullen R (2011) The phase of ongoing oscillations mediates the causal relation between brain excitation and visual perception. J Neurosci 31:11889–11893.
Durston S, Thomas KM, Yang Y, Uluğ AM, Zimmerman RD, Casey BJ. (2002) A neural basis for the development of inhibitory control. Developmental Science 5:F9–F16.
Edin F, Klingberg T, Johansson P, McNab F, Tegnér J, Compte A (2009) Mechanism for top-down control of working memory capacity. Proc Natl Acad Sci USA 106:6802–6807.
Edin F, Macoveanu J, Olesen P, Tegnér J, Klingberg T (2007) Stronger synaptic connectivity as a mechanism behind development of working memory-related brain activity during childhood. J Cogn Neurosci 19:750–760.
Funahashi S, Bruce CJ, Goldman-Rakic PS (1993) Dorsolateral prefrontal lesions and oculomotor delayed-response performance: evidence for mnemonic "scotomas". J Neurosci 13:1479–1497.
Fuster JM (2008) The prefrontal cortex, 4th ed. London NW1 7BY, UK: Elsevier.
Giedd JN, Blumenthal J, Jeffries NO, Castellanos FX, Liu H, Zijdenbos A, Paus T, Evans AC, Rapoport JL (1999) Brain development during childhood and adolescence: a longitudinal MRI study. Nat Neurosci 2:861–863.
Gogtay N, Thompson PM (2010) Mapping gray matter development: Implications for typical development and vulnerability to psychopathology. Brain and Cognition 72:6–15.
Goldman-Rakic PS (1995) Cellular basis of working memory. Neuron 14:477–485.
Haegens S, Nácher V, Luna R, Romo R, Jensen O (2011) α-Oscillations in the monkey sensorimotor network influence discrimination performance by rhythmical inhibition of neuronal spiking. Proc Natl Acad Sci USA 108:19377–19382.
Harnishfeger KK (1995) The development of cognitive inhibition: Theories, definitions, and research evidence. In: Interference and Inhibition in Cognition, pp 175–204. San Diego: Academic Press.
Harnishfeger KK, Bjorklund D (1994) A developmental perspective on individual differences in inhibition. Learning and Individual Differnces 6:331–355.
Harrison SA, Tong F (2009) Decoding reveals the contents of visual working memory in early visual areas. Nature 458:632–635.
Hashimoto T, Nguyen QL, Rotaru D, Keenan T, Arion D, Beneyto M, Gonzalez-Burgos G, Lewis DA (2009) Protracted developmental trajectories of GABAA receptor alpha1 and alpha2 subunit expression in primate prefrontal cortex. Biol Psychiatry 65:1015–1023.
Howard MW, Rizzuto DS, Caplan JB, Madsen JR, Lisman J, Aschenbrenner-Scheibe R, Schulze-Bonhage A, Kahana MJ (2003) Gamma Oscillations Correlate with Working Memory Load in Humans. Cerebral Cortex 13:1369 –1374.
Janiesch PC, Krüger H-S, Pöschel B, Hanganu-Opatz IL (2011) Cholinergic control in developing prefrontal-hippocampal networks. J Neurosci 31:17955–17970.
Jensen O, Bonnefond M, VanRullen R (2012) An oscillatory mechanism for prioritizing salient unattended stimuli. Trends Cogn Sci (Regul Ed) 16:200–206.
Jensen O, Kaiser J, Lachaux J-P (2007) Human gamma-frequency oscillations associated with attention and memory. Trends Neurosci 30:317–324.
Jokisch D, Jensen O (2007) Modulation of gamma and alpha activity during a working memory task engaging the dorsal or ventral stream. J Neurosci 27:3244–3251.
Jost K, Bryck RL, Vogel EK, Mayr U (2011) Are old adults just like low working memory young adults? Filtering efficiency and age differences in visual working memory. Cereb Cortex 21:1147–1154.
Klimesch W, Sauseng P, Hanslmayr S (2007) EEG alpha oscillations: the inhibition-timing hypothesis. Brain Res Rev 53:63–88.
Klingberg T, Forssberg H, Westerberg H (2002) Increased brain activity in frontal and parietal cortex underlies the development of visuospatial working memory capacity during childhood. J Cogn Neurosci 14:1–10.
Klingberg T, Vaidya CJ, Gabrieli JD, Moseley ME, Hedehus M (1999) Myelination and organization of the frontal white matter in children: a diffusion tensor MRI study. Neuroreport 10:2817–2821.
Knight RT, Hillyard SA, Woods DL, Neville HJ (1981) The effects of frontal cortex lesions on event-related potentials during auditory selective attention. Electroencephalogr Clin Neurophysiol 52:571–582.
Lane D, Pearson D (1982) The development of selective attention. Merrill Palmer Quarterly 28:317–337.
Lebel C, Gee M, Camicioli R, Wieler M, Martin W, Beaulieu C (2012) Diffusion tensor imaging of

white matter tract evolution over the lifespan. Neuroimage 60:340–352.
Lenroot RK, Giedd JN (2006) Brain development in children and adolescents: insights from anatomical magnetic resonance imaging. Neurosci Biobehav Rev 30:718–729.
Lörincz ML, Crunelli V, Hughes SW (2008) Cellular dynamics of cholinergically induced alpha (8-13 Hz) rhythms in sensory thalamic nuclei in vitro. J Neurosci 28:660–671.
Lorincz ML, Kékesi KA, Juhász G, Crunelli V, Hughes SW (2009) Temporal framing of thalamic relay-mode firing by phasic inhibition during the alpha rhythm. Neuron 63:683–696.
Luna B, Garver KE, Urban TA, Lazar NA, Sweeney JA (2004) Maturation of Cognitive Processes From Late Childhood to Adulthood. Child Development 75:1357–1372.
Maris E, Oostenveld R (2007) Nonparametric statistical testing of EEG- and MEG-data. J Neurosci Methods 164:177–190.
McNab F, Klingberg T (2008) Prefrontal cortex and basal ganglia control access to working memory. Nat Neurosci 11:103–107.
Miller EK, Cohen JD (2001) An Integrative Theory of Prefrontal Cortex Function. Annual Review of Neuroscience 24:167–202.
Miller EK, Desimone R (1994) Parallel neuronal mechanisms for short-term memory. Science 263:520–522.
Nagy Z, Westerberg H, Klingberg T (2004) Maturation of white matter is associated with the development of cognitive functions during childhood. J Cogn Neurosci 16:1227–1233.
Noudoost B, Moore T (2013) Parietal and prefrontal neurons driven to distraction. Nat Neurosci 16:8–9.
Olesen PJ, Macoveanu J, Tegnér J, Klingberg T (2007) Brain activity related to working memory and distraction in children and adults. Cereb Cortex 17:1047–1054.
Oostenveld R, Fries P, Maris E, Schoffelen J-M (2011) FieldTrip: Open source software for advanced analysis of MEG, EEG, and invasive electrophysiological data. Comput Intell Neurosci 2011:156869.
Oppenheim A, Schafer R (1989) Discrete-Time Signal Processing. In: Discrete-Time Signal Processing, pp 447–448. Prentice-Hall.
Palva S, Kulashekhar S, Hämäläinen M, Palva JM (2011) Localization of cortical phase and amplitude dynamics during visual working memory encoding and retention. J Neurosci 31:5013–5025.
Pascual-Leone J (1970) A mathematical model for the transition rule in Piaget's development stages. Acta Psychologica 32:301–345.
Paus T (2005) Mapping brain maturation and cognitive development during adolescence. Trends Cogn Sci (Regul Ed) 9:60–68.
Pesaran B, Pezaris JS, Sahani M, Mitra PP, Andersen RA (2002) Temporal structure in neuronal activity during working memory in macaque parietal cortex. Nat Neurosci 5:805–811.
Petermann F, Petermann U (2010) HAWIK-IV. In, Huber. Bern.
Raznahan A, Shaw P, Lalonde F, Stockman M, Wallace GL, Greenstein D, Clasen L, Gogtay N, Giedd JN (2011) How does your cortex grow? J Neurosci 31:7174–7177.
Ridderinkhof KR, Van der Molen MW, Band GPH, Bashore TR (1997) Sources of Interference from Irrelevant Information: A Developmental Study. Journal of Experimental Child Psychology 65:315–341.
Rodriguez R, Kallenbach U, Singer W, Munk MHJ (2004) Short- and long-term effects of cholinergic modulation on gamma oscillations and response synchronization in the visual cortex. J Neurosci 24:10369–10378.
Roux F, Wibral M, Mohr HM, Singer W, Uhlhaas PJ (2012) Gamma-band activity in human prefrontal cortex codes for the number of relevant items maintained in working memory. J Neurosci 32:12411–12420.
Sander MC, Werkle-Bergner M, Lindenberger U (2012) Amplitude modulations and inter-trial phase stability of alpha-oscillations differentially reflect working memory constraints across the lifespan. Neuroimage 59:646–654.
Sauseng P, Klimesch W, Heise KF, Gruber WR, Holz E, Karim AA, Glennon M, Gerloff C, Birbaumer N, Hummel FC (2009) Brain oscillatory substrates of visual short-term memory capacity. Curr Biol 19:1846–1852.
Scheeringa R, Mazaheri A, Bojak I, Norris DG, Kleinschmidt A (2011) Modulation of visually evoked cortical FMRI responses by phase of ongoing occipital alpha oscillations. J Neurosci 31:3813–3820.
Schiff A, Knopf M (1985) The effect of task demands on attention allocation in children of different ages. Child Dev 56:621–630.
Sowell ER, Peterson BS, Thompson PM, Welcome SE, Henkenius AL, Toga AW (2003) Mapping cortical change across the human life span. Nat Neurosci 6:309–315.
Sowell ER, Thompson PM, Holmes CJ, Batth R, Jernigan TL, Toga AW (1999) Localizing age-related changes in brain structure between childhood and adolescence using statistical parametric mapping. Neuroimage 9:587–597.
Spaak E, Bonnefond M, Maier A, Leopold D., Jensen O (2012) Layer-specific entrainment of gamma-band neural activity by the alpha rhythm in monkey visual cortex. Current Biology.
Tallon-Baudry C, Bertrand O, Peronnet F, Pernier J (1998) Induced gamma-band activity during the delay of a visual short-term memory task in humans. J Neurosci 18:4244–4254.
Tewes U (1991) HAWIE-R. Hamburg-Wechsler-Intelligenztest für Erwachsene. In, Huber. Bern. **Thomson D**

(1982) Spectrum estimation and harmonic analysis. Proc IEEE:1055–1096.
Todd JJ, Marois R (2004) Capacity limit of visual short-term memory in human posterior parietal cortex. Nature 428:751–754.
Traub RD, Bibbig A, LeBeau FEN, Buhl EH, Whittington MA (2004) Cellular mechanisms of neuronal population oscillations in the hippocampus in vitro. Annu Rev Neurosci 27:247–278.
Tseng KY, O'Donnell P (2005) Post-pubertal emergence of prefrontal cortical up states induced by D1-NMDA co-activation. Cereb Cortex 15:49–57.
Uhlhaas PJ, Roux F, Rodriguez E, Rotarska-Jagiela A, Singer W (2010) Neural synchrony and the development of cortical networks. Trends in Cognitive Sciences 14:72–80.
Uhlhaas PJ, Roux F, Singer W, Haenschel C, Sireteanu R, Rodriguez E (2009) The development of neural synchrony reflects late maturation and restructuring of functional networks in humans. Proc Natl Acad Sci U S A 106:9866–9871.
Vijayan S, Kopell NJ (2012) Thalamic model of awake alpha oscillations and implications for stimulus processing. Proc Natl Acad Sci USA.
Vogel EK, McCollough AW, Machizawa MG (2005) Neural measures reveal individual differences in controlling access to working memory. Nature 438:500–503.
Voytek B, Canolty RT, Shestyuk A, Crone NE, Parvizi J, Knight RT (2010) Shifts in gamma phase-amplitude coupling frequency from theta to alpha over posterior cortex during visual tasks. Front Hum Neurosci 4:191.
Voytek B, Soltani M, Pickard N, Kishiyama MM, Knight RT (2012) Prefrontal cortex lesions impair object-spatial integration. PLoS ONE 7:e34937.
Werkle-Bergner M, Freunberger R, Sander MC, Lindenberger U, Klimesch W (2012) Inter-individual performance differences in younger and older adults differentially relate to amplitude modulations and phase stability of oscillations controlling working memory contents. Neuroimage 60:71–82.
Yanagisawa T, Yamashita O, Hirata M, Kishima H, Saitoh Y, Goto T, Yoshimine T, Kamitani Y (2012) Regulation of motor representation by phase-amplitude coupling in the sensorimotor cortex. J Neurosci 32:15467–15475.

6

General Conclusions

6.1 Summary

The current thesis investigated neural oscillations with magnetoencephalogaphy (MEG) during working-memory (WM) and resting-state (RS) activity with the aim to characterize the frequencies and functional networks related to higher cognitive processes and to examine their developmental changes during adolescence. Three experiments were conducted to address these questions. The main finding is that alpha and gamma-band activity co-occur during both task and RS activity, suggesting that these frequencies as well as their interactions reflect core properties of large-scale networks. Moreover, the present findings support and extend previous data which have established functional relationships between gamma-band activity and higher cognitive processes by showing that the coupling of alpha and gamma-band activity may provide a mechanism for the gating of information. Finally, the developmental data suggest important and late occurring modifications in alpha and gamma-band activity which are involved in the maturation of WM capacity and distractor inhibition during adolescence.

Relevance of Alpha and Gamma-Band Activity for Working-Memory In psychology, working memory (WM) refers to the ability to maintain information in memory for short periods of time (Baddeley and Hitch, 1974). As a core component of WM, distractor inhibition is involved in the suppression of interfering information (Dempster, 1995), and both functions have been crucially implicated in central aspects of cognition (Bjorklund and Harnishfeger, 1995; Brainerd, 1995). The emerging view suggests that distractor inhibition and WM involve the recruitment of distributed functional networks comprising both higher neocortical as well as subcortical areas (Yoon et al., 2006; Edin et al., 2007; McNab and Klingberg, 2008; Curtis and Lee, 2010), but the mechanisms through which relevant information is selected and maintained remain unclear.

One possibility is that distributed networks utilize gamma and alpha oscillations to selectively gate and maintain relevant information (Jensen et al., 2012). To test this hypothesis, we recorded MEG activity in healthy adult participants (N = 22) during a task in which WM-load and the number of task-irrelevant items (distractors) were manipulated. Our results show a specific relationship between the amplitude of activity in the gamma (60-80 Hz) frequency range and the number of relevant WM-items. Critically, the cortical sources underlying WM-related 60-80 Hz activity were localized in the intra-parietal lobe (IPL) and prefrontal cortex (PFC), two brain regions which have been implicated in the functional networks underlying WM (Butters and Pandya, 1969; Butters et al., 1971; Fuster and Bauer, 1974; Bauer and Fuster, 1976; Funahashi et al., 1993; Goldman-Rakic, 1995; Honey et al., 2002; Curtis and D'Esposito, 2003; Mottaghy, 2006).

The findings from experiment one raise the possibility that gamma power in the IPL and in the PFC reflect different aspects of WM maintenance (Miller and Cohen, 2001; Kane and Engle, 2002). This is supported by the fact that gamma-band activity in parietal cortex was modulated by the number of stimuli presented in the memory array but not by the number of relevant items, which suggests that the modulation of 60-80 Hz activity reflects the scanning and maintenance of the spatial positions of possible WM locations. Based on the findings from experiment one we thus propose that the coupling between PFC and the IPL through coherent oscillations (Fries, 2005) may serve as a link for the readout of behaviorally relevant item positions. This interpretation is in line with recent evidence from electro-physiological recordings in non-human primates which show that selective synchronization at gamma frequencies modulates the effective connectivity between separate brain regions thereby strengthening the input of relevant information (Bosman et al., 2012).

The results from experiment one also showed oscillatory activity in the alpha (10-14Hz) range in BA 6. The localization of alpha-band delay activity in BA6 further supports the interpretation of gamma-band delay activity as a maintenance and readout mechanism of spatial maps which code for WM locations. Indeed, transcranial magnetic stimulation (TMS) of SMA has been observed to impair the ability to reproduce memorized gaze positions (Müri et al., 1995). In addition, recent theoretical and empirical work has related alpha oscillations with phasic fluctuations of neural firing, brain metabolism and perceptual detection rates (Klimesch et al., 2007; Busch et al., 2009; Lorincz et al., 2009; Jensen and Mazaheri, 2010; Dugué et al., 2011; Haegens et al., 2011; Scheeringa et al., 2011; Vijayan and Kopell, 2012), suggesting that alpha

oscillations in BA6 could reflect fluctuations of neural excitability in the occulomotor network. In agreement with these data, we propose a theoretical model in which alpha oscillations support long-range interactions between IPL and PFC by linking gamma-band activity through coherent windows of excitability (Fig. 7.1).

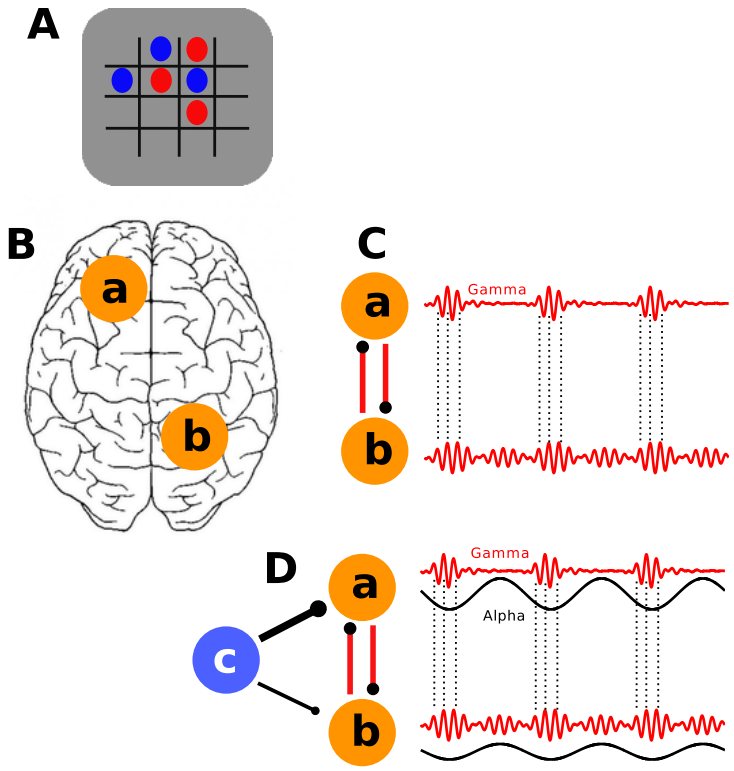

Figure 6.1: **Theoretical model of alpha based gamma modulation during WM maintenance.** Theoretical model explaining the read out of relevant information during the distractor condition (synthetic data shown for illustration; adapted from (Buzsáki and Wang, 2012)). The model is based on the results of experiment one as well as on evidence showing that gamma-band activity is modulated by the phase of ongoing and task-related alpha oscillations (Chorlian et al., 2006; Osipova et al., 2008; Cohen et al., 2009; Miller et al., 2010; Voytek et al., 2010; Foster and Parvizi, 2012; Spaak et al., 2012; Yanagisawa et al., 2012). **A:** Example of the stimuli presented during the distractor condition. **B:** Schematic view of the human brain showing hot spots of gamma-band activity implicated in WM maintenance during the distractor condition. **C:** Phase synchronization at gamma frequencies between two areas during WM maintenance. The number of gamma cycles reflects the number of items represented by each brain area. Relevant information is maintained by gamma oscillations in the PFC, whereas gamma-band activity in the IPL reflects the maintenance of all possible WM positions. Synchronization between gamma oscillations in both areas strengthens the input of relevant items in the IPL, thereby facilitating the read-out of relevant information. **D:** Gamma phase synchronization between two cortical sites, whose gamma power is differentially modulated by a common alpha rhythm. Gamma phase synchronization can only occur between gamma cycles which are coupled with the phase of highest network excitability. In addition, the differential amplitude modulation of gamma-band activity reflects the maintenance of relevant items in PFC as well as the maintenance of all possible WM positions in the IPL.

6.2 Alpha-Gamma Coupling in Thalamo-Cortical Networks

The thalamus has for long been considered as a passive relay structure. However, recent findings show that the thalamus actively modulates neocortical activity according to behavioral demands (Saalmann and Kastner, 2009). Furthermore,

emerging evidence suggests that such directed interactions may involve the synchronization of thalamo-cortical (TC) activity at alpha frequencies (Saalmann et al., 2012). This hypothesis is particularly compelling as long standing evidence has implicated the thalamus in the generation of synchronous slow-frequency activity in TC networks (Da Silva et al., 1973; Maiorchik et al., 1978; Shuliak and Trush, 1983; Jahnsen and Llinás, 1984; von Krosigk et al., 1993; Wang and Rinzel, 1993). However, direct evidence for the modulation of neocortical activity through thalamic alpha oscillations is so far lacking.

In experiment two, we therefore recorded RS-activity in a large sample (N=45) of healthy participants with MEG to study the modulation of neocortical activity through TC synchronization. To address this question, we combined measures of phase-amplitude coupling (PAC) between alpha (8-13 Hz) and gamma-band (30-70 HZ) activity with measures of TC synchronization and TC information transfer. Importantly, this approach allowed us to examine the modulation of neocortical activity via the synchronization of alpha activity in TC networks. Furthermore, because source localization of deep structures with MEG is challenging, we tested the physiological plausibility of our measurements by measuring TC conduction latencies with transfer entropy (TE) (Schreiber, 2000).

The results from experiment two revealed that the phase of thalamic alpha oscillations exerts a directed influence on the amplitude of neocortical gamma-band activity in the precuneus and the posterior cingulate cortex, two brain regions which are reciprocally connected with the higher order nuclei of the dorsal thalamus (Morgane et al., 2005; Cavanna and Trimble, 2006). Moreover, our data demonstrate synchronous alpha oscillations between the thalamus and the parietal regions in which TC interactions were found. Finally, the validity of our findings is supported by conduction latencies which were consistent with transmission delays reported by previous investigations of alpha oscillations in TC networks (Da Silva et al., 1973; Bollimunta et al., 2011).

Furthermore, we observed that gamma-band power in posterior-medial parietal (PPM) cortex was greatest at the peak of thalamic alpha activity, while in the visual cortex gamma-band activity was strongest near the trough of the alpha cycle. Electrophysiological recordings and computational models of TC circuits show that during strong phasic inhibition the spiking of relay-mode neurons and pyramidal cells will occur near the trough of the alpha cycle, whereas during weaker inhibition spiking activity will be coupled to the peak of the alpha cycle (Lorincz et al., 2009; Vijayan and Kopell, 2012). Accordingly, it is conceivable

that the differential temporal framing of cortical gamma-band activity reflects differences in the strength of phasic inhibition in TC networks.

As a result, alpha based entrainment of gamma-band activity may also promote the routing of information flow (Lorincz et al., 2009) which could lead to the emergence of state-dependent networks by biasing the sensitivity of TC networks towards internally generated vs. sensory activity (Fig. 7.2). Our interpretation is in line with fMRI- and combined EEG/fMRI-studies which show that during eyes closed RS-activity, alpha power in the visual cortex is associated with a decrease of functional connectivity between the visual cortex and the thalamus (Scheeringa et al., 2012) while functional connectivity between the thalamus and the PPM is enhanced (Gur et al., 1995). Our findings may thus reflect the intrinsic properties of functional relations in TC networks involving key regions of the default mode network (DMN) during RS (Zhang et al., 2008).

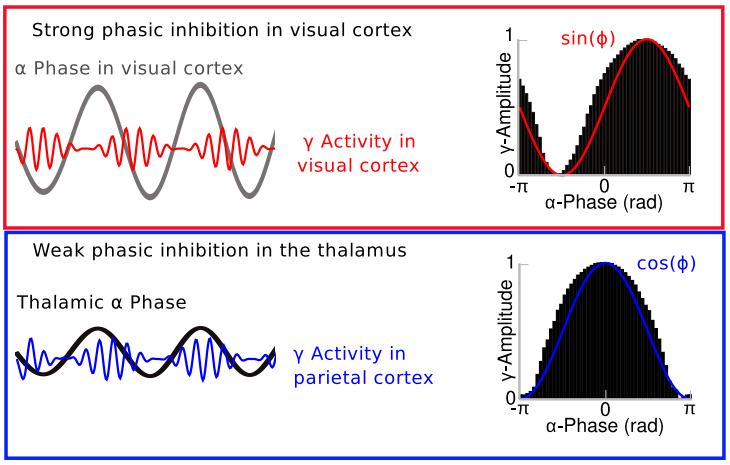

Figure 6.2: **Alpha Gamma Coupling in RS-networks.** Cartoon illustrating the possible implication of differential alpha-gamma coupling (synthetic data shown for illustration). The cartoon is based on the present findings and results reported by Lörincz et al. (17) and Vijayan and Kopell (18). **Upper panel:** Strong input (burst mode) to inhibitory interneurons in the thalamus will result in the occurrence of cortical gamma-band activity near the trough of cortical alpha oscillations. Accordingly, cortical gamma-band activity will occur during strong TC inhibition, thereby reducing the probability of signal propagation to other areas. **Lower panel:** Weak inputs (single spike mode) to thalamic interneurons will result in the occurrence of cortical gamma-band activity near the peak of thalamic alpha oscillations, ie during reduced inhibition. As a result, the output of an area may become more efficient in driving other regions. Note that when gamma-band activity occurs near the trough of the alpha cylce the phase-amplitude distribution will have the shape of a $\sin(\phi)$ function, whereas the occurrence of gamma-band activity near the peak of alpha will resemble a $\cos(\phi)$ function (synthetic data).

6.3 MEG as a Tool for Cognitive Neuroscience: Methodological Implications

In addition to providing novel evidence for the role of alpha and gamma-band activity in large-scale networks, the current work has also implications for the use of MEG as a non-invasive imaging technique to study brain functions and

cognition. Previous studies using non-invasive EEG/MEG-data which have tested the role of neural oscillations for cognition, have largely relied on correlational analyses to investigate the relationships between changes in the amplitude and synchrony of low- and high-frequency oscillations and cognitive processes (Tallon-Baudry and Bertrand, 1999; Jensen et al., 2007). However, because mechanistic relationships are difficult to test with such approaches, the precise role of distinct frequencies as well as brain regions underlying WM, for example, remained unclear.

Recent advances in multivariate statistical learning techniques (Haynes and Rees, 2006) have significantly advanced the possibilities of inferring mechanistic links between fluctuations in brain states and behaviour. Specifically, through extracting statistical regularities which are measurable only across single trial fluctuations and which cannot be detected by classical approaches relying on single trial averaging, these techniques allow the decoding of information carried by non-invasively recorded brain signals. Decoding techniques have been successfully applied to fMRI and EEG measurements (Lebedev et al., 2008; Harrison and Tong, 2009; Bradberry et al., 2010). However, so far it has remained unclear to what extent MEG-data could be utilized to infer higher cognitive processes from fluctuations of single-trial oscillatory activity. The decoding of 60-80 Hz activity using source reconstruction methods revealed that ongoing changes in PFC gamma-band power were closely related to the maintenance of relevant items in WM. Our findings are in line with recent evidence which demonstrates that single trial fluctuations of neural activity can be decoded to predict sensory and motor information (Harrison and Tong, 2009).

In addition, our decoding of MEG-data demonstrates that gamma-band signals from the frontal brain regions can be reliably measured and contain significant information content. This is relevant because gamma-band activity in EEG/MEG-recordings has been frequently observed in sensory and motor regions, while robust evidence for the involvement of frontal regions has been so far lacking. The current data thus suggest that MEG-signals carry also robust information about higher brain regions and associated cognitive processes.

A related question is the suitability of using MEG to infer properties of cortical and subcortical networks. Deep subcortical brain structures such as the thalamus and hippocampus form densely connected networks with many neocortical regions (Sherman and Guillery, 2000; Buzsáki and Wang, 2012). Source imaging of these structures with non-invasive techniques may therefore greatly contribute

to advance our understanding of subcortico-cortical interactions. However, because magnetic fields decay rapidly with increasing distance, source localization of subcoritcal activity in MEG recordings remains challenging. Thus, so far most electrophysiological experiments in humans involving subcortical structures are conducted in surgical patients (Cohen et al., 2009; Axmacher et al., 2010). A limited number of MEG studies, however, have reported thalamic and hippocampal sources (Ribary et al., 1991; Tesche, 1996a, 1996b; Gross et al., 2001; Bish et al., 2004, 2004; Jerbi et al., 2007; Lou et al., 2010; Poch et al., 2011).

Experiment two of this thesis considered the coupling between the phase of thalamic alpha and the power of brain-wide gamma in MEG recordings of RS-activity by reconstructing neural activity in source space using a beamforming approach. The results show that gamma-band activity in the neocortex is modulated by the phase of thalamic alpha oscillations, thereby providing important evidence for the emerging view that thalamic alpha oscillations may importantly contribute to the coordination of neocortical communication (Saalmann and Kastner, 2009; Schmid et al., 2012). Importantly, the biophysical validity of our results is supported by 1) previous evidence from electrophysiological recordings which have reported similar TC conduction latencies (Da Silva et al., 1973; Bish et al., 2004; Bollimunta et al., 2011) , 2) anatomical studies showing that several thalamic nuclei have a longitudinal (anterior-posterior) neuronal architecture (Yelnik et al., 1984), thereby supporting the possibility that thalamic sources may actively contribute to a measurable MEG signal (Ahlfors et al., 2010) and finally 3) theoretical and empirical findings which highlight the possibility that RS activity may be particularly sensitive to detect thalamic generators of alpha activity (Attal et al., 2007).

Thus, although the findings require further validation, the present approach provides a first step towards the non-invasive detection of TC interactions with MEG. Furthermore, if MEG proves to be capable of monitoring thalamic activity, it may have important clinical implications because TC dysfunctions have been centrally involved in the pathophysiology of several severe psychiatric disorders, such as schizophrenia (O'Donnell and Grace, 1998; Pinault, 2011).

6.4 Outlook

The present thesis demonstrates that alpha and gamma-band activity in TC and PFC networks are crucial for higher cognitive processes and RS-networks. Our

preliminary developmental findings suggest that both alpha and gamma oscillations undergo important developmental changes during adolescence, which raises further questions as to the precise relationship with ongoing changes in TC-networks. Evidence from fMRI data (Fair et al., 2010; Casey et al., 2011) support the possibility that TC interactions undergo major modifications during adolescence, highlighting that this is indeed a plausible hypothesis that requires further testing. Accordingly, future studies will therefore utilize the methods developed in the present thesis to examine the involvement of TC networks and PFC in the maturation of higher cognitive processes during development.

6.5 References

Ahlfors SP, Han J, Belliveau JW, Hämäläinen MS (2010) Sensitivity of MEG and EEG to source orientation. Brain Topogr 23:227–232.

Attal Y, Bhattacharjee M, Yelnik J, Cottereau B, Lefèvre J, Okada Y, Bardinet E, Chupin M, Baillet S (2007) Modeling and detecting deep brain activity with MEG & EEG. Conf Proc IEEE Eng Med Biol Soc 2007:4937–4940.

Axmacher N, Henseler MM, Jensen O, Weinreich I, Elger CE, Fell J (2010) Cross-frequency coupling supports multi-item working memory in the human hippocampus. Proc Natl Acad Sci USA 107:3228–3233.

Baddeley A, Hitch G (1974) Working memory. In: The psychology of learning and motivation (Bower G, ed), pp 47–89. New York: Academic Press.

Bauer RH, Fuster JM (1976) Delayed-matching and delayed-response deficit from cooling dorsolateral prefrontal cortex in monkeys. J Comp Physiol Psychol 90:293–302.

Bish JP, Martin T, Houck J, Ilmoniemi RJ, Tesche C (2004) Phase shift detection in thalamocortical oscillations using magnetoencephalography in humans. Neurosci Lett 362:48–52.

Bjorklund DF, Harnishfeger KK (1995) 5 - The evolution of inhibition mechanisms and their role in human cognition and behavior. In: Interference and Inhibition in Cognition (Frank N. Dempster and Charles J. Brainerd, eds), pp 141–173. San Diego: Academic Press.

Bollimunta A, Mo J, Schroeder CE, Ding M (2011) Neuronal mechanisms and attentional modulation of corticothalamic α oscillations. J Neurosci 31:4935–4943.

Bosman CA, Schoffelen J-M, Brunet N, Oostenveld R, Bastos AM, Womelsdorf T, Rubehn B, Stieglitz T, De Weerd P, Fries P (2012) Attentional stimulus selection through selective synchronization between monkey visual areas. Neuron 75:875–888.

Bradberry TJ, Gentili RJ, Contreras-Vidal JL (2010) Reconstructing three-dimensional hand movements from noninvasive electroencephalographic signals. J Neurosci 30:3432–3437.

Brainerd CJ (1995) 4 - Interference processes in memory development: The case of cognitive triage. In: Interference and Inhibition in Cognition (Frank N. Dempster and Charles J. Brainerd, eds), pp 105–139. San Diego: Academic Press.

Busch NA, Dubois J, VanRullen R (2009) The phase of ongoing EEG oscillations predicts visual perception. J Neurosci 29:7869–7876.

Butters N, Pandya D (1969) Retention of delayed-alternation: effect of selective lesions of sulcus principalis. Science 165:1271–1273.

Butters N, Pandya D, Sanders K, Dye P (1971) Behavioral deficits in monkeys after selective lesions within the middle third of sulcus principalis. J Comp Physiol Psychol 76:8–14.

Buzsáki G, Wang X-J (2012) Mechanisms of gamma oscillations. Annu Rev Neurosci 35:203–225.

Casey B, Jones RM, Somerville LH (2011) Braking and Accelerating of the Adolescent Brain. J Res Adolesc 21:21–33.

Cavanna AE, Trimble MR (2006) The precuneus: a review of its functional anatomy and behavioural correlates. Brain 129:564–583.

Chorlian DB, Porjesz B, Begleiter H (2006) Amplitude modulation of gamma band oscillations at alpha frequency produced by photic driving. Int J Psychophysiol 61:262–278.

Cohen MX, Axmacher N, Lenartz D, Elger CE, Sturm V, Schlaepfer TE (2009) Good vibrations: cross-frequency coupling in the human nucleus accumbens during reward processing. J Cogn Neurosci 21:875–889.

Curtis CE, D'Esposito M (2003) Persistent activity in the prefrontal cortex during working memory. Trends Cogn Sci (Regul Ed) 7:415–423.

Curtis CE, Lee D (2010) Beyond working memory: the role of persistent activity in decision making. Trends Cogn Sci (Regul Ed) 14:216–222.
Da Silva FH, Van Lierop TH, Schrijer CF, Van Leeuwen WS (1973) Organization of thalamic and cortical alpha rhythms: spectra and coherences. Electroencephalogr Clin Neurophysiol 35:627–639.
Dempster FN (1995) 1 - Interference and inhibition in cognition: An historical perspective. In: Interference and Inhibition in Cognition (Frank N. Dempster and Charles J. Brainerd, eds), pp 3–26. San Diego: Academic Press.
Dugué L, Marque P, VanRullen R (2011) The phase of ongoing oscillations mediates the causal relation between brain excitation and visual perception. J Neurosci 31:11889–11893.
Edin F, Klingberg T, Stödberg T, Tegnér J (2007) Fronto-parietal connection asymmetry regulates working memory distractibility. J Integr Neurosci 6:567–596.
Fair DA, Bathula D, Mills KL, Dias TGC, Blythe MS, Zhang D, Snyder AZ, Raichle ME, Stevens AA, Nigg JT, Nagel BJ (2010) Maturing thalamocortical functional connectivity across development. Front Syst Neurosci 4:10.
Foster BL, Parvizi J (2012) Resting oscillations and cross-frequency coupling in the human posteromedial cortex. Neuroimage 60:384–391.
Fries P (2005) A mechanism for cognitive dynamics: neuronal communication through neuronal coherence. Trends Cogn Sci (Regul Ed) 9:474–480.
Funahashi S, Bruce CJ, Goldman-Rakic PS (1993) Dorsolateral prefrontal lesions and oculomotor delayed-response performance: evidence for mnemonic "scotomas". J Neurosci 13:1479–1497.
Fuster JM, Bauer RH (1974) Visual short-term memory deficit from hypothermia of frontal cortex. Brain Res 81:393–400.
Goldman-Rakic PS (1995) Cellular basis of working memory. Neuron 14:477–485.
Gross J, Kujala J, Hamalainen M, Timmermann L, Schnitzler A, Salmelin R (2001) Dynamic imaging of coherent sources: Studying neural interactions in the human brain. Proc Natl Acad Sci USA 98:694–699.
Gur RC, Mozley LH, Mozley PD, Resnick SM, Karp JS, Alavi A, Arnold SE, Gur RE (1995) Sex differences in regional cerebral glucose metabolism during a resting state. Science 267:528–531.
Haegens S, Nácher V, Luna R, Romo R, Jensen O (2011) α-Oscillations in the monkey sensorimotor network influence discrimination performance by rhythmical inhibition of neuronal spiking. Proc Natl Acad Sci USA 108:19377–19382.
Harrison SA, Tong F (2009) Decoding reveals the contents of visual working memory in early visual areas. Nature 458:632–635.
Haynes J-D, Rees G (2006) Decoding mental states from brain activity in humans. Nat Rev Neurosci 7:523–534.
Honey GD, Fu CHY, Kim J, Brammer MJ, Croudace TJ, Suckling J, Pich EM, Williams SCR, Bullmore ET (2002) Effects of Verbal Working Memory Load on Corticocortical Connectivity Modeled by Path Analysis of Functional Magnetic Resonance Imaging Data. NeuroImage 17:573–582.
Jahnsen H, Llinás R (1984) Ionic basis for the electro-responsiveness and oscillatory properties of guinea-pig thalamic neurones in vitro. J Physiol (Lond) 349:227–247.
Jensen O, Bonnefond M, VanRullen R (2012) An oscillatory mechanism for prioritizing salient unattended stimuli. Trends Cogn Sci (Regul Ed) 16:200–206.
Jensen O, Kaiser J, Lachaux J-P (2007) Human gamma-frequency oscillations associated with attention and memory. Trends Neurosci 30:317–324.
Jensen O, Mazaheri A (2010) Shaping functional architecture by oscillatory alpha activity: gating by inhibition. Front Hum Neurosci 4:186.
Jerbi K, Lachaux J-P, N'Diaye K, Pantazis D, Leahy RM, Garnero L, Baillet S (2007) Coherent neural representation of hand speed in humans revealed by MEG imaging. Proc Natl Acad Sci USA 104:7676–7681.
Kane MJ, Engle RW (2002) The role of prefrontal cortex in working-memory capacity, executive attention, and general fluid intelligence: An individual-differences perspective. Psychonomic Bulletin$ Review 9:637–671.
Klimesch W, Sauseng P, Hanslmayr S (2007) EEG alpha oscillations: The inhibition–timing hypothesis. Brain Research Reviews 53:63–88.
Lebedev MA, O'Doherty JE, Nicolelis MAL (2008) Decoding of temporal intervals from cortical ensemble activity. J Neurophysiol 99:166–186.
Lorincz ML, Kékesi KA, Juhász G, Crunelli V, Hughes SW (2009) Temporal framing of thalamic relay-mode firing by phasic inhibition during the alpha rhythm. Neuron 63:683–696.
Lou HC, Gross J, Biermann-Ruben K, Kjaer TW, Schnitzler A (2010) Coherence in consciousness: paralimbic gamma synchrony of self-reference links conscious experiences. Hum Brain Mapp 31:185–192.
Maiorchik VE, Arkhipova NA, Vasin NY (1978) Thalamocortical projections and genesis of synchronous spindle activity in the EEG. Hum Physiol 4:629–636.
McNab F, Klingberg T (2008) Prefrontal cortex and basal ganglia control access to working memory. Nat

Neurosci 11:103–107.
Miller EK, Cohen JD (2001) An integrative theory of prefrontal cortex function. Annu Rev Neurosci 24:167–202.
Miller KJ, Hermes D, Honey CJ, Sharma M, Rao RPN, Den Nijs M, Fetz EE, Sejnowski TJ, Hebb AO, Ojemann JG, Makeig S, Leuthardt EC (2010) Dynamic modulation of local population activity by rhythm phase in human occipital cortex during a visual search task. Front Hum Neurosci 4:197.
Morgane PJ, Galler JR, Mokler DJ (2005) A review of systems and networks of the limbic forebrain/limbic midbrain. Prog Neurobiol 75:143–160.
Mottaghy FM (2006) Interfering with working memory in humans. Neuroscience 139:85–90.
Müri RM, Rivaud S, Vermersch AI, Léger JM, Pierrot-Deseilligny C (1995) Effects of transcranial magnetic stimulation over the region of the supplementary motor area during sequences of memory-guided saccades. Exp Brain Res 104:163–166.
O'Donnell P, Grace AA (1998) Dysfunctions in multiple interrelated systems as the neurobiological bases of schizophrenic symptom clusters. Schizophr Bull 24:267–283.
Osipova D, Hermes D, Jensen O (2008) Gamma power is phase-locked to posterior alpha activity. PLoS ONE 3:e3990.
Pinault D (2011) Dysfunctional thalamus-related networks in schizophrenia. Schizophr Bull 37:238–243.
Poch C, Fuentemilla L, Barnes GR, Düzel E (2011) Hippocampal theta-phase modulation of replay correlates with configural-relational short-term memory performance. J Neurosci 31:7038–7042.
Ribary U, Ioannides AA, Singh KD, Hasson R, Bolton JP, Lado F, Mogilner A, Llinás R (1991) Magnetic field tomography of coherent thalamocortical 40-Hz oscillations in humans. Proc Natl Acad Sci USA 88:11037–11041.
Saalmann YB, Kastner S (2009) Gain control in the visual thalamus during perception and cognition. Curr Opin Neurobiol 19:408–414.
Saalmann YB, Pinsk MA, Wang L, Li X, Kastner S (2012) The pulvinar regulates information transmission between cortical areas based on attention demands. Science 337:753–756.
Scheeringa R, Mazaheri A, Bojak I, Norris DG, Kleinschmidt A (2011) Modulation of visually evoked cortical FMRI responses by phase of ongoing occipital alpha oscillations. J Neurosci 31:3813–3820.
Scheeringa R, Petersson KM, Kleinschmidt A, Jensen O, Bastiaansen MC (2012) EEG alpha power modulation of fMRI resting state connectivity. Brain Connect.
Schmid MC, Singer W, Fries P (2012) Thalamic coordination of cortical communication. Neuron 75:551–552.
Schreiber (2000) Measuring information transfer. Phys Rev Lett 85:461–464.
Sherman SM, Guillery RW (2000) Exploring the Thalamus, 1st ed. Academic Press.
Shuliak BA, Trush VD (1983) Possible mechanism of the thalamic pacemaker of alpha-rhythm and fusiform activity. Biofizika 28:686–692.
Spaak E, Bonnefond M, Maier A, Leopold D., Jensen O (2012) Layer-specific entrainment of gamma-band neural activity by the alpha rhythm in monkey visual cortex. Current Biology.
Tallon-Baudry, Bertrand (1999) Oscillatory gamma activity in humans and its role in object representation. Trends Cogn Sci (Regul Ed) 3:151–162.
Tesche CD (1996a) MEG imaging of neuronal population dynamics in the human thalamus. Electroencephalogr Clin Neurophysiol Suppl 47:81–90.
Tesche CD (1996b) Non-invasive imaging of neuronal population dynamics in human thalamus. Brain Res 729:253–258.
Vijayan S, Kopell NJ (2012) Thalamic model of awake alpha oscillations and implications for stimulus processing. Proc Natl Acad Sci USA.
Von Krosigk M, Bal T, McCormick DA (1993) Cellular mechanisms of a synchronized oscillation in the thalamus. Science 261:361–364.
Voytek B, Canolty RT, Shestyuk A, Crone NE, Parvizi J, Knight RT (2010) Shifts in gamma phase-amplitude coupling frequency from theta to alpha over posterior cortex during visual tasks. Front Hum Neurosci 4:191.
Wang XJ, Rinzel J (1993) Spindle rhythmicity in the reticularis thalami nucleus: synchronization among mutually inhibitory neurons. Neuroscience 53:899–904.
Yanagisawa T, Yamashita O, Hirata M, Kishima H, Saitoh Y, Goto T, Yoshimine T, Kamitani Y (2012) Regulation of motor representation by phase-amplitude coupling in the sensorimotor cortex. J Neurosci 32:15467–15475.
Yelnik J, Percheron G, François C (1984) A Golgi analysis of the primate globus pallidus. II. Quantitative morphology and spatial orientation of dendritic arborizations. J Comp Neurol 227:200–213.
Yoon JH, Curtis CE, D'Esposito M (2006) Differential effects of distraction during working memory on delay-period activity in the prefrontal cortex and the visual association cortex. Neuroimage 29:1117–1126.
Zhang D, Snyder AZ, Fox MD, Sansbury MW, Shimony JS, Raichle ME (2008) Intrinsic functional relations between human cerebral cortex and thalamus. J Neurophysiol 100:1740–1748.

7

Zusammenfassung

7.1 Überblick

Die Adoleszenz, d.h. die Reifungsphase des Jugendlichen zum Erwachsenen, stellt einen zentralen Abschnitt in der menschlichen Entwicklung dar, der mit tief greifenden emotionalen und kognitiven Veränderungen verbunden ist. Neure Studien (Bunge et al., 2002; Durston et al., 2002; Casey et al., 2005; Crone et al., 2006; Bunge and Wright, 2007) machen deutlich, dass sich die funktionelle Architektur des Gehirns während der Adoleszenz grundlegend verändert und dass diese Veränderungen mit der Reifung höherer kognitiven Funktionen in der Adoleszenz assoziiert sein könnten. Messungen des Gehirn-Volumens mit Hilfe der Magnet-Resonanz-Tomographie (MRT) zum Beispiel zeigen eine nicht-lineare Reduktion der grauen und eine Zunahme der weißen Substanz während der Adoleszenz (Giedd et al., 1999; Sowell et al., 1999, 2003). Des weiteren treten in dieser Zeit Veränderungen in exzitatorischen und inhibitorischen Neurotransmitter-Systemen auf (Tseng and O'Donnell, 2005; Hashimoto et al., 2009). Zusammen deuten diese Ergebnisse darauf hin, dass während der Adoleszenz ein Umbau der kortikalen Netzwerke stattfindet, der wichtige Konsequenzen für die Reifung neuronaler Oszillationen haben könnte. Im Anschluss an eine Einführung im Kapitel 2, fasst Kapitel 3 der vorliegenden Dissertation die Vorbefunde bezüglich entwicklungsbedingter Veränderungen in der Amplitude, Frequenz und Synchronisation neuronaler Oszillationen zusammen und diskutiert den Zusammenhang zwischen der Entwicklung neuronaler Oszillationen und der Reifung höhere kognitiver Funktionen während der Adoleszenz. Ebenso werden die anatomischen und physiologischen Mechanismen, die diesen Veränderungen möglicherweise zu Grunde liegen könnten, theoretisch vorgestellt. Die in Kapitel 4-6 vorgestellten eigenen empirischen Arbeiten untersuchen neuronale Oszillationen mit Hilfe der Magnetoencephalographie (MEG), um die Frequenzbänder und die funktionellen Netzwerke zu charakterisieren, die mit höheren kognitiven Prozessen und deren

Entwicklung in der Adoleszenz assoziiert sind. Hierzu wurden drei Experimente durchgeführt, bei denen MEG-Aktivität während der Bearbeitung einer Arbeitsgedächtnisaufgabe und im Ruhezustand aufgezeichnet wurde. Die Ergebnisse dieser Experimente zeigen, dass Alpha Oszillationen und Gamma-Band Aktivität sowohl task-abhängig als auch im Ruhezustand gemeinsam auftreten. Darüber hinaus ergänzen die vorliegenden Untersuchungen Vorarbeiten, indem sie eine Wechselwirkung zwischen beiden Frequenzbändern aufgezeigt wird, die als ein Mechanismus für das gezielte Weiterleiten von Informationen dienen könnte. Die in Kapitel 6 vorgestellten Entwicklungsdaten weisen weiterhin darauf, dass in der Adoleszenz späte Veränderungen im Alpha und Gamma-Band stattfinden und dass diese Veränderungen involviert sind in die Entwicklung der Arbeitsgedächtnis-Kapazität und die Entwicklung der Fähigkeit, Distraktoren zu inhibieren. Abschliessend werden in Kapitel 7, die in dieser Dissertation vorgestellten Arbeiten, aus einer übergeordneten Perspektive im Gesamtzusammenhang diskutiert.

7.2 Relevanz von Alpha und Gamma Oszillationen für das Arbeitsgedächtnis

Das Arbeitsgedächtnis (AG) ist ein funktioneller Bestandteil des Erinnerungsvermögens, der es ermöglicht, Informationen für kurze Zeit im Gedächtnis zu halten (Baddeley and Hitch, 1974). Da die Kapazität des AGs begrenzt ist (Miller, 1994; Cowan, 2001), müssen irrelevante Informationen inhibiert werden, um Interferenzen mit der Aufrechterhaltung der relevanten Informationen zu vermeiden (Awh and Vogel, 2008). Ein zentraler Bestandteil des AG ist deshalb die Fähigkeit, interferierende Informationen (Distraktoren) zu inhibieren (Dempster, 1995). Neuere Ansichten gehen davon aus, dass die Aufrechterhaltung von Informationen im AG und die Inhibition von Distraktoren ein verteiltes funktionelles Netzwerk rekrutiert, zudem sowohl höhere kortikale als auch subkortikale Areale gehören (Yoon et al., 2006; Edin et al., 2007; McNab and Klingberg, 2008; Curtis and Lee, 2010). Die Mechanismen, die der Aufrechterhaltung relevanter Informationen und der Inhibition von Distraktoren zu Grunde liegen, bleiben jedoch weithin unbekannt. Ein möglicher Mechanismus ist, dass neuronale Netzwerke gamma und alpha Oszillationen benutzen, um selektiv relevante Information temporär aktiv zu halten und weiterzuleiten (Jensen et al., 2012). In Kapitel 4 (Experiment 1) wurde diese Hypothese in einer Stichprobe gesunder erwachsener Probanden (n = 22) untersucht. Zu diesem Zweck wurde ein AG-Paradigma verwendet, bei dem sowohl die Anzahl der relevanten AG-Items als auch die Anzahl task-irrelevanter Items (Distraktoren) manipuliert wurde. Die Ergebnisse dieser Studie zeigen einen

Zusammenhang zwischen der Amplitude der Aktivität im gamma (60-80 Hz) Frequenzbereich und der Anzahl der im AG gespeicherten task-relevanten Items. Besonders hervorzuheben ist, dass die kortikalen Quellen der 60-80 Hz Aktivität im intra-parietalen Lobus (IPL) und im präfrontalen Kortex (PFC) lokalisiert wurden: zwei Areale, die bereits durch eine Vielzahl von Studien mit dem funktionalen AG-Netzwerk assoziiert worden sind (Butters and Pandya, 1969; Butters et al., 1971; Fuster and Bauer, 1974; Bauer and Fuster, 1976; Funahashi et al., 1993; Goldman-Rakic, 1995; Honey et al., 2002; Curtis and D'Esposito, 2003; Mottaghy, 2006). Darüber hinaus deuten die Ergebnisse von Experiment 1 darauf hin, dass die gamma Power im IPL und im PFC unterschiedliche Aspekte der Informationverarbeitung im AG reflektieren (Miller and Cohen, 2001; Kane and Engle, 2002). Dieses Resultat könnte möglicherweise auf ein Verarbeiten und Aufrechterhalten aller relevanten und irrelevanten Item-Positionen im IPL hindeuten, wobei kohärente Oszillationen (Fries, 2005) eine Verbindung zwischen PFC und IPL herstellen könnten, über den das Auslesen der relevanten Item-Positionen erfolgen würde. Die Ergebnisse von Experiment 1 zeigen ebenfalls eine starke Zunahme oszillatorischer Aktivität im supplementär motorischen Areal (SMA) im alpha Frequenzbereich, wodurch die Interpretation der gamma Power im IPL und PFC als Mechanismus für die Aufrechterhaltung und das Auslesen räumlicher Informationen weiter unterstützt wird. Die Stimulierung des SMAs durch transkranielle Magnet-Stimulation (TMS) führt zu einer Beeinträchtigung der Fähigkeit, Item-Positionen im Blickfeld aus dem Gedächtnis abzurufen (Müri et al., 1995). Darüber hinaus haben neuere theoretische und empirische Arbeiten alpha Oszillationen mit phasischen Fluktuationen neuronaler Entladungsraten aber auch perzeptuellen Erkennungs-Raten in Verbindung gebracht (Klimesch et al., 2007; Busch et al., 2009; Lorincz et al., 2009; Jensen and Mazaheri, 2010; Dugué et al., 2011; Haegens et al., 2011; Scheeringa et al., 2011; Vijayan and Kopell, 2012). Die Lokalisierung der alpha Aktivität in BA 6 könnte daher Fluktuationen der neuronalen Erregbarkeit im okulo-motorischen Netzwerk reflektieren. In Übereinstimmung mit diesen Daten schlagen wir ein theoretisches Modell vor, welches die Langstrecken-Interaktion zwischen IPL und PFC unterstützt, indem gamma-Band Aktivität durch gemeinsame Erregbarkeitsfenster im alpha-Band synchronisiert wird.

7.3 Alpha-Gamma Kopplung in thalamo-kortikalen Netzwerken

Der Thalamus wurde lange Zeit als passive Relais-Struktur betrachtet. Neuere Studien zeigen jedoch, dass der Thalamus in Abhängigkeit von

Verhaltensanforderungen aktiv an der Modulation neokortikaler Aktivität beteiligt ist (Saalmann and Kastner, 2009). Des weiteren deuten aufkommende Befunde darauf hin, dass solch gerichtete Interaktionen durch die Synchronisation von alpha Oszillationen in thalamo-kortikalen (TK) Netzwerken implementiert sein könnten (Saalmann et al., 2012). Diese Hypothese ist vor allem deswegen überzeugend, weil zahlreiche Studien den Thalamus mit der Generierung von synchroner langsamer rhythmischer Aktivität in TK-Netzwerken in Zusammenhang gebracht haben (Da Silva et al., 1973; Maiorchik et al., 1978; Shuliak and Trush, 1983; Jahnsen and Llinás, 1984; von Krosigk et al., 1993; Wang and Rinzel, 1993). Einen direkten Beweis für die Modulierung neokortikaler Aktivität durch thalamische alpha Oszilationen gibt es jedoch bisher noch nicht. Um diese Hypothese zu untersuchen, wurde in Kapitel 5 (Experiment 2) die Modulierung neokortikaler Aktivität durch TK-Synchronisation bei gesunden erwachsenen Probanden (n = 45) mit MEG im Ruhezustand untersucht. Zu diesem Zweck wurde die Phasen-Amplituden Kopplung (PAK) zwischen alpha- und gamma-Band Aktivität zusammen mit der TK-Synchronisation und dem TK-Informationstransfer gemessen. Dieser Ansatz ermöglichte es uns, die Modulierung neokortikaler Aktivität durch die Synchronisation von alpha Oszillationen in TK-Netzwerken zu untersuchen. Da die Lokalisierung subkortikaler Strukturen mit MEG schwierig ist, wurde die physiologische Plausibilität unserer Messungen validiert, indem mit Hilfe der Transfer-Entropy (TE) (Schreiber, 2000) die Dauer von TK-Übertragungszeiten gemessen wurde. Die Ergebnisse von Experiment 2 zeigen, dass die Phase thalamischer alpha Oszillationen einen gerichteten Einfluss auf die Amplitude neokortikaler gamma-Band Aktivität im Precuneus und im posterioren cingulären Kortex hat, zwei Hirn-Areale, die über reziproke Verbindungen mit dem dorsalen Thalamus verbunden sind (Morgane et al., 2005; Cavanna and Trimble, 2006). Darüber hinaus zeigen unsere Daten, dass beide Areale über alpha Oszillationen mit dem Thalamus synchronisiert sind. Die Validität unserer Befunde wird außerdem durch die gemessenen TK-Latenz-Zeiten unterstützt, welche mit Ergebnissen aus invasivenStudien übereinstimmen (Da Silva et al., 1973; Bollimunta et al., 2011). Unsere Befunde zeigen außerdem, dass die gamma-Band Aktivität im posterioren-medialen parietalen Kortex (PPM) mit dem Schwingungsberg der alpha Oszillationen im Thalamus gekoppelt ist, während im visuellen Kortex die gamma Amplitude mit dem Schwingungstal des alpha Zyklusses korreliert. Elektrophysiologische Studien und Computer-Simulationen zeigen, dass starke phasische Inhibition im Thalamus dazu führt, dass Relais-Nervenzellen im Thalamus zeitgleich mit dem Schwingungstal des alpha Zyklus feuern. Schwache Inhibition hingegen führt dazu, dass die Aktivität von Relais-Zellen eher zeitgleich mit dem Schwingungsberg des alpha Zyklus

gekoppelt ist (Lorincz et al., 2009; Vijayan and Kopell, 2012). Folglich wäre es also denkbar, dass die differenzielle Modulierung der kortikalen gamma-Band Aktivität Unterschiede in der Stärke der Inhibition in TK-Netzwerken reflektiert. Eine mögliche Konsequenz dieser Inhibitions-abhängigen differenziellen Modulierung wäre eine Förderung des Informationsflusses in TK-Netzwerken durch eine Modulierung der gamma-Band Aktivität durch die Phase der alpha Oszillationen (Lorincz et al., 2009). Indem die Sensitivität von TK-Netzwerken zugunsten von intern generierter Aktivität erhöht würde, könnten dadurch zustandsabhängige Netzwerke formiert werden. Unsere Interpretation stimmt mit fMRI und simultanen EEG/fMRI Studien überein, die eine gleichzeitige Zunahme von alpha Oszillationen im visuellen Kortex und eine Abnahme der funktionellen Konnektivität zwischen dem visuellen Kortex und dem Thalamus im Ruhezustand zeigen (Scheeringa et al., 2012), während die funktionelle Konnektivität zwischen Thalamus und PPM im Ruhezustand erhöht ist (Gur et al., 1995). Unsere Befunde könnten somit die intrinsischen Eigenschaften funktioneller Wechselwirkungen in TK-Netzwerken widerspiegeln.

7.4 Relevanz von Alpha und Gamma-Band Aktivität für die Entwicklung höherer kognitiver Funktionen in der Adoleszenz

In Kapitel 6 wurde die funktionelle Relevanz von alpha- und gamma-Band Aktivität für die Entwicklung höherer kognitiver Funktionen in der Adoleszenz untersucht. Dabei wurde insbesondere die Hypothese untersucht, dass entwicklungsbedingte Veränderungen der alpha und gamma Power mit der Reifung funktioneller AG-Netzwerke assoziiert sind. Unsere vorläufigen Ergebnisse deuten darauf hin, dass sich die oszillatorische Aktivität im alpha und gamma Frequenzbereich während der Adoleszenz verändert und dass ein Zusammenhang zwischen der Entwicklung der oszillatorischen Aktivität in beiden Frequenzbändern und der Entwicklung des AG-Netzwerkes existiert. Diese Daten werfen die Frage auf, inwieweit entwicklungsbedingte Veränderungen in der funktionellen Architektur von TK-Netzwerken an diesen Ergebnissen beteiligt sein könnten. Diese Hypothese wird durch fMRI Studien gestützt, die darauf hindeuten, dass in der Adoleszenz wichtige Veränderungen in TK-Netzwerken stattfinden (Fair et al., 2010; Casey et al., 2011). Auf Grund der noch unklaren empirischen Befundlage ist es daher wichtig, diese Hypothese durch zusätzliche Studien mit Hilfe der in dieser Dissertation entwickelten Ansätze genauer zu untersuchen.